Tks5 interactome reveals ER-associated machinery translation in invadosomes.

Léa Normand[1], Benjamin Bonnard[1], Margaux Sala[1], Sylvaine Di-Tommaso[1,2], Cyril Dourthe[1,2], Anne-Aurélie Raymond[1,2], Jean-William Dupuy[2,3], Luc Mercier[4], Jacky G. Goetz[4], Violaine Moreau[1], Elodie Henriet[1#] and Frédéric Saltel[1,2#].

[1]University of Bordeaux, Inserm, UMR1312, BRIC, BoRdeaux Institute of onCology, 146 Rue Léo Saignat, Bordeaux, F-33000, France.

[2]University of Bordeaux, CNRS, INSERM, TBM-Core, US5, UAR 3427, OncoProt, F-33000 Bordeaux, France Labeled LNCC.

[3]University of Bordeaux, Bordeaux Proteome, F-33000 Bordeaux, France.

[4]Inserm U1109, MN3T, Strasbourg, France ; Université de Strasbourg, Strasbourg, France ; LabEx Medalis, Université de Strasbourg, Strasbourg, France ; Fédération de Médecine Translationnelle de Strasbourg (FMTS), Strasbourg, F-67000, France.

[#] These authors contributed equally to this work.

Corresponding author: frederic.saltel@inserm.fr

Summary

Invadosomes are invasive F-actin structures exhibiting different organizations that degrade the extracellular matrix. The study uses their universal marker, Tks5, to provide new data about invadosome molecular composition and reveal the role of ER-associated translation machinery in invadosome formation and function.

Abbreviations

CHX: cycloheximide

ECM: extracellular matrix

EIF4B: eukaryotic translation initiation factor 4B

ER: endoplasmic reticulum

RPS6: ribosomal subunit S6

Abstract:

The ability to progress and invade through the extracellular matrix is a characteristic shared by both normal and cancer cells through the formation of structures called invadosomes gathering invadopodia and podosomes. These invadosomes are plastic and dynamic structures that can adopt different organizations depending on the cell types and the environment such as rosettes, dots or linear invadosomes. In this study, we used the specific invadosome marker Tks5 (SH3PXD2A), to identify common features in these different organizations. Tks5 immunoprecipitation coupled with mass spectrometry analysis allowed us to identify common proteins in these different models. We identified elements of the translation machinery, in particular the EIF4B protein, but also endoplasmic reticulum (ER) proteins as part of the invadosome structure. Providing new data on invadosome molecular composition through Tks5 interactome, we identified that ER-associated translation machinery is recruited to invadosome and involved in their formation, persistence and function in all types of invadosomes.

Keywords: cancer, Tks5, invadosomes, ER, translation

Introduction

The ability to progress and invade through the surrounding environment is a characteristic shared by both normal and tumor cells. Extracellular matrix (ECM) breaching such as basement membrane or fibrillar collagen rich matrices is needed in physiological conditions such as embryogenesis or wound healing but is also required at the early stages of the metastatic cascade. During metastasis, cells will invade their surrounding matrix thanks to invadosomes. Invadosomes are dynamic actin-based structures that allow cells to interact and remodel the ECM through the recruitment of metalloproteinases[1,2]. Invadosome formation has been shown to depend on different factors such as soluble factors like growth factors[3–5] or the mechanical properties[6,7] and composition of the ECM[8]. These structures, classified as podosomes and invadopodia, respectively in normal cells and tumor cells, can adopt different organizations such as rosettes, aggregates or dots[6]. These plastic and dynamic structures are able to sense and adapt to their environment composition. Laminin can promote the formation of dots[9,10], while fibrillar type I collagen matrix leads to a re-organization along the fibers forming linear invadosomes[9,11] demonstrating a microenvironment-induced remodeling. This morphological plasticity is associated with a variation of the molecular composition of the structures: podosomes present a ring of adhesive proteins which is absent in invadopodia or linear invadosomes[11]. While podosomes and invadopodia are integrin-dependent structures, linear invadosome formation specifically depends on the discoidin domain receptor 1 (DDR1)[9,12]. On the other hand, actin-binding proteins like cortactin, the Arp2/3 complex, the neuronal Wiskott-Aldrich syndrome protein (N-WASP) and the GTPase Cdc42 are shared by all invadosome structures, but are also present in other actin structures[13–15]. However, the Tks5 scaffolding protein appears as a specific and common marker to all types of invadosomes[15]. Indeed, this protein is enriched in invadosomes but not in focal adhesion, filopodia, membrane ruffle or lamellipodia[16]. Tks5, a Src substrate protein, is required for invadosome formation[16]. Tks5 was discovered by Lock et *al.* in 1998 and is part of the p47 family[17]. It contains two major domains, the PX one that allows anchoring to the membrane, and the SH3 domain that allows protein-protein interaction. In addition to its major role in invadosome formation, Tks5 is also involved in cell division in bladder cancer and in cell proliferation via its action during the G1 phase of the cell cycle[18,19]. Tks5 belongs to a family containing also the Tsk4 protein involved in ECM degradation and in podosomes formation, while Tks5 is involved in all invadosome formation[20].

Even if several studies over the last few years have aimed at better defining molecular composition involved in invadosome formation[21,22], the common or specific markers for each structures in regard to their plasticity need to be investigated.

The aim of this article was to identify new and common molecular components present in all types of invadosome forms, namely rosettes, dots and linear invadosomes. To do so, we performed Tks5 interactome in different invadosome models. We used two cellular models, a murine fibroblast cell line expressing a constitutive activated form of the oncogene Src, NIH3T3-Src and a human epidermoid carcinoma cancer cell line, A431, this in two ECM contexts to generate rosettes, dots and linear invadosomes.

We identified 88 proteins commonly enriched in Tks5 interactome from four different types of invadosomes. While several identified proteins were already known to be involved in the formation or function of invadosomes (CD44, cortactin, ADAM15 or MMP14), we highlighted 54 new proteins not described to be involved into invadosome formation and/or function. Among these proteins, a large proportion was related to translation machinery confirming data obtained in a previous study[21]. We identified the eukaryotic translation initiation factor 4B (EIF4B) into invadosomes. We confirmed that translation and EIF4B are involved in the matrix degradation activity. Furthermore, we showed that the presence of endoplasmic reticulum (ER) proteins is required for invadosome persistence. These findings provide a better understanding of the invadosome regulation through the ER-associated translation machinery.

Results

Invadosomes variability and plasticity.

In order to compare the different invadosome structures, we chose two complementary cellular models. The Src-transformed mouse fibroblast NIH-3T3-Src cell line that present invadosomes as rosettes when cultured on a gelatin substrate and the A431 human epidermoid carcinoma cell line which form invadopodia as dots[23] (Figure 1a-b). As expected, the fibrillar collagen matrix led to their reorganization as linear invadosomes with a co-localization of F-actin and Tks5 along the collagen fibers in both cell lines[23] (Figure 1a-b). These elements demonstrate the variety of shapes and plasticity of invadosomes. Thus, Tks5 is a universal marker of rosettes, dots and linear invadosomes, and is the best candidate to investigate common invadosome features.

Proteomics analysis of Tks5 interactome in invadosomes.

To determine Tks5 interactome in these different invadosome types, we transfected NIH-3T3-Src and A431 cells with GFP-tagged Tks5 encoding plasmid. As expected, GFP-Tks5 colocalizes with endogenous Tks5 in all types of invadosomes (Figure 2a). We realized immunoprecipitation against GFP in both cell lines on plastic and type I collagen conditions (Supp Figure 1a). Indeed, on plastic, the cells behave as on a gelatin coating and thus form the same types of invadosomes, i.e. dots for A431 cells and rosettes for NIH-3T3-Src cells. Tks5 interactome was then assessed by LC-MS/MS mass spectrometry and the results are show in the Supplemental Table 1.

We first determined the specific molecular signature associated with each invadosome organization (Supp Table 1-5). We commonly identified an enrichment in mitochondrial, endoplasmic reticulum (ER) and Golgi proteins (Supp Figure 1b-g). The gene set enrichment analysis (GSEA) performed on Tks5 interactome from linear invadosomes (A431 and NIH-3T3-Src cells) showed an enrichment for cell adhesion proteins such as CD34 and TSPAN6 absent in other invadosome organizations (Supp Figure 1f). These data show that depending on each organization, invadosomes exhibit specific proteins probably involved in their structure or function. Similarly, we also showed specific enrichment of translation proteins

although each is organization specific: EIF5A in rosettes, RPS15 in dots or EIF2B4 in linear invadosomes (Supp Figure 1c, e, g).

We performed a comparative analysis with published data regarding proteins associated with Tks5 in 293T cells [22], and also identified cortactin (CTTN), the molecular chaperone Hsp90B1, the elongation factor EEF2 or the beta-actin protein (ACTB) (Supp Figure 2a, left panel). Similarly, another recent study that used proximity-labelling proteomic assay to identify Tks5 interactome in invadopodia in MDA-MB-231 cells, also identified CTTN, the microtubule-associated protein 4 (MAP4), the reticulon 4 protein (RTN4), the metalloproteinase ADAM15 and the eukaryotic translation initiation factor 4A3 (EIF4A3)[24] (Supp Figure 2a, right panel). Since cortactin is well known to be present in all types of invadosomes, it can be used as a positive control to our approach[25,26].

We then focused on proteins that were common to all invadosomes and identified 88 proteins present in dots, rosettes and linear invadosomes in the two cell types (Figure 2b-d). Among the 88 common proteins, 34 proteins such as CTTN, LAMP1, ADAM15 or MMP14 were previously identified in literature as components of in invadosomes, validating our mass spectrometry experiment. In order to validate identified proteins known to interact with Tks5[24,27,28], we stained by immunofluorescence the receptor CD44 in all types of invadosomes and confirmed the co-localization of CD44 with Tks5 in all organizations of invadosomes (Figure 2e). Interestingly, the pattern of CD44 is different in rosettes where it colocalize with the actin, in comparison with dots and linear invadosome where CD44 surrounds the actin. Similarly, MAP4 co-localized with Tks5 in dots and linear invadosomes in A431 cells (Supp Figure 2b). These results were obtained from cells overexpressing Tks5-GFP but were also confirmed in WT cells, not overexpressing Tks5-GFP (data not shown). These experiments confirm the correct co-localization between Tks5 and the proteins CD44 and MAP4, identified in Tks5 interactome by mass spectrometry analysis.

However, a large proportion of identified protein has never been described to be present in invadosomes such as RPL19, RTN4 or EIF3A (Figure 2c). The GSEA performed on the 88 common proteins showed an enrichment in translation signaling (52% of total proteins) with an enrichment of RNA binding and structural constituent of ribosomes proteins (Figure 2d), including determinant elements of translation machinery such as RPL19, EIF4B or RPS6 (Supp Figure 2c). RPS6 is a component of the 40S subunit of the ribosome that allows the reading of mRNA[29]. EIF4B, on the other hand, is a translation factor that is part of the pre-initiation complex[30]. This complex, in association with the 40S subunit, allows to start mRNA translation. This result confirms the presence of the translation machinery at invadosomes,

already identified by our team in NIH-3T3-Src cells using proteomics on laser captured rosette-like invadosomes (Ezzoukhry et *al.).*

All together these results validate our experimental approach leading to the identification of new Tks5 partners into all types of invadosomes and suggest a link between Tks5 and the translation machinery.

The translation machinery is present in all types of invadosomes.

As we identified the translation machinery as a common feature shared by all the invadosome structures, we decided to focus our analysis on these translation proteins. Interestingly, other molecular studies of invadosomes, whether global or linked to Tks5, have identified proteins linked to translation[21,22,24,31] (Supp Figure 2d). Briefly, Mallawaaratchy et *al.* identified proteins enriched in invadopodia of glioblastoma cells by mass spectrometry, Ezzoukhry et *al.* identified translation proteins enriched in invadosomes by laser microdissection combined with mass spectrometry, Stylli et *al.* identified proteins linked to Tks5 by co-immunoprecipitation and mass spectrometry in dots of 293T cells and Thuault et *al.* identified proteins linked to Tks5 by biotynilation technique in dots of MDA-MB-231. The RPS6 staining and the co-localization with Tks5 validated the presence of ribosomal proteins in all invadosomes (Figures 3a, 3b). We also showed the co-localization of the translational initiation factor, EIF4B, which was previously found enriched in rosettes[21], with Tks5 in all organizations of invadosomes in both cell lines (Figure 3c and 3d). The presence of ribosomal proteins and translation factors in all invadosomes supports the hypothesis on an active translation in all these structures. Moreover, comparative analysis, using dataset obtained from Tks5 interactome from NIH-3T3-Src cells harboring rosettes and published rosettes proteome[21], showed an enrichment in ribosomal and translation proteins (Supp Figure 2e-f). We commonly identified 79 proteins including 39 related to translation proteins (Supp Figure 2f). Among these 39 proteins, 20 are ribosomal proteins (Supp Figure 2f) which confirms the presence of ribosomes into invadosome rosettes as observed in Ezzoukhry et al.

Involvement of the translation machinery in invadosome function.

In order to investigate and confirm the role of translation in all invadosomes formation and matrix degradation activity from both cell lines, we treated A431 and NIH-3T3-Src cells seeded on gelatin or type 1 collagen with the translation inhibitor cycloheximide (CHX) (Supp Figure 3). Our previous study demonstrated that CHX blocked the formation of rosettes in a short time, after one hour of treatment[21]. By using Western Blot and SUrface SEnsing of

translation (SUnSET) assay, we first showed that CHX treatment reduced global translation in all conditions (Supp Figure 3a and 3b). We next confirmed that CHX treatment in NIH-3T3-Src model prevented invadosome rosette formation (Figure 4a, 4b) as previously described[21]. No significant differences for dots and linear invadosomes formation was measured by immunofluorescence quantification between CHX and control group (DMSO) (Supp Figure 3c and 3d). However, CHX treatment limited invadosome degradation activity by A431 and NIH-3T3-Src cells on gelatin and collagen matrices (Figure 4c, 4d). These results showed that global translation is involved in degradation capacity of all invadosomes and formation only in rosette organization.

As we identified EIF4B in all invadosomes (Figure 2c; Supp Figure 2c), we assessed the role of EIF4B in invadosome degradation activity. By using small interfering RNA (siRNA) strategy we silenced EIF4B expression in both cell lines (Supp Figure 3e) and demonstrated that EIF4B depletion prevented invadosome rosette formation in NIH-3T3-Src model and linear invadosome formation in A431 model (Supp Figure 3f). However, EIF4B depletion reduced matrix degradation activity in all organizations of invadosomes from both cell lines (Figure 4e, 4f). These results showed that EIF4B is involved in degradation capacity of all invadosomes.

These data confirm the involvement of the translation and more specifically of the EIF4B protein in the matrix degradation activity of all invadosomes.

Recruitment of ER into invadosome rosettes.

In addition to translation proteins, the mass spectrometry analysis highlighted the presence of ER-related proteins such as RTN4, LRRC59 or RRBP1 in all invadosomes linked with Tks5 (Figure 2c). Ribosomes and ER proteins have previously been identified in the proteome of invadosome rosettes[21].

In order to assess the involvement of the ER in invadosome formation and function we used the rosette model, which is the largest invadosome structure, facilitating analysis and imaging. We used lifeact-mRuby-expressing NIH-3T3-Src cells transfected with KDEL-GFP to detect ER presence. By video microscopy, we showed that the ER was recruited at the level of the rosette in formation and that there was an enrichment of the ER inside the actin core, as previously described in fixed cells[21] (Figure 5a, Video 1). Furthermore, time-lapse imaging clearly shows that the RE is not present in all the cytoplasm and revealed that the ER forms “arms” leading to a “ER flow” heading towards the forming rosette then accumulating within

the actin core (Figure 5a, Vidéo 1). The transversal sections confirm the enrichment as we can clearly see that the ER arm is inserted within the rosette actin core (Figure 5a). 3D reconstruction allowed us to visualize the accumulation of the ER within the rosette core (Figure 5b). In order to confirm the presence of ER at the level of rosettes, we performed correlative light and electron microscopy (CLEM). Correlation between actin fluorescent images and electron microscopy allowed the identification of ER tubules associated with the rosettes (Figure 5c).

In order to determine the dynamic of ER recruitment during invadosome formation, time-lapse imaging was performed. The analysis revealed that ER recruitment occurs before actin polymerization and formation of rosette-like invadosomes (Figure 5d, Video 2). In addition, we showed that the maintenance of the structures requires the presence of ER (Figure 5e upper panel, Video 3a) while a drop in ER recruitment is associated with a collapse of the structure (Figure 5e lower panel, Video 3b). 3D reconstruction confirmed that the collapse of the rosette structure is associated with a withdrawal of the ER within the structure with the "ER flow" heading towards the interior of the cell (Figure 5f). These results therefore confirm the presence but also a potential involvement of the ER in the rosette formation and maintenance over time.

Involvement of ER-associated machinery translation in invadosome formation.

As we identified the presence and the determinant role of translation and ER in invadosome formation, we investigated the role of ER-associated translation in invadosome formation and matrix degradation activity. Previously published results showed the involvement of the ER in the formation and function of invadosomes via the involvement of the protrudin protein or by the involvement of the calnexin/erp57 protein complex respectively[32,33]. To determine the role of ER-associated translation in the dynamic of invadosome rosettes formation, we performed a time-lapse experiment with cells treated with CHX to inhibit translation (Figure 6a, Video 4). Translation inhibition led to the collapse of the rosette structure while the ER was still present at the 'previous invadosome site" without re-formation of invadosomes (even if some actin polymerization events were recorded) (Figure 6a, Video 4). This result suggests that ER-associated translation is mandatory for invadosome persistence.

To further characterize the involvement ER-associated translation in invadosome formation, we treated cells with Sec 61 translocon inhibitor (ES1) which blocks the translocation of proteins to the ER. Indeed, Sec61 is a well-described ER marker that allows protein insertion

into the ER but also is a key player for ribosomes docking to the ER[34]. Furthermore, Sec61 was identified by our mass spectrometry analysis for A431 cells on plastic and collagen (Supp Table 1) and localized with invadosome structures (Figure 6b). ES1 treatment on A431 and NIH-3T3-Src cells seeded on gelatin or type 1 collagen matrix led to a decreased number of all organizations of invadosomes (Figure 6c). These results therefore suggest that the translation machinery must be adapted somewhat depending on the matrix context. This would explain why the translation machinery is only involved in the degradation function for dots and linear invadosomes while it is involved in the formation and degradation function for rosettes, which are larger structures.

All together, these results demonstrate that the ER-associated translation machinery identified in Tks5 interactome is an essential element to maintain the formation of all types of invadosomes.

Discussion

We provided here a molecular characterization of all types of invadosomes by identifying the interactome of the common and universal invadosome marker Tks5. We used co-immunoprecipitation coupled with mass spectrometry to identify new proteins shared by different invadosome types such as dots, rosettes and linear invadosomes (Figure 1). This strategy allowed us to identify proteins already known in the literature but also to identify new ones. We showed that Tks5 is linked to translation proteins and confirm that translation is involved in the degradation function in all types of invadosomes, including linear invadosomes.

Indeed, we identified 46 translation proteins with some already known in the literature to be involved in invadosome activity such as IGF2BP2, IGF2BP3 and FGD1[35–38]. Regarding the other proteins identified and already described in invadosomes, microtubule-associated proteins and especially MAP4 and LAMP1 were described in podosomes[24,27,39] and ITGA5 was described in invadopodia[31]. PTBP1 was also identified in podosomes as participating in their formation[40]. We further demonstrated here that the matrix receptor CD44 which was previously described in podosomes and invadopodia but not in linear invadosomes[28,41] is also a common marker of invadosomes (Figure 2). These known proteins allowed us to serve as quality control for mass spectrometry experiments.

Thanks to mass spectrometry experiments, we were also able to validate the presence of translation proteins in linear invadosomes. We identified the presence of EIF4B and RPS6 proteins in all invadosome organizations (Figure 3). Interestingly, these two proteins are known in the literature to be targeted by the mTOR/ S6K1 pathway. Indeed, S6K1 is be able to directly phosphorylate EIF4B to allow the recruitment of EIF4A and EIF3 as well as the RPS6 protein to initiate translation[42]. While we demonstrated that global translation is mandatory for degradation activity induced by invadosomes, the inhibition of global translation did not prevent invadosome formation (excepted for rosettes) (Figure 4). Nevertheless, we also showed that ER-associated translation regulates all type of invadosomes formation suggesting that ER has a major role in invadosome formation and the associated degradation activity. We hypothesize that ribosome docking to ER, through Sec61, enhances protein synthesis of determinant elements for invadosome formation. A recent study demonstrated that an early increase of Sec61 enhanced the expression of pro-invasive

proteins, followed by an expansion of the ER and the Golgi, leading to the delivery of these pro-invasive proteins to the cell membrane[43].

In addition to the translation proteins identified, proteins present in the ER have also been highlighted by our proteomic analysis such as RTN4 or LRRC59. Since ER is also involved in protein translation, this suggested the presence of a complex translation mechanism within all invadosomes. We showed that the ER is recruited at the rosette, so enrichment of the ER could be linked to the rosette functioning properly, notably for its degradation capacity. In addition, our data show that removal of the ER leads to a collapse of the rosette structure suggesting a link between ER and invadosome formation and degradation activity. Furthermore, we showed that the ER was necessary for initiating and maintaining the invadosome rosettes (Figure 5 and 6). Indeed, the spatiotemporal aspect of invadosome formation in the initiation, stabilization or collapse phases is a major question[44,45]. Here, we show that the ER plays a main role in these different stages.

In literature, Pedersen et *al*. also showed the involvement of ER in invadosome formation: protrudin mediated ER-endosome contact site promotes cell invasion through the translocation of MT1-MMP endosome to the plasma membrane leading to invadopodia outgrowth and degradation[32]. Moreover, one of our recent study showed that two ER proteins, calnexin and ERp57, can be trafficked to invadosomes and are essential for ECM degradation[33]. These results therefore suggest the presence of a complex allowing invadosomes to have their own translation machinery to facilitate cell invasion with local translation of specific mRNA[21,46]. Tks5 could therefore act as a molecular crossroads allowing translational proteins to cluster in the same place, leading to rapid localization and greater efficiency for the cell in the formation and function of invadosomes.

In order to better understand the link between the translation and the ER in all types of invadosomes, we first targeted the EIF4B protein, identified by mass spectrometry. Using siRNA strategy, we showed that EIF4B is required in degradation function. Recent studies already showed the involvement of EIF4B in invasion. Indeed, Cao and al. showed that the pathway PIM1/EIF4B/c-MET pathway was involved in tumor migration and invasion in lung adenocarcinoma[47]. In the same way, the GMAN/p-EIF4B pathway leads to cell proliferation and invasion in hepatocellular carcinoma (HCC)[48].

We also identified many proteins associated with EIF3 and EIF4 complexes such as EIF3C, EIF4A3, EIF4E or EIF3H in at least three out of four types of invadosomes. Similarly, these complexes are already known in the literature to participate in the process of cell invasion.

The YTHDF1/EIF3C axis is involved in the invasion process in ovarian cancer[49], EIF3H participates to the invasion of hepatocellular carcinoma[50] and the EIF4A3/FLOT1 pathway promotes invasion and tumor proliferation in lung adenocarcinoma[51]. These results suggest the involvement of these complexes in the degradation mechanism that could be common to all types of invadosomes.

Altogether, these results provide new knowledge specifically into invasive structures and on the invasion process more broadly. Indeed, we reported new molecular components common to all types of invadosomes through the identification of Tks5 interactome. This thus provides a better understanding of the mode of operation of invadosomes, in particular via the involvement of the ER-associated translation machinery which is involved into invadosome formation.

Material and methods

Antibodies and reagent

Anti-GFP (catalog number ab6673) antibody was purchased from Abcam. Anti-Tks5 (G-7, catalog number sc-376211), and anti-CD44 (DF1485, catalog number sc-7297) were purchased from Santa Cruz Biotechnology, Inc. Anti-MAP4 (AG1741, catalog number 11229-1-AP) was purchased from Proteintech. Anti-RPS6 (S369, catalog number AP22299a) was purchased from Abgent. Anti-DDK (OTI2F7, catalog number TA500288) was purchased from OriGene Technologies, Inc. Anti-EIF4B (catalog number 3592) was purchased from Cell Signaling Technology. Secondary antibodies for immunofluorescence IRDye® 680RD Conjugated Goat anti-mouse (926-68070, LI-COR Biotech.), IRDye® 680RD Conjugated Goat anti-rabbit, (926-68071, LI-COR Biotech.), IRDye® 800CW Conjugated Goat anti-mouse (926-32210, LI-COR Biotech.), IRDye® 800CW Conjugated Goat anti-rabbit (926-32211, LI-COR Biotech.). The Atto 647N conjugated Goat anti-mouse-IgG was purchased from Sigma-Aldrich (catalog number 50185). DAPI (catalog number H21486), phalloidin (catalog number FP-BZ-9630) were purchased from Interchim. Type I collagen from rat tail(catalog number 354236) was purchased from Corning. Sec61 translocon was inhibited by pharmacological approach using Eeyarestatin 1 (ES1, catalog number E1286 Sigma-Aldrich) at 5µM during 1 hour. Species-specific fluorescent far-red coupled secondary antibody for western blot IRDye 680CW goat (polyclonal) anti-rabbit IgG (H+L) (catalog number 926-68070) or IRDye 800CW goat (polyclonal) anti-mouse IgG (H+L) (catalog number 926-32210) were purchased from LI-COR Biotech. GM6001 MMP Inhibitor (catalog number CC10), Cycloheximide (CHX) (catalog number 01810) and Manganese(II) (catalog number M7899) were purchased from Sigma-Aldrich.

Cell culture

The A431 cell line was generously donated by Dr. Julie Dechanet-Merville (CNRS 5164, Bordeaux) and authenticated. NIH-3T3-Src cells were generously donated by Dr. Sara Courtneidge (Université of Portland, USA). A431 and NIH-3T3-Src cells were maintained in DMEM high glucose (Gibco) supplemented with 10% fetal bovine serum (FBS, 139 Sigma Aldrich) at 37°C in a 5% CO2 incubator. In this study, we used A431 and NIH-3T3-Src cells transduced with a lentiviral plasmid expressing Tks5 fused to GFP, and the cell line was named A431-Tks5-GFP and NIH3T3-Src-Tks5-GFP.

Lentiviral transduction

A431 and NIH-3T3-Src cells were seeded in a 6-well plate, then transduced after 24 h at a multiplicity of infection of 10 µg, either with a lentiviral plasmid containing Tks5 couple to GFP, or with the GFP alone plasmid encoding as a control . The transduced cells were selected using puromycin treatment at 1µg/mL. Co-transduction of lifeact-mRuby and KDEL-GFP NIH-3T3-Src cells has been performed as described above but double positive cells were selected and sorted using BD FACSAria Cell Sorter (BD Bioscience).

Transfection

EIF4B-DDK plasmid was purchased from OriGene Technologies, Inc. This plasmid was transfected (2,4 µg) using JetPrime (PolyPlus Transfection) following the manufacturer's instructions. siRNA oligonucleotides (20 nM) targeting eIF4B (Human: s4573 & s4574; Mouse: s93804 & s93805 ThermoFisher) were transfected using Lipofectamine RNAiMax (Invitrogen) according to the manufacturer's instructions.

Coating of coverslips with extracellular matrix (ECM)

Cells were seeded on gelatin coverslips with or without coating of collagen. Type I collagen (rat tail, catalog number 354236, Corning) was diluted in DPBS containing calcium and magnesium (Dulbecco's Buffered-Phosphate Saline, Gibco) at a final concentration of 0.5mg/ml and polymerized for 4 h at 37°C. Gelatin-coated coverslips were made using gelatin from Sigma-Aldrich (catalog number G1393). Coverslips were incubated with gelatin for 20 min before and then fixed with 0.5% glutaraldehyde (Electron Microscopy Science) for 40 min at room temperature. Coverslips were washed 3 times with PBS before cell seeding.

Immunofluorescence and imaging

Cells were fixed using 4% paraformaldehyde (PFA) (Electron Microscopy Sciences) for 10 min at room temperature and then rinsed 3 times with PBS. Cells were permeabilized using 0.2% Triton X-100 (catalog number T9284, Sigma-Aldrich) for 10 min at room temperature before being rinsed twice with PBS. Cells were then incubated with primary antibodies (1:100 diluted in PBS-4%BSA) for 40 min at room temperature, rinsed 3 times with PBS. The cells were then incubated with secondary antibodies (1:200 diluted in PBS-4%BSA) for 30 min at room temperature. Nuclei were stained with DAPI (1:1,000 dilution) and actin was stained with phalloidin (1:200 dilution). Coverslips were mounted on microscope slides using Fluoromount-G mounting media (catalog number 0100-01, SouthernBiotech) and were

imaged using SP5 confocal microscope (Leica, Leica Microsystems GmbH, Wetzlar, Germany). Collagen is observed by internal reflection microscopy (IRM). Images were analyzed using ImageJ or Fiji softwares.

Live-cell imaging

Cells were seeded on glass bottom dishes then image acquisitions were performed every 2 min for 4 using LiveSR spinning-disk microscope (Leica, Leica Microsystems GmbH, Wetzlar, Germany) with environmental control at 37°C and CO_2 provider. Z-stacks were performed then deconvolution imaging were used for 3D reconstruction (Imaris software).

Correlative light and electron microscopy (CLEM)

For performing CLEM of invadosome rosettes, we did micro-pattern on ACLAR® films (Catalog number 77850-12, EMS) by the laser microdissection[52]. Solution of gelatin (0.5 mg/mL) was pre-coated on these patterned ACLAR® substrates in a 24-well plate. The lifeact-mRuby expressed NIH-3T3-Src cells were then seeded at 20,000 cells/mL on ACLAR® films and incubated overnight. The film was transferred to a 35mm glass bottom dish (Catalog number P35G-1.0-20-C, MatTek) for confocal imaging (Leica SP2) using a × 63 objective (NA:1.32, Leica Microsystems). Position of the region of interest (ROI) according to the landmarks visible in transmitted light. High-magnification images of the cells and rosettes of interest were acquired as well as low-magnification images. After imaged, cells were fixed in primary fixation buffer contained 2.5% PFA (Catalog number 15713, EMS) and 2.5% GA (Catalog number 16220, EMS) in 0.1M cacodylate buffer (Catalog 11652, EMS) for 1 h at room temperature. Post-fixation was performed in 1% osmium tetroxide (Catalog number 19150, EMS) in 0.1M cacodylate buffer for 1 h on ice. Cells were stained with 2% uranyl acetate, and then dehydrated in sequential gradient alcohol baths and infiltrated with Epon resin. We then inversed the film on the top of the plastic embedding capsule (Catalog number 69910-05, EMS) following overnight polymerization at 60 °C thus embedding the intact cell monolayer of adhesion cells. The following day, the capsules were filled with fresh Epon and polymerized again overnight at 60 °C. Accurate positioning of the ROI can be relocated by a stereomicroscope according to the micro-pattern. Finally, the precise trimmed resin block was done serial sectioning (thickness: 70 nm) and all the sections were collected on slot grids for TEM observation. Micrographs were obtained at transmitted electron microscope (CM12, FEI company) with a CCD camera (ORIUS, Gatan). For the image process, overlay the

fluorescent and the EM images in Fiji, and manually rescale or rotate the data until the cell boundaries align.

Western Blot

Cells were washed once with cold PBS on ice, and then were scraped with RIPA lysis buffer containing phosphatase and protease inhibitor cocltails (catalog number 04906845001, Merck) and lysed for 30 min on ice. Cell lysates were clarified by centrifugation at 13,000g for 15 min at 4°C. Protein concentrations were determined using BCA reagent (DC™ Protein Assay, BioRad), according to the manufacturer's protocol. Lysates were heat at 95°C for 10 min and then separated by SDS-PAGE electrophoresis on 10% acrylamide gels (FastCast™ Acrylamide kit, BioRad) at 110V for 60 min. Samples were transferred onto nitrocellulose membranes using a Transblot transfer system (BioRad) and membranes were blocked using 5%BSA with0.2%Tween (catalog number P7949, Sigma-Aldrich) in TBS buffer (catalog number ET220, Euromedex) for 1 h at room temperature before being incubated with primary antibodies (1:1,000 dilutiond in blocking buffer as described above) overnight at 4°C. The next day, membranes were washed 3 times with TBST and incubated with secondary antibodies (1:5,000 dilution with 5% BSA inTBST) for 30min at room temperature. Membranes were washed 3 times with TBST before exposure using a Chemidoc system (BioRad).

Sunset assay

Cells were treated with puromycin (10mg/ml) during 10min at 37°C then washed twice in ice-cold PBS for protein extraction as described above in Western Blot section. For negative control we pre-treated cells with the translation inhibitor cycloheximide (35mM) during 10min at 37°C.

Immunoprecipitation

For immunoprecipitation experiments, 4.5 million cells were necessary and technical triplicate were performed. NIH-3T3-Src-Tks5-GFP and A431-Tks5-GFP cells were seeded on plastic or in dishes with a fibrillar collagen I matrix. Lysates were centrifuged for 15 min at 13,000g at 4°C and supernatants were immunoprecipitated with the GFP-Trap®_MA kit (Goldstandard) according to the supplier(s) recommendations. The immunoprecipitates were washed three times in lysis buffer, and then assayed using the Lowry method (DC™ Protein Assay kit, Biorad) using a spectrophotometer at 750nm.

Mass spectrometry

The steps of sample preparation and protein digestion by the trypsin were performed as previously described[53]. NanoLC-MS/MS analysis were performed using an Ultimate 3000 RSLC Nano-UPHLC system (Thermo Scientific, USA) coupled to a nanospray Q Exactive Hybrid Quadruplole-Orbitrap mass spectrometer (Thermo Scientific, USA). Each peptide extracts were loaded on a 300 µm ID x 5 mm PepMap C_{18} precolumn (Thermo Scientific, USA) at a flow rate of 20 µL/min. After a 5 min desalting step, peptides were separated on a 75 µm ID x 25 cm C_{18} Acclaim PepMap® RSLC column (Thermo Scientific, USA) with a 4-40% linear gradient of solvent B (0.1% formic acid in 80% ACN) in 108 min. The separation flow rate was set at 300 nL/min. The mass spectrometer operated in positive ion mode at a 1.8 kV needle voltage. Data were acquired using Xcalibur 3.1 software in a data-dependent mode. MS scans (m/z 350-1600) were recorded at a resolution of R = 70000 (@ m/z 200) and an AGC target of 3×10^6 ions collected within 100 ms. Dynamic exclusion of selected precursors was set to 30 s and top 12 ions were selected from fragmentation in HCD mode. MS/MS scans with a target value of 1×10^5 ions were collected with a maximum fill time of 100 ms and a resolution of R = 17500. Additionally, only +2 and +3 charged ions were selected for fragmentation. Other settings were as follows: no sheath and no auxiliary gas flow, heated capillary temperature, 200°C; normalized HCD collision energy of 27% and an isolation width of 2 m/z. Protein identification and Label-Free Quantification (LFQ) were done in Proteome Discoverer 3.0. CHIMERYS node using prediction model inferys_2.1 fragmentation was used for protein identification in batch mode by searching against a Uniprot *Homo sapiens* database (82 439 entries, release March 2023) or a UniProt Mus musculus database (55 029 entries, release March 2023). Two missed enzyme cleavages were allowed for the trypsin. Peptide lengths of 7-30 amino acids, a maximum of 3 modifications, charges between 2-4 and 20 ppm for fragment mass tolerance were set. Oxidation (M) and carbamidomethyl (C) were respectively searched as dynamic and static modifications by the CHIMERYS software. Peptide validation was performed using Percolator algorithm[54] and only “high confidence” peptides were retained corresponding to a 1% false discovery rate at peptide level. Minora feature detector node (LFQ) was used along with the feature mapper and precursor ions quantifier. The normalization parameters were selected as follows: (1) Unique peptides, (2) Precursor abundance based on intensity, (3) No normalization was applied, (4) Protein abundance calculation: summed abundances, (5) Protein ratio calculation:

pairwise ratio based and (6) Missing values are replaced with random values sampled from the lower 5% of detected values. Quantitative data were considered for master proteins, quantified by a minimum of 2 unique peptides and a fold changes ≥ 2.

Inhibition of translation machinery present in invadosomes

A431-Tks5-GFP and NIH-3T3-Src-Tks5-GFP cells were seeded on coverslips coated with gelatin (dots/rosettes) or gelatin and type I collagen (linear invadosomes). The cells were treated with 35µM of translation inhibitor cycloheximide (CHX) (01810, Sigma-Aldrich) or DMSO (control) (D8418, Sigma-Aldrich) 2 h after seeding. For cells seeded on collagen, cells were fixed 4h after seeding. For cells seeded on gelatin, cells were fixed 24 h after seeding by using 4% PFA. The immunofluorescence was performed as previously described. A total of 10 images were performed for each condition using a confocal microscope (SP5, Leica) and experiments were done in three biological replicates. The number of invadosomes were quantified using ImageJ and normalized to the number of nuclei. For Western Blot analysis, cells were seeded on plate and treated with 35µM of cycloheximide (CHX) or DMSO (control) 2h after seeding. Before extraction, cells were treated with Puromycin at a concentration of 10µg/mL. Western Blot was performed as previously described.

Image analysis of fluorescence intensities and area of gelatin degradation

Sterile coverslips were coated with Oregon Green™ 488 conjugated gelatin 488 (catalog number G13186, Thermofisher) for 20 min and fixed with 0.5% glutaraldehyde (catalog number 15960, EMS) for 40 min. Then, the same experiment as described before was performed. Coverslips were imaged under the epifluorescence microscope (Zeiss) using the x 63 oil immersion objective. A total of 15 images were acquired for each condition, and experiments were done in three biological replicates. The area of degradation was quantified using ImageJ and normalized to the number of nuclei in each image.

Statistical analysis

Data are reported as the mean ± SEM of at least three experiments. Statistical significance ($p < 0.05$ or less) was determined using analysis of variance (ANOVA) (one way, two way followed by a Bonferroni's correction), unpaired or paired student t-test as appropriate and performed with GraphPad Prism software. Significance levels are shown as p-values.

Data and material availability

The mass spectrometry proteomics data have been deposited to the ProteomeXchange Consortium via the PRIDE[55] partner repository with the dataset identifiers PXD046512 (NIH cells) and PXD046515 (A431 cells).

References

1. Ferrari, R. *et al.* MT1-MMP directs force-producing proteolytic contacts that drive tumor cell invasion. *Nat. Commun.* **10**, 4886 (2019).
2. Watanabe, A. *et al.* Critical Role of Transient Activity of MT1-MMP for ECM Degradation in Invadopodia. *PLoS Comput. Biol.* **9**, (2013).
3. Fekete, A. *et al.* EGF regulates tyrosine phosphorylation and membrane-translocation of the scaffold protein Tks5. *J. Mol. Signal.* **8**, 8 (2013).
4. Daubon, T., Spuul, P., Alonso, F., Fremaux, I. & Génot, E. VEGF-A stimulates podosome-mediated collagen-IV proteolysis in microvascular endothelial cells. *J. Cell Sci.* **129**, 2586–2598 (2016).
5. Varon, C. *et al.* Transforming Growth Factor β Induces Rosettes of Podosomes in Primary Aortic Endothelial Cells. *Mol. Cell. Biol.* **26**, 3582–3594 (2006).
6. Jerrell, R. J. & Parekh, A. Matrix Rigidity Differentially Regulates Invadopodia Activity Through ROCK1 and ROCK2. *Biomaterials* **84**, 119–129 (2016).
7. Parekh, A. *et al.* Sensing and Modulation of Invadopodia across a Wide Range of Rigidities. *Biophys. J.* **100**, 573–582 (2011).
8. Cannone, S. *et al.* Cancer Associated Fibroblast (CAF) Regulation of PDAC Parenchymal (CPC) and CSC Phenotypes Is Modulated by ECM Composition. *Cancers* **14**, 3737 (2022).

9. Juin, A. *et al.* Discoidin domain receptor 1 controls linear invadosome formation via a Cdc42–Tuba pathway. *J. Cell Biol.* **207**, 517–533 (2014).

10. Iizuka, S. *et al.* Crosstalk between invadopodia and the extracellular matrix. *Eur. J. Cell Biol.* **99**, 151122 (2020).

11. Di Martino, J. *et al.* The microenvironment controls invadosome plasticity. *J. Cell Sci.* **129**, 1759–1768 (2016).

12. Mueller, S. C. *et al.* A Novel Protease-docking Function of Integrin at Invadopodia*. *J. Biol. Chem.* **274**, 24947–24952 (1999).

13. Beaty, B. T. & Condeelis, J. Digging a little deeper: the stages of invadopodium formation and maturation. *Eur. J. Cell Biol.* **93**, 438–444 (2014).

14. Helgeson, L. A. & Nolen, B. J. Mechanism of synergistic activation of Arp2/3 complex by cortactin and N-WASP. *eLife* **2**, e00884 (2013).

15. Di Martino, J. *et al.* Cdc42 and Tks5. *Cell Adhes. Migr*. **8**, 280–292 (2014).

16. Seals, D. F. *et al.* The adaptor protein Tks5/Fish is required for podosome formation and function, and for the protease-driven invasion of cancer cells. *Cancer Cell* **7**, 155–165 (2005).

17. Lock, P., Abram, C. L., Gibson, T. & Courtneidge, S. A. A new method for isolating tyrosine kinase substrates used to identify fish, an SH3 and PX domain-containing protein, and Src substrate. *EMBO J.* **17**, 4346–4357 (1998).

18. Wang, W. *et al.* The Role of TKS5 in Chromosome Stability and Bladder Cancer Progression. *Int. J. Mol. Sci.* **23**, 14283 (2022).

19. Moodley, S., Hui Bai, X., Kapus, A., Yang, B. & Liu, M. XB130/Tks5 scaffold protein interaction regulates Src-mediated cell proliferation and survival. *Mol. Biol. Cell* **26**, 4492–4502 (2015).

20. Buschman, M. D. *et al.* The Novel Adaptor Protein Tks4 (SH3PXD2B) Is Required for Functional Podosome Formation. *Mol. Biol. Cell* **20**, 1302–1311 (2009).

21. Ezzoukhry, Z. *et al.* Combining laser capture microdissection and proteomics reveals an active translation machinery controlling invadosome formation. *Nat. Commun.* **9**, 2031 (2018).

22. Stylli, S. S. *et al.* Nck adaptor proteins link Tks5 to invadopodia actin regulation and ECM degradation. *J. Cell Sci.* **122**, 2727–2740 (2009).

23. Juin, A. *et al.* Physiological type I collagen organization induces the formation of a novel class of linear invadosomes. *Mol. Biol. Cell* **23**, 297–309 (2012).

24. Thuault, S. *et al.* A proximity-labeling proteomic approach to investigate invadopodia molecular landscape in breast cancer cells. *Sci. Rep.* **10**, 6787 (2020).

25. Mader, C. C. *et al.* An EGFR-Src-Arg-cortactin pathway mediates functional maturation of invadopodia and breast cancer cell invasion. *Cancer Res.* **71**, 1730–1741 (2011).

26. Wang, Y. *et al.* ERβ promoted invadopodia formation-mediated non-small cell lung cancer metastasis via the ICAM1/p-Src/p-Cortactin signaling pathway. *Int. J. Cancer* **153**, 1287–1299 (2023).

27. Inoue, H. *et al.* A MAP1B–cortactin–Tks5 axis regulates TNBC invasion and tumorigenesis. *J. Cell Biol.* **223**, e202303102 (2024).

28. Zhao, P. *et al.* The CD44s splice isoform is a central mediator for invadopodia activity. *J. Cell Sci.* **129**, 1355–1365 (2016).

29. Challa, S. *et al.* Ribosome ADP-Ribosylation Inhibits Translation and Maintains Proteostasis in Cancers. *Cell* **184**, 4531-4546.e26 (2021).

30. Shahbazian, D. *et al.* Control of Cell Survival and Proliferation by Mammalian Eukaryotic Initiation Factor 4B. *Mol. Cell. Biol.* **30**, 1478–1485 (2010).

31. Mallawaaratchy, D. M. *et al.* Membrane Proteome Analysis of Glioblastoma Cell Invasion. *J. Neuropathol. Exp. Neurol.* **74**, 425–441 (2015).

32. Pedersen, N. M. *et al.* Protrudin-mediated ER–endosome contact sites promote MT1-MMP exocytosis and cell invasion. *J. Cell Biol.* **219**, e202003063 (2020).

33. Ros, M. *et al.* ER-resident oxidoreductases are glycosylated and trafficked to the cell surface to promote matrix degradation by tumour cells. *Nat. Cell Biol.* **22**, 1371–1381 (2020).

34. Fuentes, L. A., Marin, Z., Tyson, J., Baddeley, D. & Bewersdorf, J. The nanoscale organization of reticulon 4 shapes local endoplasmic reticulum structure in situ. *J. Cell Biol.* **222**, e202301112 (2023).

35. Hwang, Y. S., Park, K.-K., Cha, I. H., Kim, J. & Chung, W.-Y. Role of insulin-like growth factor-II mRNA-binding protein-3 in invadopodia formation and the growth of oral squamous cell carcinoma in athymic nude mice. *Head Neck* **34**, 1329–1339 (2012).

36. Hwang, Y. S., Xianglan, Z., Park, K.-K. & Chung, W.-Y. Functional invadopodia formation through stabilization of the PDPN transcript by IMP-3 and cancer-stromal crosstalk for PDPN expression. *Carcinogenesis* **33**, 2135–2146 (2012).

37. Kim, H.-Y., Ha Thi, H. T. & Hong, S. IMP2 and IMP3 cooperate to promote the metastasis of triple-negative breast cancer through destabilization of progesterone receptor. *Cancer Lett.* **415**, 30–39 (2018).

38. Zagryazhskaya-Masson, A. *et al.* Intersection of TKS5 and FGD1/CDC42 signaling cascades directs the formation of invadopodia. *J. Cell Biol.* **219**, e201910132 (2020).

39. Tu, C. *et al.* Lysosomal cathepsin B participates in the podosome-mediated extracellular matrix degradation and invasion via secreted lysosomes in v-Src fibroblasts. *Cancer Res.* **68**, 9147–9156 (2008).

40. Li, D. *et al.* The lncRNA MIR99AHG directs alternative splicing of SMARCA1 by PTBP1 to enable invadopodia formation in colorectal cancer cells. *Sci. Signal.* **16**, eadh4210 (2023).

41. Chabadel, A. *et al.* CD44 and β3 Integrin Organize Two Functionally Distinct Actin-based Domains in Osteoclasts. *Mol. Biol. Cell* **18**, 4899–4910 (2007).

42. Magnuson, B., Ekim, B. & Fingar, D. C. Regulation and function of ribosomal protein S6 kinase (S6K) within mTOR signalling networks. *Biochem. J.* **441**, 1–21 (2011).

43. Costa, D. S. *et al.* The Caenorhabditis elegans anchor cell transcriptome: ribosome biogenesis drives cell invasion through basement membrane. *Development* **150**, dev201570 (2023).

44. Kreider-Letterman, G. *et al.* ARHGAP17 regulates the spatiotemporal activity of Cdc42 at invadopodia. *J. Cell Biol.* **222**, e202207020 (2022).

45. Badowski, C. *et al.* Paxillin Phosphorylation Controls Invadopodia/Podosomes Spatiotemporal Organization. *Mol. Biol. Cell* **19**, 633–645 (2008).

46. Zeng, H. *et al.* Spatially resolved single-cell translatomics at molecular resolution. *Science* **380**, eadd3067 (2023).

47. Cao, L. *et al.* PIM1 kinase promotes cell proliferation, metastasis and tumor growth of lung adenocarcinoma by potentiating the c-MET signaling pathway. *Cancer Lett.* **444**, 116–126 (2019).

48. Xu, J. *et al.* Long noncoding RNA GMAN promotes hepatocellular carcinoma progression by interacting with eIF4B. *Cancer Lett.* **473**, 1–12 (2020).

49. Liu, T. *et al.* The m6A reader YTHDF1 promotes ovarian cancer progression via augmenting EIF3C translation. *Nucleic Acids Res.* **48**, 3816–3831 (2020).

50. Tang, J. *et al.* The deubiquitinase EIF3H promotes hepatocellular carcinoma progression by stabilizing OGT and inhibiting ferroptosis. *Cell Commun. Signal. CCS* **21**, 198 (2023).

51. Yu, W. *et al.* EIF4A3 Acts on the PI3K–AKT–ERK1/2–P70S6K Pathway through FLOT1 to Influence the Development of Lung Adenocarcinoma. *Mol. Cancer Res.* **21**, 713–725 (2023).
52. Spiegelhalter, C., Laporte, J. F. & Schwab, Y. Correlative Light and Electron Microscopy: From Live Cell Dynamic to 3D Ultrastructure. in *Electron Microscopy* (ed. Kuo, J.) vol. 1117 485–501 (Humana Press, Totowa, NJ, 2014).
53. Henriet, E. *et al.* Argininosuccinate synthase 1 (ASS1): A marker of unclassified hepatocellular adenoma and high bleeding risk. *Hepatology* **66**, 2016 (2017).
54. Käll, L., Canterbury, J. D., Weston, J., Noble, W. S. & MacCoss, M. J. Semi-supervised learning for peptide identification from shotgun proteomics datasets. *Nat. Methods* **4**, 923–925 (2007).
55. Deutsch, E. W. *et al.* The ProteomeXchange consortium at 10 years: 2023 update. *Nucleic Acids Res.* **51**, D1539–D1548 (2022).

Acknowledgments:

The microscopy was done in the Bordeaux Imaging Center a service unit of the CNRS-INSERM and Bordeaux University, member of the national infrastructure France BioImaging supported by the French National Research Agency (ANR-10-INBS-04). The help of Magali Mondin is acknowledged. We are also grateful to platform of the unit TBMCore (US 005), Oncoprot and FACSility (US 005). We also thank Kuang-Jing Huang from U1109 for his help.

Author contributions:

L.N and B.B designed and performed experiments. S.D.T, J.W.D and A.A.R performed and interpreted mass spectrometry analysis. L.M and J.G contributed to CLEM analysis. L.N, B.B, V.M, E.H and FS wrote the manuscript, F.S designed and led the study.

Data Availability:

All data supporting the findings of this study are available from the corresponding author upon reasonable request. The mass spectrometry data are available via ProteomeXchange with the identifier PXD046512 (NIH cells) and PXD046515 (A431 cells). Source data are provided with this paper.

Funding:

Léa Normand was supported by a PhD scholarship from the SIRIC BRIO and the Région. Benjamin Bonnard was supported by the Inca. This work was supported by Fondation Ruban rose, Inca (PLBIO-2020-122) and Ligue contre le cancer (équipe labellisée 2023-DN/IP/IQ 17691).

Figure legends

Figure 1: Invadosome plasticity.
a) Confocal microscopy images of invadosome formation in NIH3T3-Src cells. The cells were seeded on gelatin or type I collagen to form rosettes and linear invadosomes respectively. Tks5 is stained in green, actin in red, nuclei in blue and collagen fibers were imaged by internal reflection microscopy (IRM). Scale bar: 40µm, zoom: 5µm. **b)** Confocal microscopy images of invadosome formation in A431 cells. The cells were seeded on gelatin or type I collagen to formed dots and linear invadosomes respectively. Tks5 is stained in green, actin in red, nuclei in blue and collagen was imaged by internal reflection microscopy (IRM). The arrows show the collagen fibers. Scale bar: 40µm, zoom: 5µm.

Figure 2: Proteomic analysis of Tks5 interactome in invadosomes.
a) Confocal microscopy images of NIH3T3-Src-Tks5-GFP and A431-Tks5-GFP cells. The cells were seeded on gelatin and type I collagen to form invadosomes and stained for Tks5 and GFP. Scale bar: 5µm. **b)** Proteins interacting with Tks5-GFP by co-immunoprecipitation in NIH3T3-Src-Tks5-GFP and A431-Tks5-GFP cells on gelatin and type I collagen. 88 common proteins were identified in every conditions. **c)** List of the 88 commons proteins identified in every conditions. The color codes are in accordance with the table Supp Figure 2c: orange: translation, green: actin cytoskeleton and blue: adhesion. **d)** Bubble plot of the proteins related pathway. **e)** Confocal microscopy images of NIH-3T3-Src and A431-Tks5-GFP cells. The cells were seeded on gelatin or type I collagen and stained for Tks5 in green, actin in red, nuclei in blue and CD44 in grey. Scale bar: 20µm, zoom: 5µm.

Figure 3: The translation machinery is present in all types of invadosomes.
a) Confocal microscopy images of NIH3T3-Src-Tks5-GFP cells. The cells were seeded on gelatin or type I collagen and stained for Tks5 in green, actin in red, nuclei in blue and RPS6 in grey. Scale bar: 40µm, zoom: 10µm. **b)** Confocal microscopy images of A431-Tks5-GFP cells. The cells were seeded on gelatin or type I collagen and stained for Tks5 in green, actin in red, nuclei in blue and RPS6 in grey. Scale bar: 40µm, zoom: 10µm. **c)** Confocal microscopy images of NIH3T3-Src-Tks5-GFP cells. The cells were seeded on gelatin or type I collagen and stained for Tks5 in green, actin in red, nuclei in blue and EIF4B in grey. Scale bar: 40µm, zoom: 10µm. **d)** Confocal microscopy image of A431-Tks5-GFP cells. The cells

were seeded on gelatin or type I collagen and stained for Tks5 in green, actin in red, nuclei in blue and EIF4B in grey. Scale bar: 40µm, zoom: 10µm.

Figure 4: Involvement of the translation machinery in invadosome activity.
a) Quantification of the numbers of invadosomes per cell treated (CHX) or not (DMSO) with cycloheximide in NIH3T3-Src-Tks5-GFP cells seeded on gelatin. Values represent the mean +/- SEM of n=3 independent experiments (10 images per condition and per replicate) and were analyzed using student t-test. **b)** Representative images of the quantification of invadosome formation in NIH3T3-Src-Tks5-GFP cells seeded on gelatin. Tks5 is stained in green and nuclei in blue. Scale bar: 40µm, zoom: 10µm. **c)** Left: Quantification of the ECM degradation properties of A431 and NIH3T3-Src-Tks5-GFP cells on gelatin treated (CHX) or not (DMSO) with cycloheximide. Values represent the mean +/- SEM of n=3 independent experiments (15 images per condition and per replicate) and were analyzed using student t-test. Right: Representative images of the quantification of ECM degradation of A431 and NIH3T3-Src-Tks5-GFP cells on gelatin. Gelatin is stained in green and nuclei in blue. Scale bar: 40µm, zoom: 10µm. **d)** Left: Quantification of the ECM degradation properties of A431 and NIH3T3-Src-Tks5-GFP cells on collagen treated (CHX) or not (DMSO) with cycloheximide. Values represent the mean +/- SEM of n=3 independent experiments (15 images per condition and per replicate) and were analyzed using student t-test. Right: Representative images of the quantification of ECM degradation of A431 and NIH3T3-Src-Tks5-GFP cells on collagen. Gelatin is stained in green and nuclei in blue. Scale bar: 40µm, zoom: 10µm. **e)** Left: Quantification of the ECM degradation properties of A431 and NIH3T3-Src-Tks5-GFP cells on gelatin treated (siEIF4B#1 and #2) or not (siCtrl) with siEIF4B. Values represent the mean +/- SEM of n=3 independent experiments (15 images per condition and per replicate) and were analyzed using student t-test. Right: Representative images of the quantification of ECM degradation of A431 and NIH3T3-Src-Tks5-GFP cells on gelatin. Gelatin is stained in green and nuclei in blue. Scale bar: 40µm, zoom: 10µm. **f)** Left: Quantification of the ECM degradation properties of A431 and NIH3T3-Src-Tks5-GFP cells on collagen treated (siEIF4B#1 and #2) or not (siCtrl) with siEIF4B. Values represent the mean +/- SEM of n=3 independent experiments (15 images per condition and per replicate) and were analyzed using student t-test. Right: Representative images of the quantification of ECM degradation of A431 and NIH3T3-Src-Tks5-GFP cells on collagen. Gelatin is stained in green and nuclei in blue. Scale bar: 40µm, zoom: 10µm.

Figure 5: Recruitment of ER into invadosome rosettes.
a) Representative images from time-lapse video microscopy of lifeact-mRuby (red)-expressing NIH-3T3-Src cells transfected with KDEL-GFP (white). The lifeact-mRuby and KDEL-GFP were measured along the yellow axis. Scale bar: 20µm. **b)** Projection of a z-stacks and Imaris surface 3D renderings are shown, visualizing that KDEL-GFP (green) localizes inside invadosome during maturation. Scale bar: 20µm. **c)** CLEM images of invadosomes of NIH-3T3-Src cells on gelatin matrix. Actin is stained in red. Red arrows show the endoplasmic reticulum. Scale bar: 10µm and 1µm. **d)** Representative images from time-lapse video microscopy of lifeact-mRuby (red)-expressing NIH-3T3-Src cells transfected with KDEL-GFP (white). Intensity level of lifeact-mRuby and KDEL-GFP were measured in initiation step in rosette. Scale bar: 5µm. **e)** Representative images from time-lapse video microscopy of lifeact-mRuby (red)-expressing NIH-3T3-Src cells transfected with KDEL-GFP (white). Intensity level of lifeact-mRuby and KDEL-GFP were measured in maintained and collapsed in rosettes. Scale bar: 5µm. **f)** Projection of a z-stacks and Imaris surface 3D renderings are shown, visualizing that KDEL-GFP (green) escape from invadosome during his collapse. Scale bar: 20µm.

Figure 6: Involvement of ER-associated machinery translation in invadosome formation.
a) Lifeact-mRuby and KDEL-GFP signals were recorded in NIH-3T3-Src cells treated with cycloheximide (CHX; 35µM) at T60 min. Scale bar: 5 µm. **b)** Confocal microscopy images of NIH-3T3-Src and A431 cells. The cells were seeded on gelatin or type I collagen and stained for Sec61 in red, nuclei in blue and Actin in grey. Scale bar: 20µm, zoom: 5µm. **c)** Upper part: Quantification of invadosome formation in A431 and NIH-3T3-Src cells seeded on gelatin or type 1 collagen treated or not (DMSO) with Sec61 translocon inhibitor (ES1) during one hour. Lower part: Representative images of the quantification of invadosomes formation in A431 and NIH3T3-Src-Tks5-GFP cells seeded on gelatin or type 1 collagen treated or not (DMSO) with ES1. The arrows show the invadosomes. Tks5 is stained in green and nuclei in blue. Scale bar: 40µm, zoom: 10µm.

Supp Figure 1: Specific molecular proteins of each invadosomes organization.
a) Western Blot analysis of the co-immunoprecipitation performed with anti-GFP antibodies in NIH3T3-Src-Tks5-GFP cells. The input, the Δ and the co-IP (IP-Tks5-GFP) fractions are shown. **b)** Bubble plot of the proteins related pathway in rosettes. **c)** Classification table of the specific proteins identified in rosette. Proteins are grouped into five main categories corresponding to translation proteins, mitochondrial proteins, ER proteins, proteins of the Golgi apparatus and microtubules proteins. **d)** Bubble plot of the proteins related pathway in dots. **e)** Classification table of the specific proteins identified in dots. Proteins are grouped into five main categories corresponding to translation proteins, mitochondrial proteins, ER proteins, proteins of the Golgi apparatus and microtubules proteins. **f)** Bubble plot of the proteins related pathway in linear invadosomes and classification table of the adhesion proteins specific to linear invadosomes organizations. **g)** Classification table of the specific proteins identified in linear invadosomes. Proteins are grouped into five main categories corresponding to translation proteins, mitochondrial proteins, ER proteins, proteins of the Golgi apparatus and microtubules proteins.

Supp Figure 2: Characterization and validation of proteins identified by mass spectrometry as partner of Tks5.
a) Table of proteins identified by mass spectrometry in at least one type of invadosomes and already identified in the literature as partner of Tks5 in 293T cells (Stylli and *al.*) and MDA-MB-231 cells (Thuault and *al.*). **b)** Confocal microscopy images of A431-Tks5-GFP cells. The cells were seeded on gelatin or type I collagen and stained for Tks5 in green, actin in red, nuclei in blue and MAP4 in grey. Scale bar: 40µm, zoom: 5µm. **c)** Classification table of the 88 common proteins identified. Proteins are grouped into three main categories corresponding to translation, adhesion and actin cytoskeleton. **d)** Table of translation proteins already identified in invadosomes in the literature **e)** Bubble plot of proteins related pathway identified by mass spectrometry thanks to Tks5 and present in data already published by Ezzoukhry and *al.* in rosettes. **f)** Summary table of crossed data obtained by mass spectrometry for the rosettes with the data from Ezzoukhry and *al.* paper.

Supp Figure 3: Translation is not involved on invadosome formation.
a) Quantification of the effect of cycloheximide treatment on A431 and NIH-3T3-Src cells by using puromycin quantification. Values represent the mean +/- SEM of n=4 independent experiments and were analyzed using student t-test. **b)** Relative western blot analysis of puromycin expression for cells treated (CHX) or not (DMSO) with cycloheximide in A431

and NIH-3T3-Src cells seeded on gelatin or collagen. **c)** Quantification of the numbers of invadosomes per cell on gelatin and collagen treated (CHX) or not (DMSO) with cycloheximide in A431-Tks5-GFP and NIH3T3-Src-Tks5-GFP cells. Values represent the mean +/- SEM of n=3 independent experiments (10 images per condition and per replicate) and were analyzed using student t-test. **d)** Representative images of invadosome formation in A431-Tks5-GFP1 and NIH3T3-Src-Tks5-GFP cells seeded on gelatin or collagen. Tks5 is stained in green and nuclei in blue. Scale bar: 40µm, zoom: 10µm. **e)** Western Blot analysis of endogenous EIF4B expression in A431 and NIH-3T3-Src cells transfected using control or EIF4B-targeting siRNA and associated quantification. Stain free was used as the loading control. Values represent the mean of n=4 independent experiments. **f)** Quantification of the numbers of invadosomes per cell on gelatin and collagen silencing (siEIF4B) or not (DMSO) for EIF4B in A431-Tks5-GFP and NIH3T3-Src-Tks5-GFP cells. Values represent the mean +/- SEM of n=4 independent experiments (10 images per condition and per replicate) and were analyzed using student t-test.

Video 1:
Time-lapse video microscopy of lifeact-mRuby (red)-expressing NIH-3T3-Src cells transfected with KDEL-GFP (white).

Video 2:
Time-lapse video microscopy of lifeact-mRuby (red)-expressing NIH-3T3-Src cells transfected with KDEL-GFP (white).

Video 3:
Time-lapse video microscopy of lifeact-mRuby (red)-expressing NIH-3T3-Src cells transfected with KDEL-GFP (white).

Video 4:
Time-lapse of Lifeact-mRuby and KDEL-GFP signals recorded in NIH-3T3-Src cells treated with cycloheximide (CHX; 35µM).

Figure 1 : Invadosomes plasticity.

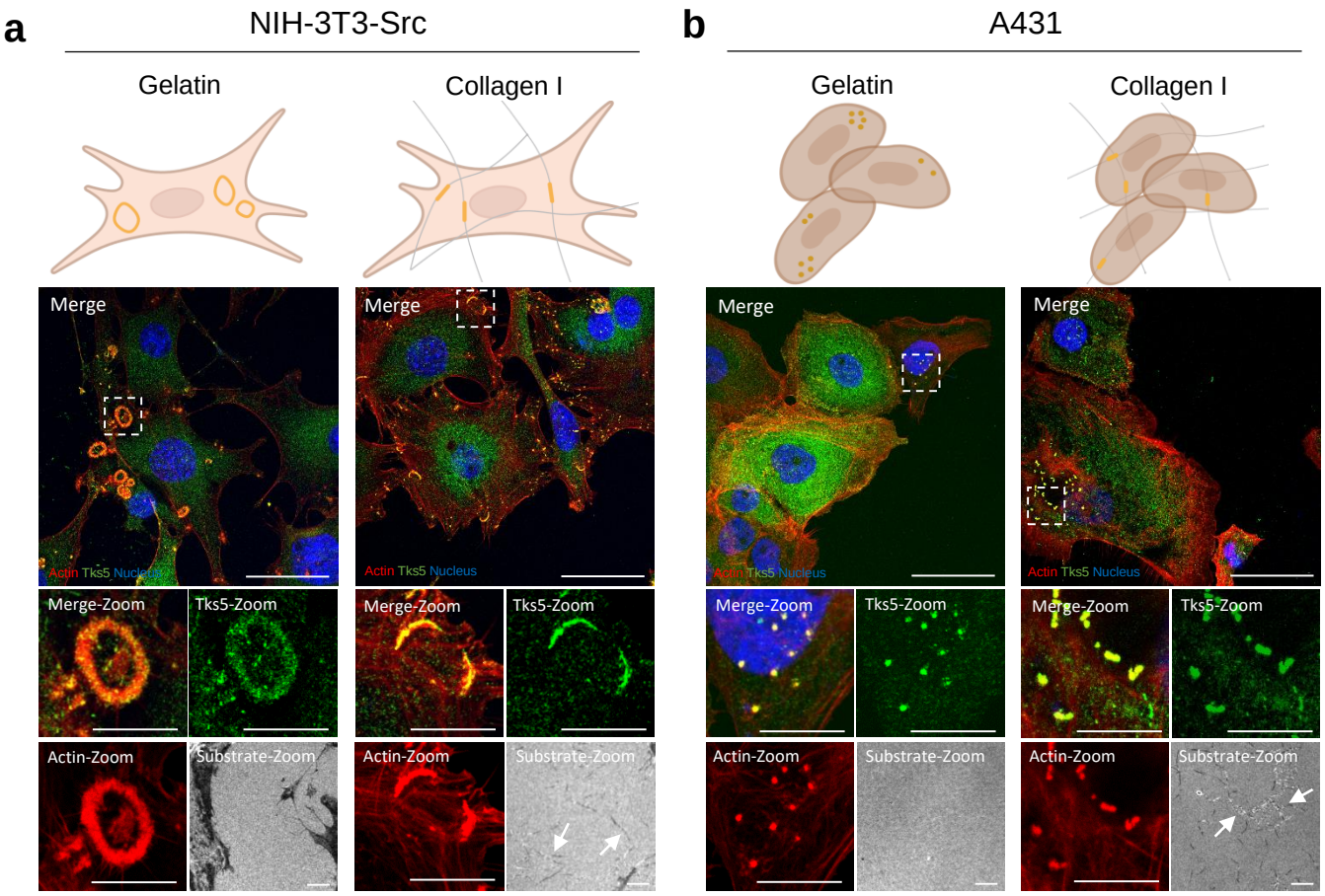

Supp Figure 1: Specific molecular signature of each invadosomes organizations.

a

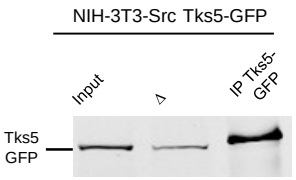

b

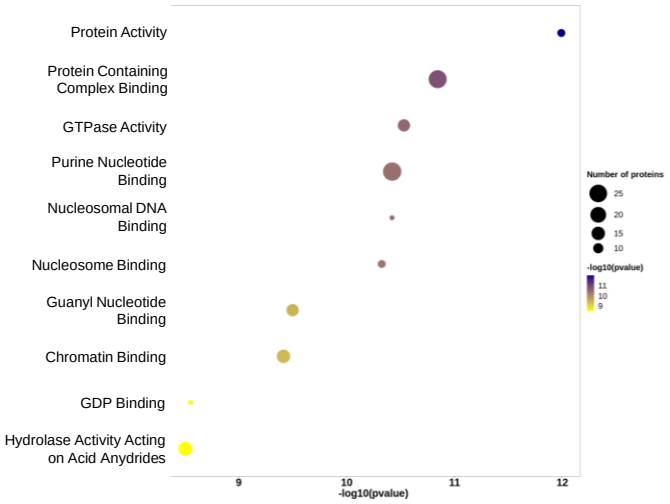

c

List of proteins present in rosettes

Translation proteins (3%)	EIF1A, EIF3S3X, EIF5A, MRPL12, NGDN
Mitochondrial proteins (8%)	AFG3L1, ATAD1, ATP5PB, MRPL12, NDUFV1, NFU1, PGAM5, RDH13, SLC25A4, SLC25A10, SLC29A1, SLC44A2
Endoplasmic reticulum proteins (6%)	CISD2, CNPY2, RAB1A, RAB1B, SEC22B, TMED9, TMX1, UBXN4
Proteins of the golgi apparatus (4%)	RAB1A, RAB1B, RAB6A, SEC22B, TMED9, TMED10
Microtubule proteins	STMN1

d

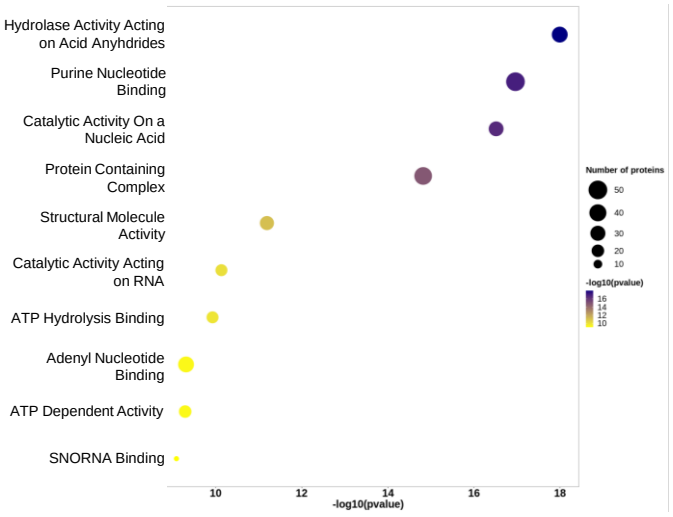

e

List of proteins present in dots

Translation proteins (9%)	BOP1, BRIX1, DDX27, EEFSEC, EIF3CL, EIF3I, EIF6, GNL2, IMP4, LARP4B, MRM3, MRPL2, MRPL15, MRPL37, MRPL47, MRPS12, MRPS15, MRPS23, MRPS34, NOP56, NSUN4, POLDIP3, RPS15, YTHDF1
Mitochondrial proteins (12%)	CHCHD3, CYC1, DIABLO, DRG1, GTF3C4, HK2, HTRA2, IMMT, MCAT, MRM3, MRPL2, MRPL15, MRPL37, MRPL47, MRPS12, MRPS15, MRPS23, MRPS34, NDUFA10, NDUFS2, NIPSNAP1, NSUN4, PRORP, PTPMT1, RAB38, RHOT1, SFXN3, SLC25A3B16, TEFM, VDAC1, VDAC2
Endoplasmic reticulum proteins (9%)	DHCR7, DNAJB11, DNAJC10, DPM1, EMC3, ERLIN2, HTRA2, PIGT, PRKAR2A, PUM3, RCN2, SEC61B, SEC62, SET, SLC35B2, SRP72, STT3A, SURF4, TAP2, TECR, TMCC1, TMEM214, TMX3, TOR1AIP2, UFL1
Proteins of the golgi apparatus (3%)	MGAT1, MYO18A, NSF, PRKAR2A, RAB34, SLC35B2, SURF4, TMEM214
Microtubule proteins (2%)	MARK3, TBCA, TMEM214, TTLL3, TUBB, TUBB4B

f

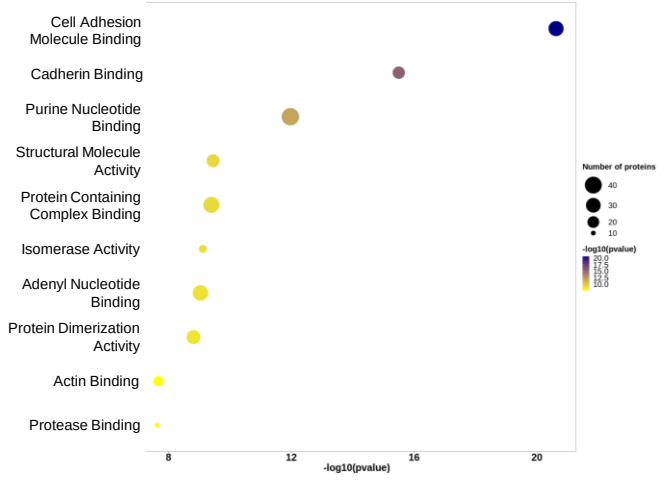

Adhesion proteins (3%)	CCN1, CD34, CD151, DAG1, ECM1, FN1, ITGB1, TSPAN6

g

List of proteins present in linear invadosomes

Translation proteins (5%)	DHX37, EEF1D, EIF2B4, EIF3J2, EIF3L, EIF5, EIF5B, ERAL1, MRPL44, PTCD1, PUM1, PYM1, RPS21, RWDD1
Mitochondrial proteins (9%)	ABCB7, ACADL, AFG3L2, AK4, AK4P3, ATP5MF, CLPX, DHODH, ECHS1, ERAL1, ETFA, ETFB, ETHE1, GFM1, GLUD1, HADH, HMGCL, HSPD1, IDH2, MFN1, MIX23, MRPL44, NDUFA4, PTCD1, PYCR1, TOMM70, YARS2
Endoplasmic reticulum proteins (6%)	ABHD12, ATL2, ATXN2, COPB1, CRELD2, ERAP1, ERLEC1, FKBP9, GOLT1B, HM13, LCLAT1, PIGK, PIGS, PLP2, SACM1L, SEC23IP, SSR1, UFD1
Proteins of the golgi apparatus (5%)	ARFGAP1, ARFIP1, COPB1, CRELD2, FAM20B, GOLGA5, GOLIM4, NSFL1C, STX6, TGOLN2, TMEM87A, USO1, VTI1A, YIPF3
Microtubule proteins (1%)	CEP170, DYNC1H1, MAP1B, MAP6, TACC2

Figure 2 : Proteomic analysis of Tks5 interactome in invadosomes.

a

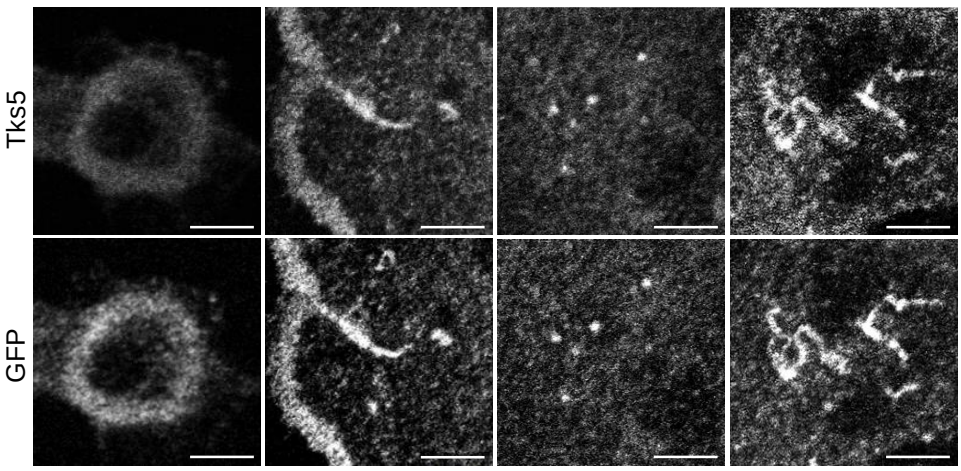

b

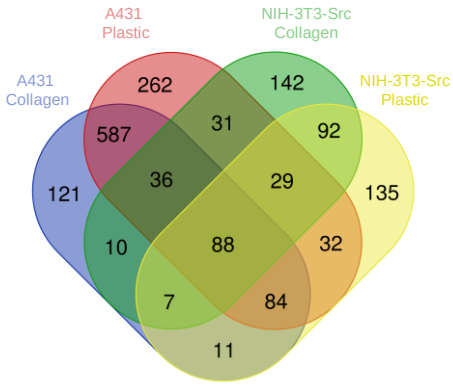

c

List of the 88 common proteins present in every conditions

Not validated in invadosomes
BASP1, BZW2, C1QBP, CLTB, DLD, EIF3A, EMD, GUSB, HNRNPAB, HNRNPU, LAMP2, LARP4, LRRC59, NUFIP2, PPM1G, PRKAG1, PRR2C2, PRRC2A, PSMD7, PUF60, PVR, RPL0, RPL3, RPL4, RPL5, RPL6, RPL7, RPL8, RPL7A, RPL13, RPL14, RPL15, RPL18A, RPL19, RPL29, RPL32, RPL36A, RPS6, RPS6KA4, RPS8, RTN4, RTRAF, SART1, SPATS2, SRSF1, STAU1, TCOF1, YBX1, YWHAB, YWHAE, YWHAG, YWHAH, YWHAQ, YWHAZ
Validated in at least one of the invadosomes organization
ADAM15, ADAM19, ASPH, BAG3, CALD1, CD44, CTTN, EIF4B, FNBP1L, FXR1, G3BP1, HNRNPA1, IGF2BP2, ITGA5, LAMP1, MAP4, MMP14, MYH9, NONO, NPM1, PABPC1, PPP1CA, PRKAA1, PTBP1, RPL10A, RPL34, RPS4X, RRBP1, SH3PXD2A, SSB, STX7, SYNCRIP, THBD, YBX3

d

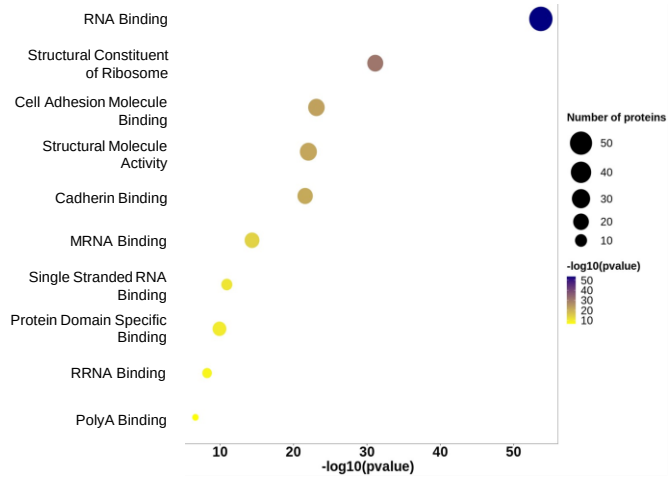

e

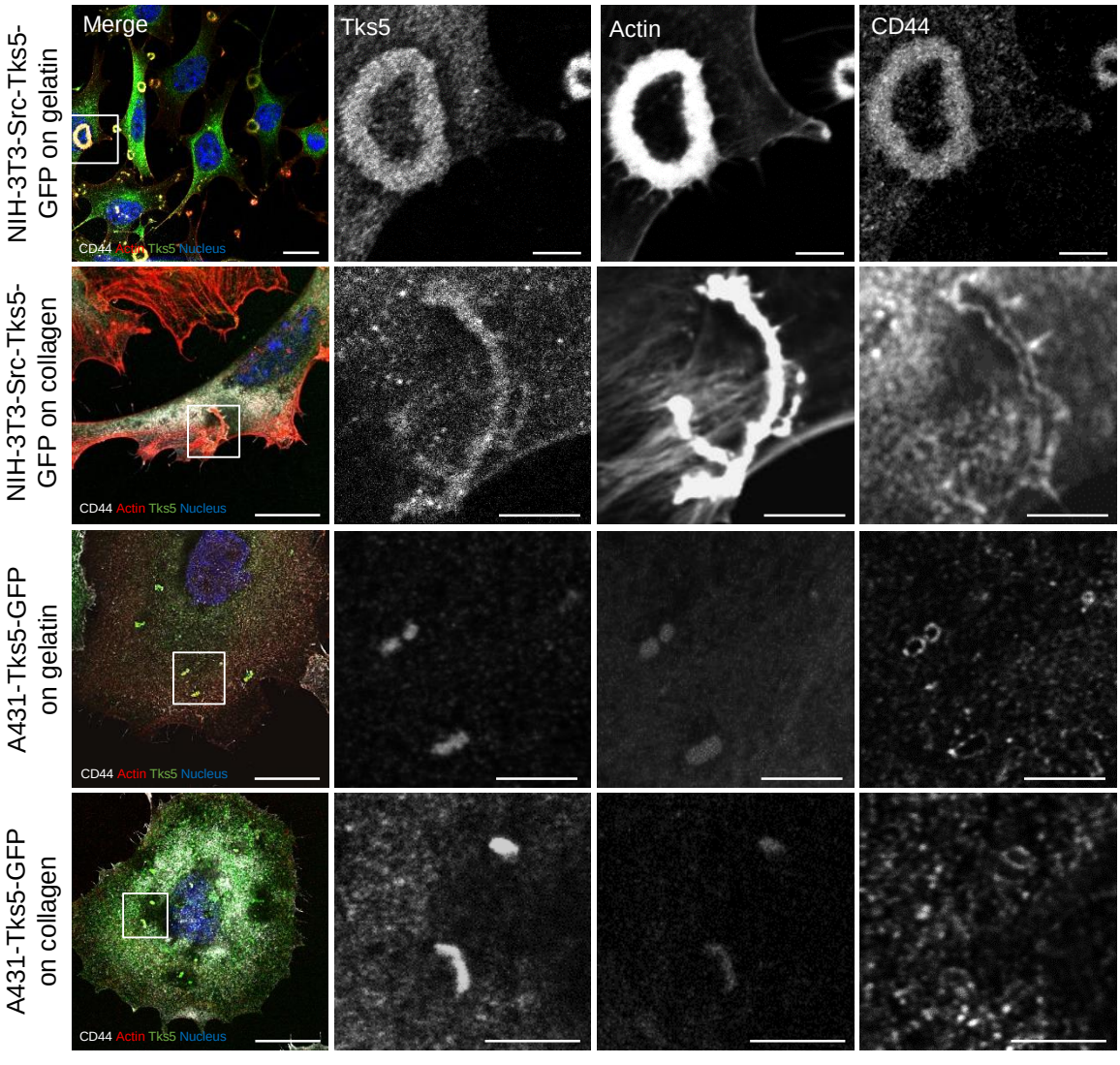

Supp Figure 2 : Characterization and validation of proteins identified by mass spectrometry as partner of Tks5.

a

Proteins	A431 Gelatin	A431 Collagen	NIH-3T3-Src Gelatin	NIH-3T3-Src Collagen
ACTB	X	X		
CRKL	X			
CTTN	X	X	X	X
DBN1			X	X
DDX3X	X	X		
EEF2	X	X		
G3BP1	X	X	X	X
GRB2	X		X	
HNRNPK	X	X		
HSP90B1		X		
MARS1	X	X		
MTHFD1	X	X		
NDRG1	X	X		
NCL	X	X		
PRKAA1	X	X	X	X
PRKAG1	X	X	X	X
RUVBL1	X			
RUVBL2	X			

Stylli and *al.*, 2009

Proteins	A431 Gelatin	A431 Collagen	NIH-3T3-Src Gelatin	NIH-3T3-Src Collagen
ADAM15	X	X	X	X
ARAG	X	X		
CD2AP				X
CTTN	X	X	X	X
DBNL			X	X
EIF2S3	X	X		
EIF4A3	X	X	X	
FGD1	X	X	X	
FNBP1	X	X	X	X
HSPA1B	X	X		
IGF2BP2	X	X	X	X
MAP4	X	X	X	X
NAP1L1	X	X		
NUDT5	X			
PDLIM1				X
PRDX4	X			
RPIA				X
RTN4	X	X	X	X
SH3PXD2A	X	X	X	X
TJP1	X	X		
USP15	X	X		
WASL	X	X		

Thuault and *al.*, 2020

b

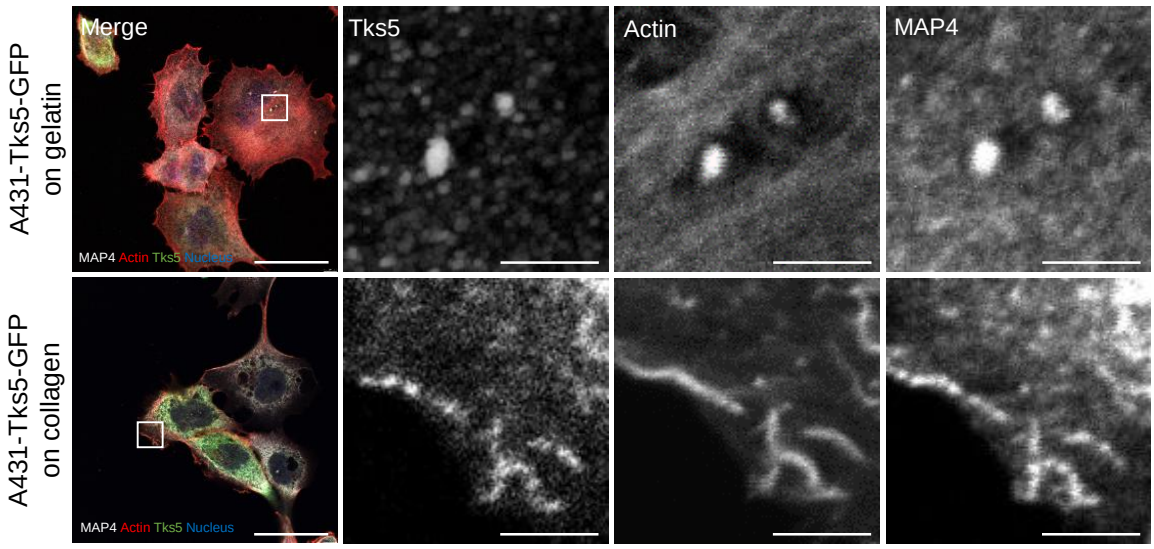

c

Translation	BZW2, EIF3A, EIF4B, FXR1, G3BP1, HNRNPA1, HNRNPAB, IGF2BP2, LARP4, NONO, NUFIP2, PABPC1, PTBP1, PUF60, RPL0, RPL3, RPL4, RPL5, RPL6, RPL7, RPL7A, RPL8, RPL10A, RPL13, RPL14, RPL15, RPL18A, RPL19, RPL29, RPL32, RPL34, RPL36, RPS4X, RPS6, RPS6KA4, RPS8, RRBP1, RTRAF, SPATS2, SRSF1, SSB, STAU1, SYNCRIP, TCOF1, YBX1, YBX3
Actin Cytoskeleton	CALD1, CTTN, EMD, FNBP1L, MYH9,
Adhesion	CD44, ITGA5, PVR
Others	ADAM15, ADAM19, ASPH, BAG3, BASP1, C1QBP, CLTB, DLD, GUSB, HNRNPU, LAMP1, LAMP2, LRRC59, MAP4, MMP14, NPM1, PPM1G, PPP1CA, PRKAA1, PRKAG1, PRR2C2, PRRC2A, PSMD7, RTN4, SART1, STX7, THBD, YWHAB, YWHAE, YWHAG, YWHAH, YWHAQ, YWHAZ

d

Stylli and *al*, 2009	DDX3X, EEF2, HNRNPK, MetRS, NCL
Thuault and *al*, 2020	EIF2S3, EIF4A3, ELP4, ELP6, EPL5, IGF2BP2, MREAA1
Mallawaaratchy and *al*, 2015	EEIF1E1, KARS1, YBX1
Ezzoukhry and *al*, 2018	ANP32A, BTF3L4, CARS, DDX3X, DDX17, EEF1A2, EEF1D, EEF1G, EEF2, EEFA1A, EFTUD2, EIF2A, EIF2S1, EIF3C, EIF3E, EIF3F, EIF3G, EIF3H, EIF3I, EIF3K, EIF3L, EIF3M, EIF4B, EIF5A, ELAVL1, EPRS, FARSA, FXR1, G3BP1, HNNRPF, HNRNPA1, HNRNPA2B, HNRNPC, HNRNPH1, HNRNPK, HNRNPL, HNRNPM, HSP90B1, HSPA5, IGF2BP1, IGF2BP2, IGF2BP3, KHSRP, MYBBPA1, NONO, PA2G4, PABPC1, PLR35A-PS3, PSMC1, PTBP1, RARS, RBM14, RPL10, RPL10A, RPL12, RPL22, RPL23, RPL23-PS3, RPL26, RPL28, RPL30, RPL31, RPL34, RPL35A, RPL36A, RPL37A, RPS3, RPS4X, RPS11, RPS13, RPS14, RPS15A, RPS16, RPS20, RPS26, RPSA, RRBP1, RSP3A, RSP12, RSP19, SERBP1, SF3A1, SF3B3, SNRPA, SRRT, SYNCRIP, TRIM28, YBX3

e

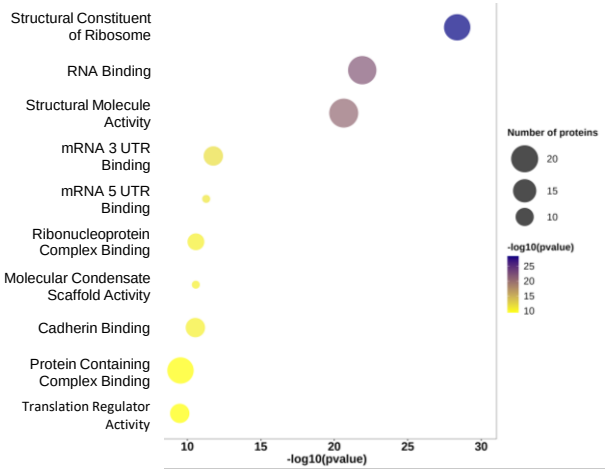

f

Proteins commonly identified in rosettes in Tks5 immunoprecipitation experiment and Ezzoukhry et al. paper
ANP32A, ARPC4, BAG3, CALD1, CAMK2D, CAPRIN1, CHMP4B, CKAP4, CLTA, CTTN, DDX17, DLST, EIF2S1, EIF3C, EIF3H, EIF4B, EIF5A, ELAVL1, FLNB, FUBP1, FXR1, G3BP1, GRPEL1, HNRNPA1, HNRNPH1, HNRNPM, HSPE1, IGF2BP1, IGF2BP2, IGF2BP3, KPNA2, LASP1, MAP4, MYBBP1A, MYEF2, MYH9, MYL6, MYOF, NACA, NONO, NPM1, PABPC1, PABPC4, PPP1CA, PRDX3, PSMA2, PTBP1, PURB, RAB5C, RAB14, RAB21, RPL10A, RPL12, RPL22, RPL23A, RPL28, RPL30, RPL34, RPL35A, RPL37A, RPS3A, RPS4X, RPS11, RPS12, RPS14, RPS15A, RPS19, RPS20, RPS26, RPS27, RRBP1, SFPQ, SNRPA, SRRT, STMN1, SYNCRIP, TARDBP, YBX3

Translation proteins highlighted in red in the table

Figure 3 : The translation machinery is present in all types of invadosomes.

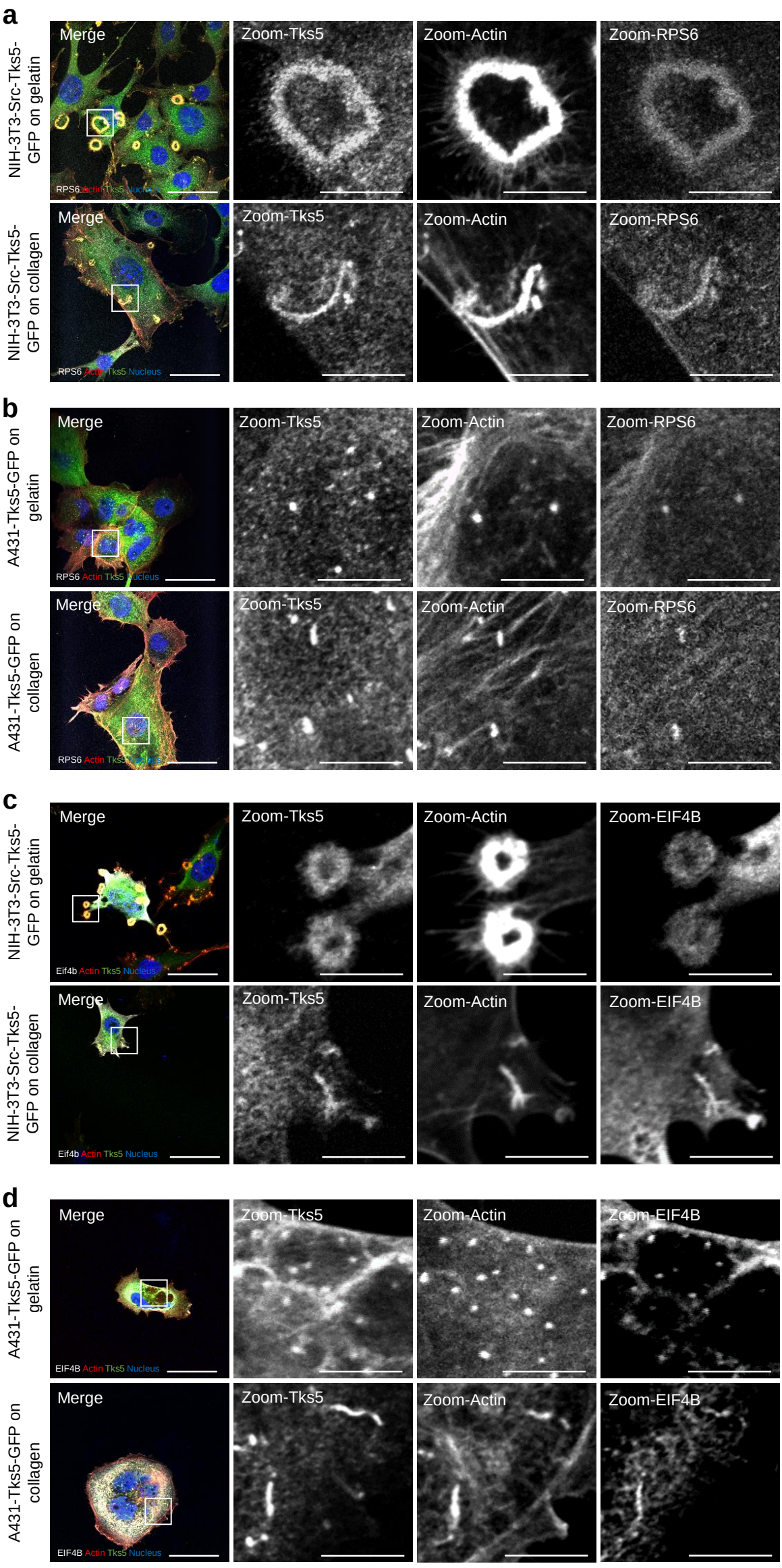

Supp Figure 3: No effect of translation on invadosomes formation.

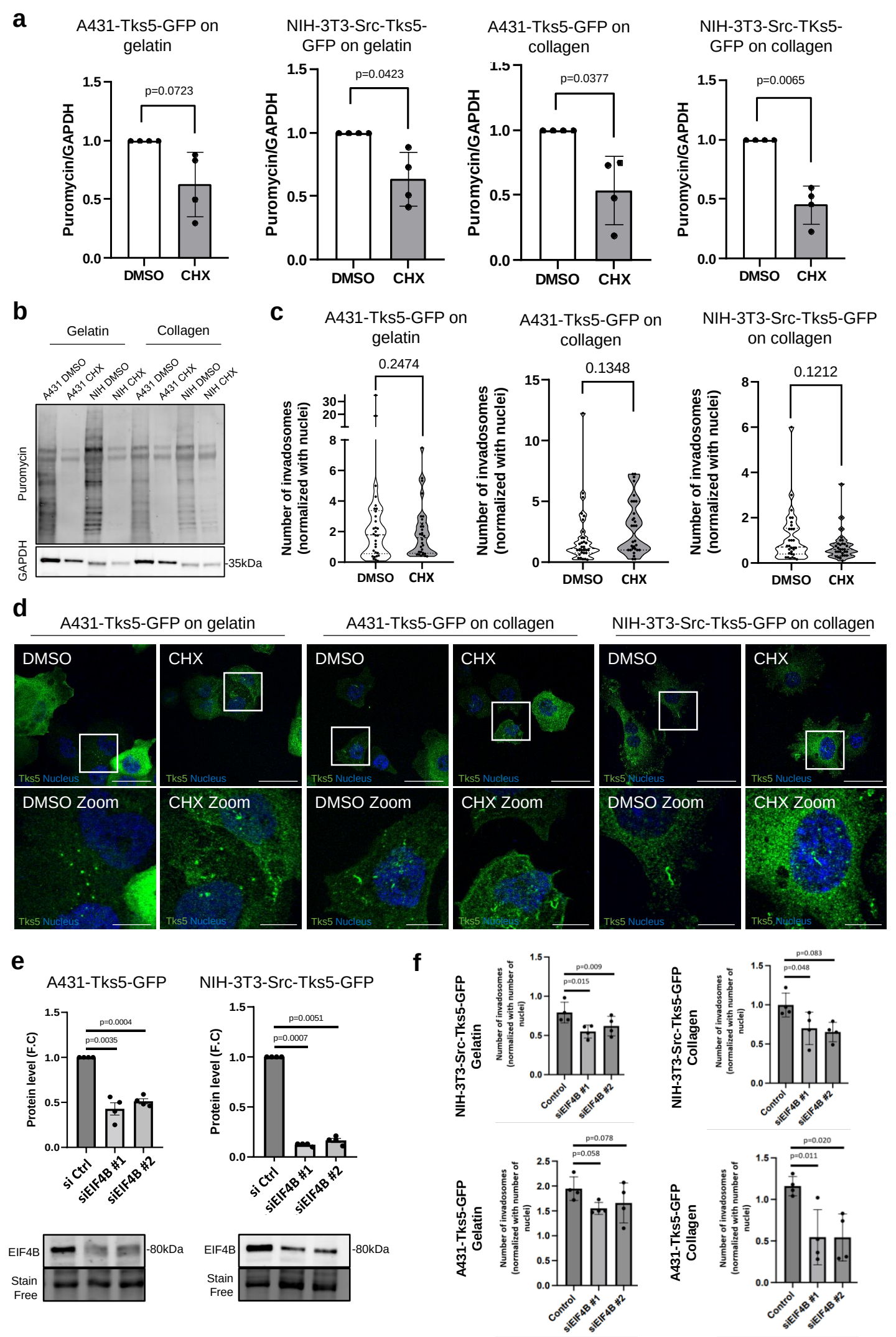

Figure 4 : Involvement of translation in invadosomes function.

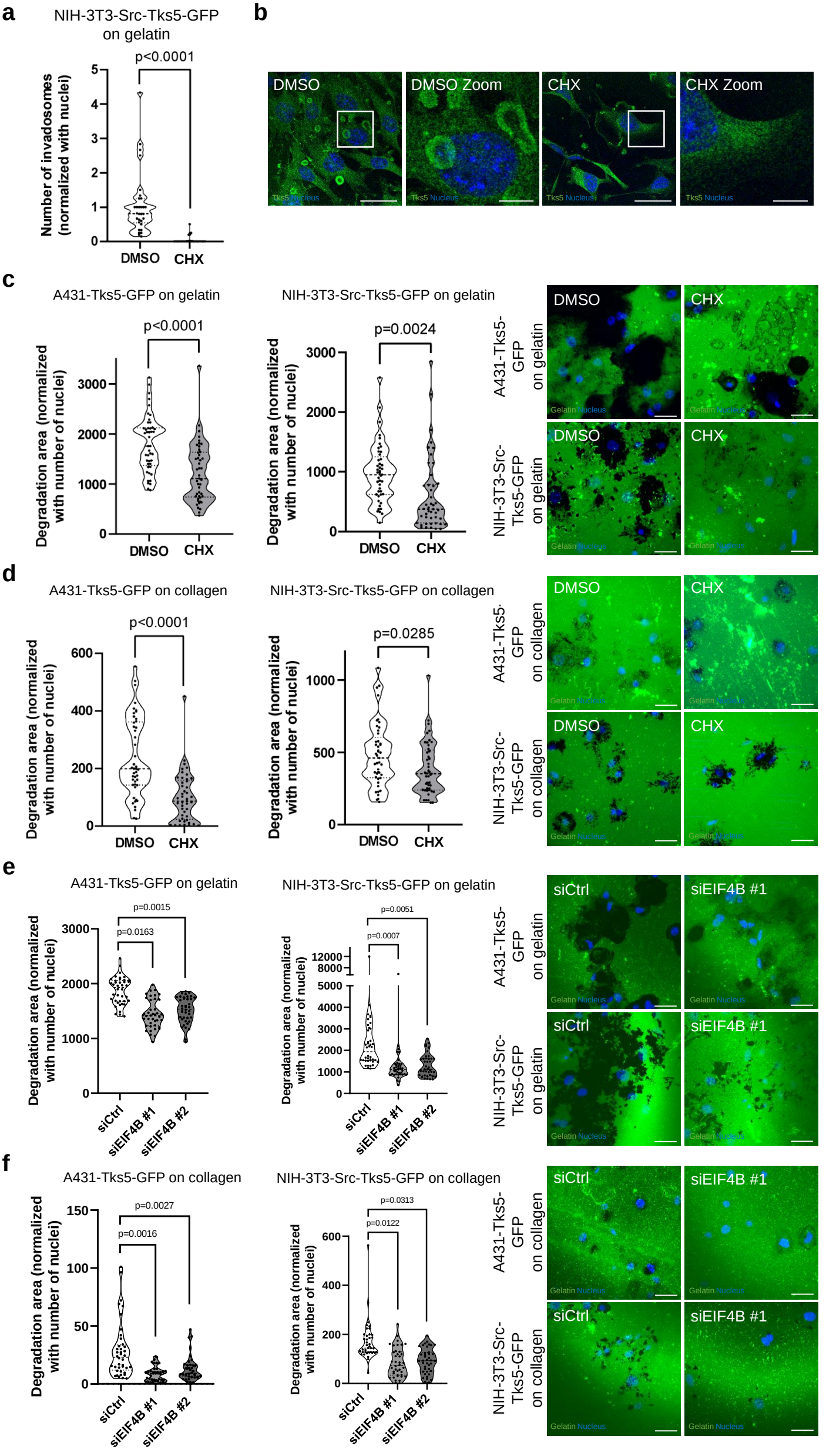

Figure 5 : Recruitment of ER into invadosomes rosettes.

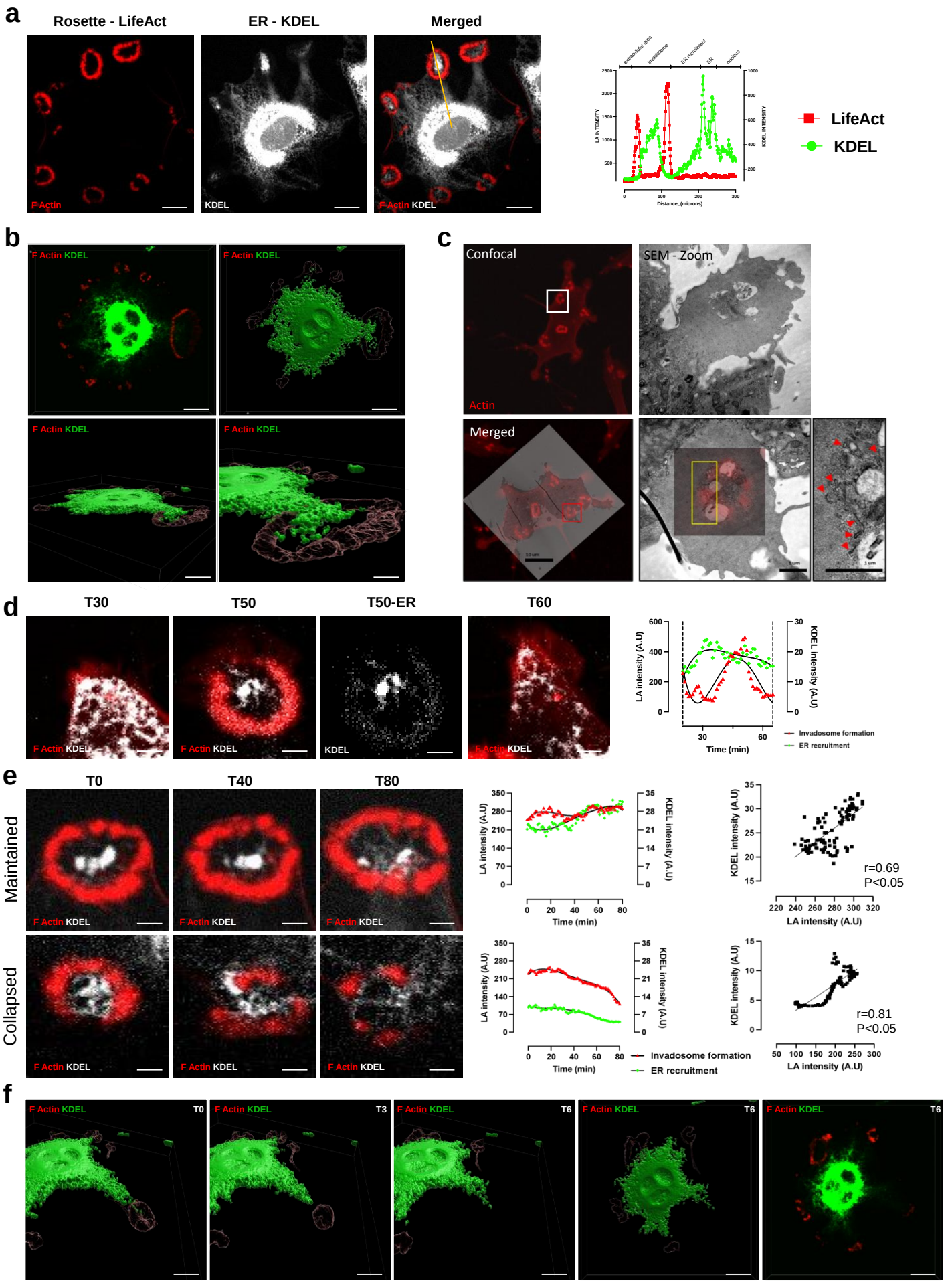

Figure 6 : Involvement of ER-associated machinery translation in invadosomes formation and function**.**

a

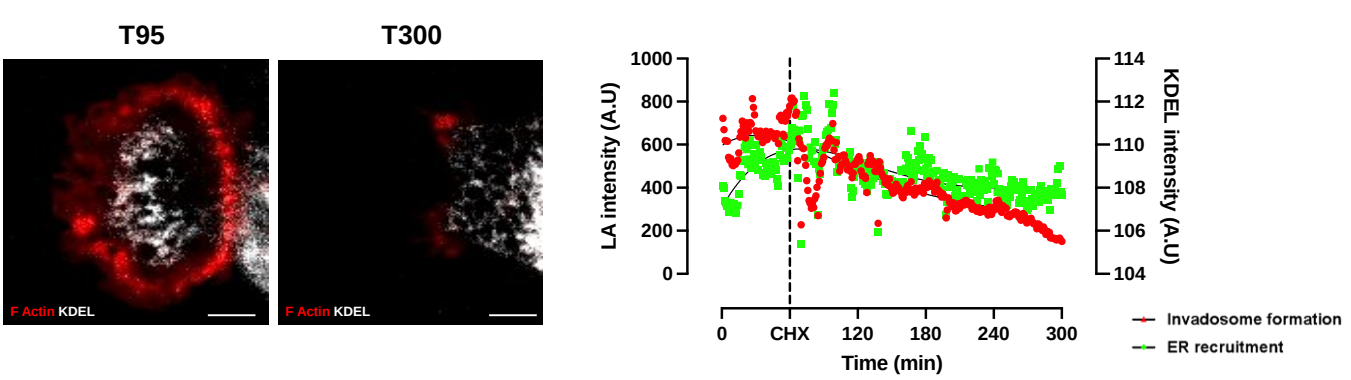

b

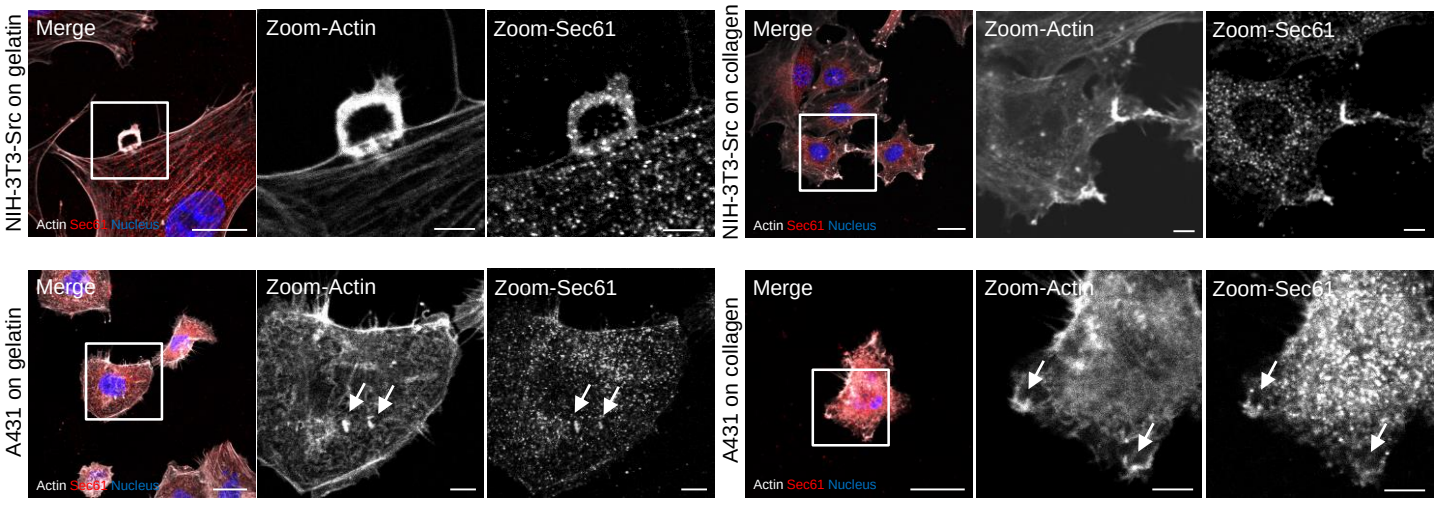

c

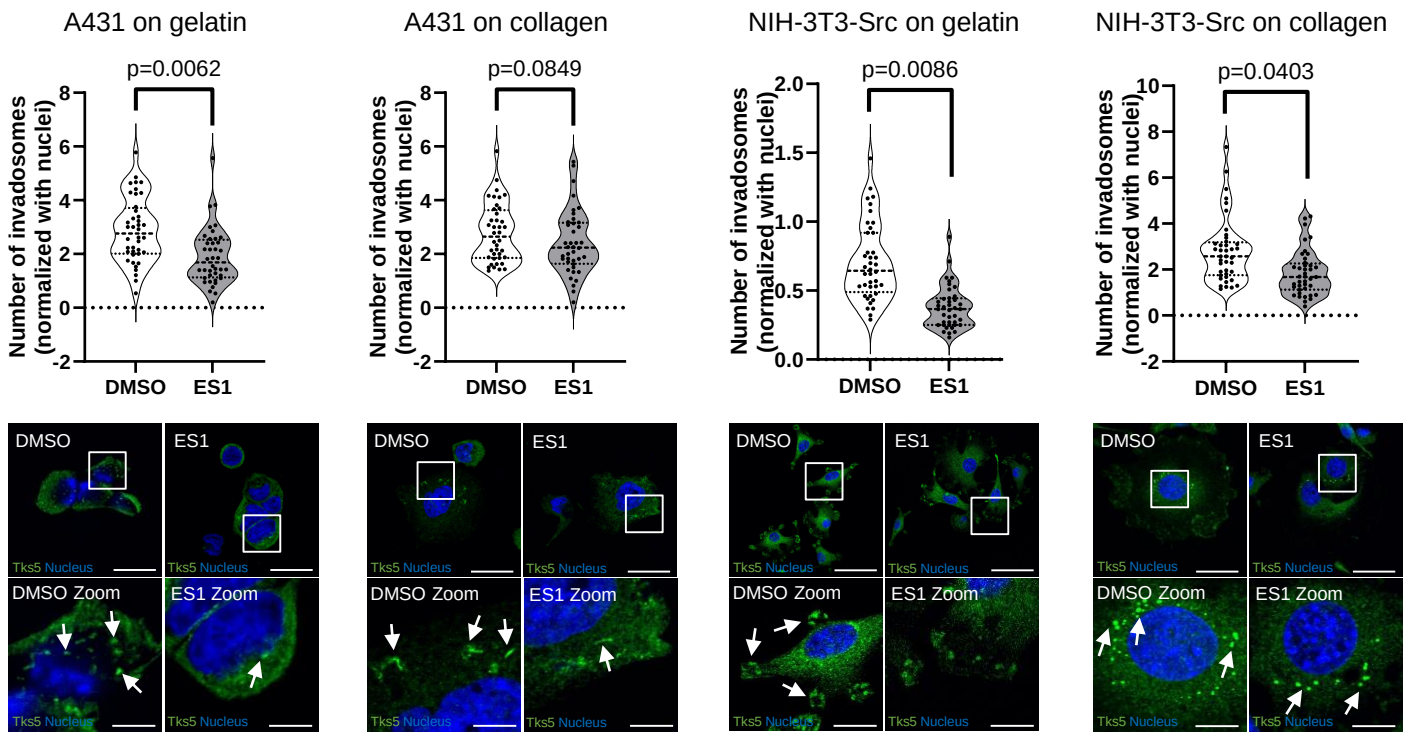

Supplemental table 1 : Summary table of proteins present in invadosomes identified by mass spectrometry analysis of Tks5 interactome

Names	Total	Elements
A431_C A431_P NIH3T3_C NIH3T3_P	88	ADAM15 ADAM19 ASPH BAG3 BASP1 BZW2 C1QBP CALD1 CD44 CLTB CTTN DLD EIF3A EIF4B EMD FNBP1L FXR1 G3BP1 GUSB HNRNPA1 HNRNPAB HNRNPU IGF2BP2 ITGA5 LAMP1 LAMP2 LARP4 LRRC59 MAP4 MMP14 MYH9 NONO NPM1 NUFIP2 PABPC1 PPM1G PPP1CA PRKAA1 PRKAG1 PRRC2A PRRC2C PSMD7 PTBP1 PUF60 PVR RPL3 RPL4 RPL5 RPL6 RPL7 RPL7A RPL8 RPL10A RPL13 RPL14 RPL15 RPL18A RPL19 RPL29 RPL32 RPL34 RPL36 RPLP0 RPS4X RPS6 RPS6KA4 RPS8 RRBP1 RTN4 RTRAF SART1 SH3PXD2A SPATS2 SRSF1 SSB STAU1 STX7 SYNCRIP TCOF1 THBD YBX1 YBX3 YWHAB YWHAE YWHAG YWHAH YWHAQ YWHAZ
A431_P NIH3T3_C NIH3T3_P	29	ALYREF BCAP31 CAV2 CCDC47 CD9 CHMP4B DLST DNAJC5 FUBP1 FUS GOLM1 HPRT1 ITGA3 LASP1 MANF NACA NHERF1 PCNP PPP1CB PPP1R12A PRDX3 PRKCSH RCN1 RCN3 RPS17 SNAP23 SOD2 SRSF5 ZRANB2
A431_C NIH3T3_C NIH3T3_P	6	CLTA EEA1 EIF3C P4HB SMNDC1 SRSF2
A431_C A431_P NIH3T3_P	84	ACSL4 AIFM1 AP2A1 AP2A2 AP2B1 AP2M1 ARHGEF40 CAPRIN1 CCDC86 CD47 CELF1 CKAP4 CSDE1 DARS1 DDX1 DDX5 DDX17 DHX15 EBNA1BP2 EIF2S1 EIF3H EIF4A3 EIF4E EXOSC9 FAU FBXO3 FGD1 FLNB FXR2 GTPBP4 H1-0 HNRNPA0 HNRNPH1 HNRNPM HNRNPUL1 IGF2BP3 ILF2 KHDRBS1 KRT6A LARP1 LARS1 MIB1 MOGS MRTO4 MYL6 MYO1E MYOF NCBP1 NIPSNAP2 NSDHL PABPC4 PAK1IP1 PCDH1 PRKAB1 PRKRA PURA PURB QARS1 RBM17 RCC2 RFC4 RPL12 RPL22 RPL28 RPL30 RPL35A RPL37A RPS3A RPS11 RPS12 RPS19 RPS26 RPS27 SEC63 SFPQ SLC25A13 SMC4 SNRPA1 SQOR TARDBP TMOD3 U2AF2 UPF1 ZC3HAV1
A431_C A431_P NIH3T3_C	36	ACOT9 ATXN2L BSG CALR CCT2 CDK1 CS CYB5R3 CYCS EIF4G1 ERO1A H1-5 HNRNPA2B1 HSD17B10 HSD17B12 HYOU1 KTN1 LGALS3 LUZP1 MAP7D1 MSN MTDH NPTN RAB11FIP1 RPL18 RPS2 SEPTIN2 SEPTIN9 SERPINH1 SF3B2 SH3KBP1 TFG TOR1AIP1 TPM1 TTC1 ZC3H15
NIH3T3_C NIH3T3_P	92	ACIN1 ACP2 ALCAM ANP32A APOBR ARGLU1 ARID1A ARPC4 BCLAF1 BIN1 BRI3BP BTF3 CAST CCDC9 CCDC124 CD63 CD81 CDH2 COLEC12 CSTF2 DBN1 DBNL DDX46 DEK DNAJC8 EEF1B EIF4H ELOB EMB EPB41L2 FKBP3 FKBP10 FXYD5 GM45713 GSR GTF2F1 H1-2 HDGF HDGFL2 HMBS HSPE1 IGF2BP1 IWS1 LGALS1 LRPAP1 MAGEA13 MAP1A MARCKS MXRA7 NES NOLC1 NPC2 NUCB1 NUCKS1 NUP50 PACSIN2 PAKAP PEX19 PGRMC1 PGRMC2 PHACTR4 PLIN3 PMF1 PPP1R18 PPP4R2 PTGES RAB11FIP5 REEP5 RHOC RPL10L RPL17 RTN3 S100A11 SARNP SGTA SIRPA SLC2A1 SNAP29 SOD1 SPARC SRSF7 THRAP3 TP53BP1 TPBG TPR TSPAN3 TXN UBAP2 UBAP2L UBQLN4 VTI1B WASHC2
A431_P NIH3T3_P	32	CDK11B CFL1 CSNK2B DDX56 DKC1 ELAVL1 G3BP2 GRB2 GRPEL1 H1-4 HP1BP3 LEMD2 NAT10 NOC4L NUDT21 OCIAD1 PRC1 PSMB2 RAB10 RAB21 RALB RPL23A RPLP2 RPS5 RPS7 RPS14 RPS20 RPS28 RRP1 RTCA SF1 UTP14A
A431_C NIH3T3_P	11	ESYT2 FMR1 GOT2 KRT16 MAN2A1 PDCD10 PSME2 RPS15A SNRPB2 SQSTM1 SRRT
A431_P NIH3T3_C	31	CALU CAPZB CDV3 CLINT1 CNPY3 DDRGK1 EFHD2 EWSR1 HNRNPA3 LNPEP MAPRE1 MYH10 NUCB2 NUDC PAWR PEX14 PFN1 PSAP PSME1 RAD23B RANGAP1 RPS24 SCAMP1 SERBP1 SERPINC1 SLC44A1 SNX1 STX4 STX12 TPM4 TWF1
A431_C NIH3T3_C	10	ARFGAP1 COL1A1 ECE1 FAM177A1 HADH KRT1 PCYOX1 PDLIM5 PLXNB2 SCP2
A431_C A431_P	587	AAAS ABCF1 ABHD10 ABI1 ABO ACAD9 ACADVL ACBD3 ACOT8 ACSL3 ACTBL2 ACTG1 ACTN1 ACTN4 ACTR2 ACTR3 ADAM10 ADAMTSL4 ADAR ADPGK AFAP1L2 AGK AHCYL1 AIFM2 AIMP1 AIMP2 AK2 AKAP12 ALDH1A3 ALDH3A2 AMY1A ANXA1 APMAP ARAF ARCN1 ARHGAP1 ARHGEF2 ARL6IP5 ARPC2 ASAH1 ASCC1 ASCC2 ASCC3 ATAD3A ATL3 ATP1A1 ATP2A2 ATP2B4 ATP5F1A ATP5F1C ATXN10 BAG4 BAIAP2L1 BCL2L13 BUB3 BYSL C1orf226 C6orf132 C7orf50 C8orf33 CAD CAND1 CANX CAPN1 CAPZA1 CAPZA2 CAVIN1 CAVIN3 CBLB CCNK CCT3 CCT4 CCT6A CCT7 CCT8 CD82 CDC5L CDC42EP1 CDCP1 CDH1 CDH3 CDK9 CDK13 CENPB CEP170B CGAS CHCHD2 CKAP5 CKMT1A CLP1 CLTC CMAS CNP COL17A1 COLGALT1 COPA COPB2 COPE COPG1 CORO1C CPNE1 CPOX CPSF6 CPSF7 CPT1A CRYBG1 CSNK1A1 CSNK2A1 CTNNA1 CTNNB1 CTNND1 CTPS1 CTSB CTSD CUL7 CYB5R1 CYFIP1 CYP2S1 DAP3 DAPK3 DCAF5 DDB1 DDOST DDX3X DDX6 DDX21 DDX24 DDX39B DDX47 DDX55 DDX60 DECR1 DHCR24 DHRS7 DHX9 DHX30 DHX36 DHX57 DIMT1 DNAJA2 DNAJA3 DNAJB12 DNAJC13 DTX3L ECH1 EDC4 EEF2 EGFR EHD2 EHD4 EIF2AK2 EIF2S2 EIF2S3 EIF3B EIF3E EIF3F EIF3G EIF3J EIF4A1 EIF4A2 EIF4G2 ELAVL2 EMC1 EMC2 EPHA2 EPRS1 ERBIN ERGIC1 ERGIC3 ERMP1 ERP29 ERP44 ESRP1 ESYT1 EXOSC2 EXOSC5 EXOSC10 F11R FAF2 FAM3C FAM83A FAM91A1 FAM98A FAM98B FAM120A FAR1 FBXO22 FH FHL2 FHL3 FIP1L1 FLII FLNA FLOT1 FNBP1 FNDC3B GAA GALNT2 GALNT3 GANAB GBA1 GEMIN4 GET3 GIPC1 GLG1 GLS GMPS GNL3 GNL3L GOLGA2 GOLGA4 GPD2 GRB7 GRSF1 GRWD1 GSN GTF3C2 H1-10 HACD3 HADHA HADHB HARS1 HDAC6 HECTD1 HELZ2 HLA-A HLA-B HMOX2 HNRNPC HNRNPD HNRNPF HNRNPK HNRNPR HNRNPUL2 HSD17B4 HSDL2 HSP90B1 HSPA1B HSPA2 HSPA5 HSPA8 HSPB1 HSPH1 IARS1 ICAM1 IDH3B IFI16 IKBIP ILF3 INF2 INPP5K IPO5 IQGAP1 ISG20L2 ITCH ITGA2 ITGAV ITGB6 IVL KARS1 KCTD12 KIAA0930 KIAA1522 KIF2A KPNB1 KRT6B KRT8 KRT17 KRT18 L1RE1 LACTB LAMA3 LAMB3 LAMC2 LANCL2 LCN2 LETM1 LGALS3BP LIMA1 LMAN1 LMAN2 LPCAT2 LRPPRC LRRC1 LRRC8A LSG1 LSR LUC7L2 MACF1 MAGEA4 MAGED2 MAN1B1 MAOA MAP7 MARK2 MARS1 MAVS MBOAT7 MCM5 MDH2 MFAP1 MICAL2 MIOS MLEC MORC2 MOV10 MRPL4 MRPS2 MRPS5 MRPS7 MRPS9 MRPS18B MRPS22 MRPS27 MRPS31 MRPS35 MSH2 MSH6 MTHFD1L MTHFD2 MTPAP MTREX MVP MX1 MYCBP2 MYO1B MYO1C MYO1D MYO5A MYO5B MYO6 NAGK NAP1L1 NCEH1 NCKAP1 NCL NCLN NCSTN NDRG1 NECTIN4 NIT2 NKRF NMNAT1 NOMO1 NOP2 NRDC NSUN2 OAS2 OAS3 OASL OAT OPA1 OSBPL8 OTUB1 P4HA2 PA2G4 PACSIN3 PARP1 PARP9 PARP12 PARS2 PBXIP1 PC PCBP2 PCYT1A PDIA3 PDIA4 PDIA5 PES1 PFKM PFKP PHLDA1 PIP5K1A PISD PKP3 PLBD2 PLEKHA5 PLOD1 PLOD2 PLOD3 PLRG1 PLSCR1 PML POLRMT PON2 POP1 POR PPFIA1 PPFIBP1 PPIB PPP2CA PPP2R1A PRKAB2 PRKAG2 PRKDC PRMT1 PRMT5 PRPF3 PRPF19 PSMA4 PSMC2 PSMC5 PSMD2 PSMD3 PSMD8 PSMD11 PTCD3 PTDSS1 PTGES2 PTGS1 PTPN1 PTPN6 PWP1 QSOX1 RAB3GAP1 RAB3GAP2 RACK1 RAE1 RARS1 RASAL2 RBM4 RBM14 RBM28 RBM39 RCL1 RDH11 RECQL RETSAT RFC2 RFC3 RFC5 RHOT2 RIOX2 RNH1 RPL9 RPL10 RPL11 RPL13A RPL17-C18orf32 RPL21 RPL23 RPL24 RPL26 RPL27 RPL27A RPL31 RPL35 RPN1 RPN2 RPS3 RPS9 RPS13 RPS16 RPS18 RPS23 RPS25 RPSA RTCB SART3 SCAMP2 SCARB2 SCFD1 SCRIB SDC4 SDHA SEC16A SEC23A SEC23B SEC24C SEC61A1 SEMA3C SERPINB1 SERPINB2 SERPINE1 SFN SGPL1 SH3BP4 SHMT2 SLC3A2 SLC7A5 SLC16A3 SLC25A22 SLC25A24 SLC27A4 SLFN5 SMAD3 SMC1A SND1 SNX9 SPATS2L SPINT1 SPOCD1 SPTAN1 SPTBN1 SPTLC1 SPTLC2 SRP54 SRP68 SRPK1 SRPRA SRPRB SRRM2 STAU2 STIM1 STOM STRAP SUMF2 SUPT16H SVIL TACSTD2 TAP1 TAPBP TARS2 TBL2 TCP1 TFAM TFB1M TFB2M TFRC TGFBI THBS1 THSD4 TIMM44 TIMM50 TJP1 TM9SF2 TM9SF4 TMCC3 TMEM43 TMPO TMTC3 TNFAIP2 TNKS1BP1 TOE1 TOP1 TOR4A TRABD TRAF7 TRAM1 TRAP1 TRIM25 TRIM28 TRIM32 TRIM56 TRIP4 TRIP10 TRMT1L TRMT2A TRMT6 TRMT10C TSPYL1 TUBB6 TUFM TUT7 U2SURP UBR4 UBTF UGGT1 UQCRC2 USP7 USP9X USP15 USP34 VAPA VAPB VAT1 VCP VDAC3 VPS26A WASL WDR1 WDR5 WDR12 WDR26 WDR82 WIPF2 XPO1 XRCC5 XRCC6 XRN1 XRN2 YTHDC2 YTHDF2 ZC3H18 ZFPL1 ZMPSTE24 ZNF385A
NIH3T3_P	135	36951 5031439G07RIK ABCB1B AFG3L1 AGO3 AK1 ANAPC1 API5 AQP1 ARF2 ARF4 ARL1 ATAD1 ATP5PB AURKB BAG2 BLVRB CAMK1 CAMK2D CBX3 CD2BP2 CDC40 CDK6 CHD4 CIAPIN1 CISD2 CNPY2 CPSF1 CSTF3 CTDSPL2 CYB5B DCAF13 DNMT1 EIF1A EIF2S3X EIF5A FAM32A GLYR1 GM20521 GNS GSTO1 HDAC1 HDAC2 HINT1 HIRIP3 HMGA2 HS2ST1 IAP IFI202 IFITM3 KPNA2 KPNA6 LAMC1 LMNB2 MACROH2A2 MRPL12 MSI2 MTA2 MYADM MYBBP1A MYEF2 NDUFV1 NFU1 NGDN NOTCH2 NRD1 NUP93 NUP107 NUP160 OTUD4 PAFAH1B3 PCM1 PDLIM7 PGAM5 PHC2 PNO1 POLR2E PRDX6 PRKAR2B PRPF4 PRPF6 PRPF31 PRPF40A PRPSAP1 PSMA2 PTBP2 PTPRE RAB1A RAB1B RAB5A RAB5C RAB6A RAB7A RAB11B RAB14 RAC1 RAD21 RALA RANBP1 RBM19 RBMS1 RDH13 RPA1 RRAS2 S100A4 SCML2 SEC22B SH3PXD2B SLC25A4 SLC25A10 SLC29A1 SLC44A2 SLTM SMARCC2 SMARCE1 SMCHD1 SNRNP40 SNRPA SRSF3 ST13 STAG1 STEAP3 STMN1 SYNE3 TMED9 TMED10 TMX1 UBE2L3 UBXN4 UTP3 UTP6 WDR33 YTHDF3 ZFAND6 ZFR
NIH3T3_C	142	2900026A02RIK 8030462N17RIK ACADL AFDN AHNAK2 AK4 ALAD ANLN ANP32E ANXA5 APOA1 ATF7IP ATXN2 BOD1L BSDC1 CAV1 CAVIN2 CCDC50 CD2AP CD34 CD151 CD200 CDC37 CEP170 CFDP1 CNPY4 COBLL1 COL1A2 CRELD2 CSF1 D17H6S53E DAD1 DAG1 DHODH DIDO1 EEF1D EFCAB14 EHD1 EIF3J2 EIF5B EPB41L3 FKBP7 FKBP9 FSTL1 FTL1 FTSJ3 GOLGA5 GOLIM4 GOLT1B GOT1 GRN HAL HEXIM1 HMGN5 HSPA13 IDI1 IRF2BP2 ITGB1 JPT2 KCNAB2 KCT2 KRT76 KRT78 LIG1 LRRFIP1 LRRFIP2 LSM14A LSS LTBP1 LTBP3 MAP1B MAP6 MARCKSL1 MCL1 MDC1 MIX23 NECTIN1 NECTIN3 NRADD NSFL1C PALM PARK7 PDAP1 PDLIM1 PDPN PGAM1 PGM1 PLAUR PLP2 PPP1R7 PPP1R11 PRRC2B PSIP1 PSMD4 PSME3 PTTG1IP PYM1 RABL6 RAD23A RAET1A RANBP3 RPIA RPS21 RSU1 RWDD1 SAFB2 SCPEP1 SEPTIN11 SERPINB6A SERPINF1 SF3B1 SFR1 SGSH SLC12A2 SNW1 SOX9 SPECC1 SPP1 SSR1 STX8 SUPT5H TACC2 TALDO1 TEX101 TGOLN2 TNFRSF10B TPD52L2 TPM3 TSPAN6 TTN TXNDC15 UBQLN1 UBQLN2 ULBP1 USO1 VAMP3 VKORC1L1 VPS26B VSIG10 VTI1A WIPF1 YIPF3
A431_P	262	ABCD3 AGTRAP AJUBA ALDH18A1 ANKLE2 ANXA8 APOBEC3B ARPC1A ARPC1B ARPC4-TTLL3 ATP2C1 B2M B3GAT3 BAIAP2 BCAS2 BOP1 BRIX1 CACYBP CALM2 CALML3 CAMK2G CCDC59 CCNT1 CDC42 CERS2 CHCHD3 CNBP COMT COQ9 CRKL CSE1L CSNK1D CYC1 DDX20 DDX27 DDX41 DHCR7 DIABLO DNAJA1 DNAJB2 DNAJB11 DNAJC3 DNAJC10 DNAJC14 DNAJC16 DOCK7 DPM1 DRG1 EEFSEC EIF3CL EIF3I EIF6 ELOA EMC3 EPB41L4B EPPK1 ERCC6 ERLIN2 EXOSC4 EXOSC6 EXOSC7 FARSA FARSB FBL FBXO31 FOSL1 FTH1 FUBP3 GEMIN5 GFPT1 GM2A GNL2 GPAA1 GPI GTF2H2 GTF3C3 GTF3C4 GTF3C5 H2A HBB HCCS hCG_1984214 HDAC10 HK2 HMGB1 HMGB2 HSP90AB4P HTATIP2 HTRA2 HYAL2 IFRD1 IMMT IMP4 IMPDH IPO7 ISG15 ITPRIP KHSRP KIF1C KRR1 KRT13 KRT15 KRT82 LAD1 LARP4B LLGL1 LRCH3 LYAR M6PR MAGT1 MARK3 MATR3 MBNL1 MCAT MFSD10 MGAT1 MPG MPHOSPH10 MPRIP MRM3 MRPL2 MRPL15 MRPL37 MRPL47 MRPS12 MRPS15 MRPS23 MRPS34 MTAP MX2 MYDGF MYH14 MYL12A MYO18A NAP1L4 NAPA NDUFA10 NDUFS2 NFX1 NIPSNAP1 NOP56 NOP58 NOS1AP NSF NSUN4 NSUN5 NTAQ1 NUDT5 NUMB P3H2 PCBP1 PCMTD1 PCNA PEX16 PFKL PIGT PLAA PLAU PLEC PLEKHG3 PNN POLDIP2 POLDIP3 POLR3A PPL PPP1R10 PPP2R2A PPP3CA PPP6C PRDX4 PRDX5 PRKAR2A PRORP PSMA1 PSMB3 PSMC1 PSMC3 PSMC6 PTBP3 PTK7 PTPMT1 PUM3 PYGL RAB5B RAB8B RAB34 RAB38 RAN RBM27 RBM33 RBM47 RCN2 RFC1 RHOT1 RIDA RPP30 RPS15 RRAGB RRP1B RRP12 RTKN RUVBL1 RUVBL2 S100A6 S100A8 SDF2 SEC61B SEC62 SET SETX SF3A1 SFXN3 SIGMAR1 SLC25A3 SLC35B2 SMN1 SNRPB SPOUT1 SPRR1B SPTY2D1 SRP14 SRP72 SSRP1 STT3A STT3B SURF4 TAP2 TBCA TBL3 TECR TEFM TIMP3 TMCC1 TMEM40 TMEM214 TMX3 TOLLIP TOM1L2 TOP3B TOR1AIP2 TPM2 TPP1 TRIM65 TRMT61A TSG101 TSR1 TTC13 TUBB TUBB4B TWNK UFL1 UNC45A USP10 VDAC1 VDAC2 VPS45 WDR3 WDR36 WDR77 YTHDF1 Z02 ZNF598
A431_C	119	ABCB7 ABHD12 ACOT7 AFAP1 AFG3L2 AGO2 AHCY AHSA1 AK4P3 ANXA8L1 ARFIP1 ATL2 ATP1B1 ATP1B3 ATP5MF-PTCD1 ATP6AP1 BZW1 CAPG CAPN2 CASP14 CAT CCN1 CD46 CHERP CLPX COPB1 CSTA DEFA1 DHX37 DSC3 DSP DYNC1H1 ECHS1 ECM1 EIF2B4 EIF3L EIF5 ERAL1 ERAP1 ERLEC1 ETFA ETFB ETHE1 FAM20B FLG FMNL3 FN1 GARS1 GFM1 GIGYF2 GLUD1 H1-3 HDLBP HEXB HM13 HMGCL HSP90AB1 HSPA4 HSPBP1 HSPD1 IDH2 IGHA1 IGKC JUP KPRP KRT80 LBR LCLAT1 LMAN2L LYZ MAPK1 MCM3 MFN1 MRPL44 NDUFA4 NECTIN2 NFKB2 NUDCD1 NUP155 P4HA1 PIGK PIGS PPT1 PROSER2 PRPS1 PSMB8 PSMD1 PSMD6 PSMD13 PSMD14 PTGFRN PUM1 PUS1 PYCR1 RNF213 S100A14 SACM1L SAMD9 SEC23IP SEPTIN8 SERPINB6 SLC38A5 SMC2 SPRYD3 STK24 STX6 SUCLG2 TBL1XR1 TMEM87A TOMM70 TYMP UBA1 UCHL5 UFD1 UMPS VPS4A VPS35 YARS2 ZG16B

Supplemental table 2 : Summary table of proteins present in A431-Tks5-GFP cells seeded on plastic identified by mass spectrometry analysis of Tks5 interactome

Accession	Gene Name	Description	Abundance Ratio: (TKS5) / (Control)
NP_000448.2	ADE2H1	5-aminoimidazole-4-carboxamide 2	9,60,93
P49327	FASN	Fatty acid synthase	264,35
P42773	RPL6	Large ribosomal subunit protein uL6	187,07
P11940	PABPC1	Polyadenylate-binding protein 1	159,48
P62917	RPL8	Large ribosomal subunit protein uL2	129,17
Q15084	PDIA6	Protein disulfide-isomerase A6	153,84
P62701	RPS4X	Small ribosomal subunit protein eS4, X isoform	152,36
P68104	EEF1A1	Elongation factor 1-alpha 1	113,97
P04406	GAPDH	Glyceraldehyde-3-phosphate dehydrogenase	110,28
P62753	RPS6	Small ribosomal subunit protein eS6	93,09
O75369	FLNB	Filamin B, beta	90,94
P08670	VIM	Vimentin	87,29
P62424	RPL7A	Large ribosomal subunit protein uL30	82,48
P14618	PKM	Pyruvate kinase, muscle	76,76
P07355	ANXA2	Annexin A2	74,98
P62979	RPS27A	Ubiquitin and ribosomal protein S27a	74,37
P62753	RPS6	Small ribosomal subunit protein eS6	71,19
P68651	PTDSS1	Phosphatidylserine synthase 1	70,35
P62914	RPL8	Large ribosomal subunit protein uL2	69,93
P68371	TUBB4B	Tubulin beta chain	65,72
P27824	CANX	Calnexin	65,60
P62829	RPL23	Large ribosomal subunit protein uL14	62,94
P07900	HSPA9	Heat shock protein family A (Hsp70) member 9	62,79
P62750	RPL23A	Large ribosomal subunit protein uL23	60,60
P62942	FKBP1A	Peptidyl-prolyl cis-trans isomerase FKBP1A	59,34
P62847	RPS24	Small ribosomal subunit protein eS24	58,64
P62266	RPS23	Small ribosomal subunit protein eS23	57,36
P62861	RPS30	Small ribosomal subunit protein eS30	56,81
P62263	RPS14	Small ribosomal subunit protein eS14	55,34
P62987	UBA52	Ubiquitin A-52 residue ribosomal protein fusion product 1	54,73
P62979	RPS27A	Ubiquitin and ribosomal protein S27a	53,48
P62805	H4C1	Histone H4	52,84
P62826	RAN	GTP-binding nuclear protein Ran	51,77
P62241	RPS8	Small ribosomal subunit protein eS8	51,76
P62917	RPL8	Large ribosomal subunit protein uL2	50,86
P62753	RPS6	Small ribosomal subunit protein eS6	50,21
P62424	RPL7A	Large ribosomal subunit protein uL30	49,77
P62829	RPL23	Large ribosomal subunit protein uL14	49,58
P62979	RPS27A	Ubiquitin and ribosomal protein S27a	49,15
P62753	RPS6	Small ribosomal subunit protein eS6	48,57
P62942	FKBP1A	Peptidyl-prolyl cis-trans isomerase FKBP1A	47,77
P62424	RPL7A	Large ribosomal subunit protein uL30	47,70
P62753	RPS6	Small ribosomal subunit protein eS6	46,75
P62829	RPL23	Large ribosomal subunit protein uL14	45,98
P62753	RPS6	Small ribosomal subunit protein eS6	45,62
P62829	RPL23	Large ribosomal subunit protein uL14	45,58
P62753	RPS6	Small ribosomal subunit protein eS6	45,53
P62829	RPL23	Large ribosomal subunit protein uL14	45,53

Supplemental table 3 : Summary table of proteins present in A431-Tks5-GFP cells seeded on collagen identified by mass spectrometry analysis of Tks5 interactome

Accession	Gene Name	Description	Abundance Ratio: (TKS5) / (Control)
Q5TC25	SHIP010	SH2 and PH domain-containing protein 2A	634,03
P18124	RPL7	Large ribosomal subunit protein uL30	81,80
A0A8Q3SHY9	ATAP112	Actin filament associated protein 1 like 2	73,20
A5A3E3	ADAM15	Disintegrin and metalloproteinase domain-containing protein 15	69,28
P62388	RPL10	Large ribosomal subunit protein uL10	69,05
P62241	RPS8	Small ribosomal subunit protein eS8	57,90
P46779	RPL7	Large ribosomal subunit protein uL18	55,49
P62263	RPLA0	Small ribosomal subunit protein eS4, X isoform	50,19
Q00839	HNRNPU	Heterogeneous nuclear ribonucleoprotein U	48,73
P62279	RPS11	Small ribosomal subunit protein eS13	43,96
P62424	RPL8	Large ribosomal subunit protein eL8	43,68
P63081	YWHAG	14-3-3 protein gamma	42,73
P56819	PRKAG1	5'-AMP-activated protein kinase subunit gamma-1	42,71
P62753	RPS6	Small ribosomal subunit protein eS6	42,61
P35614	RPL14	Large ribosomal subunit protein eL14	42,51
P62917	RPL8	Large ribosomal subunit protein eL8	41,90
P62424	RPL7A	Large ribosomal subunit protein eL8	41,54
Q7Z569	PRKRA	interferon-inducible double-stranded RNA-dependent protein kinase activator A	36,14
P62267	RPS23A	Small ribosomal subunit protein eS1	35,60
P62829	RPL23	Large ribosomal subunit protein eL23	34,51
P62913	RPL11	Large ribosomal subunit protein uL5	34,55
Q12965	MYO1E	Unconventional myosin-Ie	34,23
P62753	RPS6	Small ribosomal subunit protein eS6	33,86
P62908	RPS3	Small ribosomal subunit protein eS3	32,68
Q8N8G1	ESRP1	Epithelial splicing regulatory protein 1	30,92
P14618	HNRNPD	Heterogeneous nuclear ribonucleoprotein D0	30,20
P49910	GLIPR2	Golgi-associated plant pathogenesis-related protein 1	29,11
P62854	RPS26	Small ribosomal subunit protein eS26	28,67
P25143	RPL15A	Large ribosomal subunit protein eL15	28,64
Q96I24	FUBP3	Glutamate-rich WD repeat-containing protein 1	28,52
O75191	ARL6IP5	PRA1 family protein 3	28,43
Q9Y385	ACOT9	Acyl-coenzyme A thioesterase 9, mitochondrial	28,20
Q7Z460	KIF4A	Chromosome-associated kinesin KIF4A	27,93
Q96DU9	TSPYL1	Testis-specific Y-encoded-like protein 1	27,68
Q96CF6	MRPS18B	Small ribosomal subunit protein mS40	27,62
P40926	IDH2	Isocitrate dehydrogenase [NADP], mitochondrial	27,53
H9J07	RPL34	Large ribosomal subunit protein eL34	26,89
Q15757	LAMA3	Laminin subunit alpha-3	26,66
O15127	SCAMP2	Secretory carrier-associated membrane protein 2	26,34
Q13153	PAK1	5'-AMP-activated protein kinase catalytic subunit alpha-1	26,11
Q9UJV4	CORO1C	Coronin-1C	25,09
P62701	STAU1	Double-stranded RNA-binding protein Staufen homolog 1	24,92
Q12965	01E	Interlevkin enhancer-binding factor 2	24,51
P62826	GDIMH4	Gem-associated protein 4	24,45
A0A0J3RRM4	PTBP1	Polypyrimidine tract-binding protein 1	24,28
Q8Y446	PRP3	Pleiokinshin-3	22,74
A0A0G8PHA2	INF2	Inverted formin 2	23,80
Q9H0J3	ADAM19	Disintegrin and metalloproteinase domain-containing protein 19	23,69
P53621	COPA	Coatomer subunit alpha	23,57
Q9NYH8	OXLD1	Glutamate-ammonia-ligase domain-containing protein 1	23,26
Q8N4N9	ATL2	Atlastin-2	22,18
P61163	ACTR2	Actin-related protein 2	22,87
P30626	TMODS	Tropomodulin-3	22,48
P01834	IGKC	Immunoglobulin kappa constant	22,19
P02751	FN1	Fibronectin	21,87
P46561	PTDSS1	Phosphatidylserine synthase 1	21,79
P60953	RDC1	ATP-dependent DNA helicase Q1	21,54
Q8NC45	FAM98A	Protein FAM98A	21,51
P49419	ALDH7A1	Alpha-aminoadipic semialdehyde dehydrogenase	21,45
Q9Y678	PPAR3	Peroxisomal acyl-coenzyme A thioesterase 3	20,72
Q13724	MOGS	Mannosyl-oligosaccharide glucosidase	20,60
P55084	TMODS	Tropomodulin-2	20,48
A0A5F8H4W7	SACM1L	OCS like phosphatidylinositide phosphatase	20,12
P15880	RPS2	Small ribosomal subunit protein uS5	20,00
P69905	HBA2	Hemoglobin subunit alpha	19,94
P07996	THBS1	Thrombospondin-1	19,92
P62913	RPL11	Large ribosomal subunit protein uL5	19,62
Q13310	PABPC4	Polyadenylate-binding protein 4	19,60
Q9Y5Q8	SRP68	Signal recognition particle subunit SRP68	19,55
Q9NYU2	UGGT1	UDP-glucose:glycoprotein glucosyltransferase 1	19,55
P52272	HNRNPM	Heterogeneous nuclear ribonucleoprotein M	19,46
P81274	FGD1	FYVE, RhoGEF and PH domain-containing protein 1	19,45
A0A0U1RQ35	FNBP1	Formin binding protein 1	19,29
A0A5H7VQ2	FXR1	RNA-binding protein FXR1	19,03
A0A0U1RQ2	DDX17	RNA helicase	18,93
Q9NN9	NMNAT3	Nicotinic/nicotinamide mononucleotide adenylyltransferase 1	18,93
A0A0A0MSW9	TAPBP	Tapasin	18,76
P11387	TOP1	DNA topoisomerase I	18,75
P62258	YWHAE	14-3-3 protein epsilon	18,73
P31943	HNRNPH1	Heterogeneous nuclear ribonucleoprotein U-like protein 1	18,70
O94813	ASCC2	Activating signal cointegrator 1 complex subunit 2	18,65
P63010	AP2B1	AP-2 complex subunit beta	18,60
Q5TCZ1	H1-10	Histone H1.10	18,14
Q9NQC3	RTN4IP1	Reticulon-4-interacting protein 1, mitochondrial	17,80
Q8E211	DHX9	ATP-dependent RNA helicase A	17,80
Q2KQU3	MAPT01	MAPT domain-containing protein 1	17,69
P60660	ISG4P1	Rac GTPase-activating like protein ISG4P1	17,43
Q8V7T6	MBL1	C-type lectin-like protein MBL	17,41
Q9H4B6	LIMA1	LIM domain and actin-binding protein 1	17,40
P23396	RPS3	Small ribosomal subunit protein uS3	17,37
Q8ZMH3	UPF2	UPF2 domain-containing protein	17,29
Q5JWF	UCHL5	Ubiquitin carboxyl-terminal hydrolase (Fragment)	17,20
Q12797	ASPH	Aspartyl/asparaginyl beta-hydroxylase	17,18
O15162	PLSCR1	Ca2+ induced Scaffold protein 1	16,94
Q9UJ71	RBM17	Splicing factor 45	16,93
Q9H8U6	C7orf50	Uncharacterized protein C7orf50	16,89
Q96ZR7	DDX24	ATP-dependent RNA helicase DDX24	16,84
P68366	PRR23A	Protein PRR23A	16,64
A0Y2N6	ATAD2A	ATPase family AAA domain containing 2A (Fragment)	16,43
A0A7X2WQ3	RPL19	Ribosomal protein L19	16,32
P27348	YWHAQ	14-3-3 protein theta	16,41
Q8N174	PCDH1	Protocadherin-1	16,40
P30050	RPL12	Large ribosomal subunit protein uL11	16,16
P05121	PAI1	Plasminogen activator inhibitor 1	16,03
Q6I7N5	MYO1B	Unconventional myosin-Ib	15,83
A0A5B9BT8	MYH9	Myosin heavy chain 9	15,62
Q16666	IFI16	Gamma-interferon-inducible protein 16	15,46
H6I7T8	RPL21	Large ribosomal subunit protein eL21	15,45
P06213	GBA1	Glucosylceramidase	15,45
P13674	P4HA1	Prolyl 4-hydroxylase subunit alpha-1	15,42
P35226	ABCF1	ATP binding cassette subfamily F member 1	15,39
P62266	RPS23	Small ribosomal subunit protein uS12	15,36
P62841	DAP3	Small ribosomal subunit protein mS29	15,13
Q8N3C6	PARP9	Protein mono-ADP-ribosyltransferase PARP9	15,09
A0A087WZ09	ABO	ABO, alpha 1-3-N-acetylglucosaminyltransferase and alpha 1-3-galactosyltransferase	14,98
Q9UJU0	PRKAG2	5'-AMP-activated protein kinase subunit gamma-2	14,94
Q9P209	RBBP1	Ribosome-binding protein 1	14,87
Q9P206	KIAA1522	Uncharacterized protein KIAA1522	14,79
Q9UKX5	TIMP3	Metalloproteinase inhibitor 3	14,74
Q96A54	LRRC59	Leucine-rich repeat-containing protein 59	14,73
O43865	AHCYL1	S-adenosylhomocysteine hydrolase-like protein 1	14,66
Q8WXI9	LLGPL	Leucine zipper protein 1	14,63
Q92499	DDX1	ATP-dependent RNA helicase DDX1	14,50
O00329	STAM1	STAM1	14,46
P84077	ARF1	ADP-ribosylation factor 1	14,14
Q99985	SEMA3C	Semaphorin-3C	14,02
O00533	IGF2BP3	Insulin-like growth factor 2 mRNA-binding protein 3	13,95
O00425	SPATS2L	SPATS2-like protein	13,92
A0A0A0MVL6	RPL17-C18orf32	60S ribosomal protein L17	13,82
A0A7X2V5S	NONO	Non-POU domain-containing octamer binding	13,65
A0A0B4DT72	NXRF	NFKB-repressing factor	13,61
P30101	PDIA3P	DNA-directed RNA polymerase, mitochondrial	13,61
H0YK28	RPL28	60S ribosomal protein L28	13,18
Q6UWP7	UCLA71	Lysocerebrosidase acyltransferase 1	13,18
Q72WH4	ZC3HAV1	Zinc finger CCCH-type antiviral protein 1	13,13
P52630	TBRG4	Transcription intermediary factor 1 beta	12,98
Q96ZN1	MYOF	Myoferlin	12,97
Q07065	CKAP4	Cytoskeleton-associated protein 4	12,79
P49327	FASN	Fatty acid synthase	12,77
Q8NFW8	CMAS	N-acylneuraminate cytidylyltransferase	12,74
Q9Y394	DHRS7	Dehydrogenase/reductase SDR family member 7	12,66
Q5JPE7	PRR12C	Protein PRR12C	12,64
H0YT23	BASP1	Brain acid soluble protein 1	12,63
A0A5F8DP5	ASCC1	Activating signal cointegrator 1 complex subunit 1	12,59
Q8N8N7	LSG1	Large subunit GTPase 1 homolog	12,58
Q15020	SART3	Squamous cell carcinoma antigen recognized by T-cells 3	12,58
Q92900	UPF1	Regulator of nonsense transcripts 1	12,57
A0F8B8	EIF1P2	Eukaryotic translation initiation factor 1 pseudogene 2	12,51
A0A0B4PF7	PPT1	Palmitoyl-protein thioesterase 1	12,49
H0YJ21	CAPG	Macrophage-capping protein	12,43
P32322	PYCR1	Pyrroline 5-carboxylate reductase 1, mitochondrial	12,38
Q9Y618	NCOR2	Nuclear receptor corepressor 2	12,37
Q92665	MRPS31	Small ribosomal subunit protein mS31	12,35
O00401	WASL	Actin nucleation-promoting factor WASL	12,33
Q15365	TNRA61	Transducing chain-associated membrane protein 1	12,17
O75909	CCNL	Cyclin-L	12,13
Q16698	DECR1	2,4-dienoyl-CoA reductase [(3E)-enoyl-CoA-producing], mitochondrial	12,00
Q9Y399	ATG3	Ubl-activating enzyme ATG3 homolog	11,97
H7BY16	NCL	Nucleolin	11,96
O14908	GPC1	PDZ domain-containing protein GPC1	11,95
A0A0B7P2V2	PDK2	Pyruvate dehydrogenase (acetyl-transferring) kinase isozyme 2, mitochondrial	11,90
Q01170	CSRP1236	Uncharacterized protein CSRP1236	11,90
Q8N917	YWHAH	14-3-3 protein eta	11,79
Q62MP9	TVD64	Thrombospondin type-1 domain-containing protein 4	11,73
P62979	RS27A	Ribosomal protein eS27	11,70
O14464	CAPRIN1	Caprin-1	11,70
P23284	PPIB	Peptidyl-prolyl cis-trans isomerase B	11,62
P15941	PABPC1	Polyadenylate-binding protein 1	11,59
E7ER63	ZC3H18	Zinc finger CCCH-type containing 18	11,50
Q96AE5	CCDC86	Coiled-coil domain-containing protein 86	11,47
Q8TC05	LARS1	Leucine--tRNA ligase, cytoplasmic	11,45
P51665	PSMD7	26S proteasome non-ATPase regulatory subunit 7	11,44
O14920	IKKAB300	Uncharacterized protein IKKAB300	11,39
Q96AY3	FAM120A	Constitutive activator of PPAR-gamma-like protein 1	11,27
H0YB68	CCT3	T-complex protein 1 subunit gamma	11,25
A0A496B6B4	FIP1L1	Pre-mRNA 3'-end-processing factor FIP1	11,25
P08659	EPAS1	Endothelial PAS domain-protein 1	11,17
Q9H4S9	CDC5L	Cell division cycle 5-like protein	11,13
O94832	MYO1D	Unconventional myosin-Id	11,12
Q15650	TRP4	Activating signal cointegrator 1	11,11
P07900	HSP90AA1	Heat shock protein HSP 90-alpha	11,07
P03011	LINE-1	LINE-1 retrotransposable element ORF1 protein	11,07
P41091	EIF2S3	Eukaryotic translation initiation factor 2 subunit 3	11,07
P09693	AP2A1	AP-2 complex subunit mu	11,03
P07355	AP2A1	AP-2 complex subunit alpha-1	11,01
P02452	COL1A1	Collagen alpha-1(I) chain	10,97
P06396	GSN	Gelsolin	10,95
Q92616	GTPBP4	GTP-binding protein 4	10,91
Q9NWV13	RBM28	RNA-binding protein 28	10,89
P62879	RPL27A	Large ribosomal subunit protein uL15	10,74
E7EVA0	MAP4	Microtubule-associated protein	10,74
O43263	DAPK2	Death-associated protein kinase 3	10,67
P05362	ICAM1	Intercellular adhesion molecule 1	10,61
Q9H8P7	TBL2	Transducin beta-like protein 2	10,67
Q96A25	SVIL	Supervillin	10,65
O00623	CON1	CON family member 1	10,61
Q07112	EDF1	Retinoid dehydrogenase 11	10,58
Q8WVM8	SCFD1	Sec1 family domain-containing protein 1	10,53
Q14192	FHL2	Four and a half LIM domains protein 2	10,51
P31151	CAT8	Calcium-activated potassium channel subunit alpha 1	10,51
A0A7X2BRN3 | MYO5C | Unconventional myosin-Vc | 10,51 |
Q53EP0 | FNDC3B | Fibronectin type III domain-containing protein 3B | 10,50 |
Q13049 | TRIM32 | E3 ubiquitin-protein ligase TRIM32 | 10,48 |
A0A0B9RHJ8 | MCM3 | DNA replication licensing factor MCM3 | 10,48 |
Q6TA4 | DDX5 | Probable ATP-dependent RNA helicase DDX5 | 10,46 |
Q96QG0 | CYP20A1 | Cytochrome P450 20A1 | 10,45 |
A0A0A0MT38 | NGDN1 | Neuroblast differentiation-associated protein Neuroguidin | 10,41 |
P55268 | RL22 | Large ribosomal subunit protein eL22 | 10,31 |
Q8N8F4 | FAM89A1A | Protein FAM89A1A | 10,25 |
A0A0G0WV3 | MRPL57 | Mitochondrial ribosomal protein L57 | 10,24 |
P55263 | MRPL54 | Mitoribosome-associated protein 54 | 10,21 |
Q13126 | PPP1R1 | Liprin-alpha-1 | 10,19 |
Q70CQ2 | USP34 | Ubiquitin carboxyl-terminal hydrolase 34 | 10,19 |
Q8N5S6 | ATAP1 | Actin filament associated protein 1 | 10,19 |
Q9UJ27 | MDN1 | Ribosome biogenesis protein MDN1 | 10,17 |
H0YBF1 | LDH2 | Lipocalin 2 | 10,15 |
H0J731 | RPL24 | Large ribosomal subunit protein eL24 | 10,13 |
A0A0G0QF37 | KIF23A | Kinesin-like protein | 10,11 |
O75616 | ERAL1 | GTPase Era, mitochondrial | 10,08 |
Q9H3K6 | BOLA2 | Synaptocan-4 | 10,07 |
Q8N9H1 | CHD4L2 | Coiled-coil helix-coiled-coil-helix domain-containing protein 2 | 10,06 |
P49748 | ACADVL | Very long-chain specific acyl-CoA dehydrogenase, mitochondrial | 9,97 |
O95476 | SDR1 | Sphingosine-1-phosphate lyase 1 | 9,96 |
O15031 | PLXNB2 | Plexin-B2 | 9,93 |
Q12906 | ILF3 | Interleukin enhancer-binding factor 3 | 9,91 |
A0A0B9B4L5 | GOLGA2 | Golgin A2 | 9,89 |
O13033 | DDB2 | Sphingosine-1-phosphate lyase 1 | 9,86 |
Q8N6N5 | SQOR | Sulfide quinone oxidoreductase, mitochondrial | 9,81 |
Q96EY4 | TBL1M | Transducin beta-like protein 1, mitochondrial | 9,81 |
A0A7P0TAU8 | DAS3 | 2-5' oligoadenylate synthase | 9,80 |
P67809 | YBX1 | Y-box binding protein 1 | 9,78 |
A0A0G0BPH1 | AFMA1 | Apoptosis inducing factor mitochondria associated 1 | 9,74 |
Q7Z775 | TBK7 | TBK/TIs ubiquitin | 9,74 |
Q8WUR0 | ZC3H15 | Zinc finger CCCH domain-containing protein 15 | 9,66 |
P62829 | GRL1A | Glutamine--tRNA ligase | 9,62 |
P62829 | RPL23 | Large ribosomal subunit protein uL14 | 9,56 |
Q14706 | MANZA1 | Alpha-mannosidase 2 | 9,54 |
Q8P258 | BCC2 | Protein BCC2 | 9,43 |
P46781 | RPS9 | Small ribosomal subunit protein uS4 | 9,42 |
H0YD26 | HAOH4 | enoyl-CoA hydratase | 9,40 |
Q9H4U0 | PLEKHA5 | Pleckstrin homology domain-containing family A member 5 | 9,39 |
Q6DD88 | ATL3 | Atlastin-3 | 9,39 |
P39727 | RPL22 | Ribosomal protein L22 | 9,37 |
Q96CF6 | CDPQ1 | Customer subunit gamma-1 | 9,37 |
A0A0B4H4K0 | ZRPR1 | Leucine-rich protein-coupled receptor containing | 9,35 |
A0A0A0MW8 | V | SCRIB | 9,32 |
Q14451 | GRB7 | Growth factor receptor-bound protein 7 | 9,27 |
Q8TD8C | DTX3L | E3 ubiquitin-protein ligase DTX3L | 9,23 |
A0A7X2EE1 | ARHGEF12 | Rho guanine nucleotide exchange factor 2 | 9,23 |
P62104 | YWHAZ | 14-3-3 protein zeta/delta | 9,13 |
Q9H4D6 | KIN2 | 1-2'-oligoadenylate synthase 2 | 9,09 |
Q07828 | CALU | Calnexin-related protein CSurf-132 | 9,07 |
P54819 | AK2 | Adenylate kinase 2, mitochondrial | 9,06 |
P29728 | OAS2 | 2'-5'-oligoadenylate synthase 2 | 9,05 |
Q92599 | SEPT9A6 | Septin-8 | 9,02 |
Q96G8 | CDT1 | Geminated yeast protein-1 | 8,95 |
Q12849 | GRS1 | G-rich sequence factor 1 | 8,95 |
Q6PTS | TRAB0 | Trafd domain containing | 8,95 |
A0A0B4 | EMV1 | Endoplasmic reticulum vesicle transmembrane protein 1 | 8,86 |
Q6N2Z1 | CNVM1 | Caveolae-associated protein 1 | 8,82 |
A0A3B3RTL6 | CSN5 3 | Chromosome 8 open reading frame 33 | 8,82 |
P27797 | CALR | Calreticulin | 8,79 |
Q8P21 | DDX50 | Probable ATP-dependent RNA helicase DDX50 | 8,78 |
Q96B42 | TRMT6C | E3 ubiquitin-protein ligase TRIM15A | 8,73 |
Q5JTK7 | FMR1 | Fragile X mental retardation protein 1 | 8,71 |
Q6DS26 | SYNCRP | Heterogeneous nuclear ribonucleoprotein Q | 8,70 |
A0A5F8JHN | ALDH3A2 | Aldehyde dehydrogenase | 8,70 |
A0A0A0MQ2P | CDK1 | Cell division cycle 2, G1 to S and G2 to M, isoform CRA_a | 8,68 |
P54136 | RARS1 | Arginine--tRNA ligase, cytoplasmic | 8,67 |
Q14314 | FDXD | Protein disulfide isomerase A5 | 8,66 |
Q15642 | TRIP13 | Cdc42-interacting protein 4 | 8,65 |
A0A0G3SX1 | KIAA2442 | RAS protein activator like 2 | 8,62 |
P11498 | PC | Pyruvate carboxylase, mitochondrial | 8,61 |
O76031 | CLPX | ATP-dependent Clp protease ATP-binding subunit clpX-like, mitochondrial | 8,60 |
Q9UJ78 | HECTD1 | E3 ubiquitin-protein ligase HECTD1 | 8,58 |
P20810 | CSS | Filaggrin | 8,55 |
P30566 | PAH4A6 | 14-3-3 protein beta/alpha | 8,51 |
Q9H3S4 | DDX57 | Probable ATP-dependent RNA helicase DDX57 | 8,50 |
P84022 | SMAD3 | Mothers against decapentaplegic homolog 3 | 8,43 |
Q96F07 | CCC1 | Structural maintenance of chromosomes protein 4 | 8,42 |
A0A2R5VQ4 | 1 SV | Tight junction protein ZO-2 | 8,41 |
A0A0A0MJ33 | CSN5 3A1 | Cullin 5 | 8,41 |
Q8N3C0 | ASCC3 | Activating signal cointegrator 1 complex subunit 3 | 8,33 |
Q14739 | LBR | Delta(14)-sterol reductase LBR | 8,28 |
P07355 | ANXA2 | Annexin A2 | 8,27 |
P51861 | ZZZ3 | Zinc finger ZZ-type and ankyrin domain protein 3 | 8,23 |
Q8ZH2 | KRN1 | 5'-3' exoribonuclease 1 | 8,22 |
P60287 | ACP2 | Protein 28S rRNA (cytosine(4447)-C(5)-)-methyltransferase | 8,16 |
Q13011 | ECH1 | Delta(3,5)-Delta(2,4)-dienoyl-CoA isomerase, mitochondrial | 8,15 |
P05164 | MPO | Serpin-H1 | 8,15 |
Q96AQ6 | PBEF1 | Pre-B-cell leukemia transcription factor-interacting protein 1 | 8,15 |
P29590 | PML | Protein PML | 8,13 |
P62942 | FKBP12 | Peptidyl-prolyl cis-trans isomerase FKBP12 | 8,11 |
O43143 | DHX15 | ATP-dependent RNA helicase DHX15 | 8,04 |
Q15019 | SEPT9A2 | Septin-2 | 8,03 |
P62917 | RPL8 | Small ribosomal subunit protein uS8m | 8,03 |
P50895 | YBX3 | Y-box binding protein 3 | 8,03 |
Q96A26 | SPATS2 | Spermatogenesis-associated serine-rich protein 2 | 8,01 |
P49902 | EDN2 | eIF5-mimic protein 2 | 7,97 |
Q16531 | DDB1 | DNA damage-binding protein 1 | 7,95 |
Q96NY4 | MTPAP | Poly(A) RNA polymerase, mitochondrial | 7,94 |
P07476 | IVL | Involucrin | 7,94 |
P05783 | KRT18 | Keratin, type I cytoskeletal 18 | 7,91 |
O43767 | ACTN4 | Alpha-actinin-4 | 7,90 |
P04040 | CAT | Catalase | 7,87 |
Q9Y230 | RUVBL2 | Inner mitochondrial membrane protein | 7,85 |
P14868 | DARS | Aspartate--tRNA ligase, cytoplasmic | 7,77 |
A0A3B3RTT5 | RPL29 | 60S ribosomal protein L29 | 7,75 |
A0A496A8D8 | 4 SV | Exocrine component 4 | 7,74 |
Q15038 | PSMD8 | 26S proteasome non-ATPase regulatory subunit 6 | 7,74 |
Q02962 | AAAP2 | A-kinase anchor protein 12 | 7,72 |
Q14004 | CDK13 | Cyclin-dependent kinase 13 | 7,72 |
P07910 | ACTN3 | Actin-related protein 3 | 7,72 |
Q96AF3 | RBM4 | RNA-binding protein 4 | 7,70 |
A0A0E7W7X | 1 | HMOX2 | 7,70 |
Q8NV7 | ATAD3A | ATPase family AAA domain-containing protein 3A | 7,69 |
P78527 | PRKDC | DNA-dependent protein kinase catalytic subunit | 7,66 |
Q96NW7 | SPIN90 | SPIN domain-containing 3 | 7,60 |
Q13435 | SF3B2 | Splicing factor 3B subunit 2 | 7,59 |
Q99755 | RPS6KL1 | Phosphatidylinositol 4-phosphate 5-kinase type-1 alpha | 7,59 |
Q14376 | GPAT3 | Acetyl-type protease inhibitor 1 | 7,53 |
A0A4B | 4 | HEMGN | 7,52 |
P0C0S5 | DNMT3 | DNA adenine N(6)-methyltransferase | 7,52 |
P05556 | CDH10 | Cadherin subfamily 2 | 7,51 |
Q01169 | TNFAIP3 | Tumor necrosis factor alpha-induced protein 2 | 7,50 |
Q70UQ0 | RBBP | Inhibitor of nuclear factor kappa-B kinase-interacting protein | 7,49 |
O96N99 | PDIA6 | Protein disulfide isomerase | 7,48 |
P50895 | ARD1B | Trifunctional enzyme subunit beta, mitochondrial | 7,48 |
O75367 | EIF4B | Eukaryotic translation initiation factor 4B | 7,48 |
P05388 | RPLP0 | Ribosomal protein P0 | 7,46 |
O00159 | MYO1C | Unconventional myosin-Ic | 7,46 |
Q8NHP8 | FLBD2 | Putative phospholipase B-like 2 | 7,43 |
P02533 | KRT14 | Keratin, type I cytoskeletal 14 | 7,41 |
P08238 | GLS3 | Beta-glucuronidase | 7,37 |
A0A496B7B4 | 4 | PGS1 | 7,35 |
P48200 | MAGEA4 | Melanoma-associated antigen 4 | 7,25 |
Q15582 | TGFBI | Transforming growth factor-beta-induced protein ig-h3 | 7,21 |
P08874 | PARP1 | Poly (ADP-ribose) polymerase 1 | 7,19 |
Q15084 | AARS1 | Lysine--tRNA ligase | 7,12 |
P09525 | EF2AK2 | Interferon-induced, double-stranded RNA-activated protein kinase | 7,12 |
P04897 | SHMT2 | Serine hydroxymethyltransferase, mitochondrial | 7,11 |
P61250 | GARS1 | Glycine--tRNA ligase | 7,08 |
Q16644 | MTDH | Protein YRC | 7,03 |
P08579 | SNRNP2 | U2 small nuclear ribonucleoprotein B'' | 7,01 |
Q6DS68 | PLOD3 | Multifunctional procollagen lysine hydroxylase and glycosyltransferase LH3 | 7,01 |
O75676 | RPS6KA4 | Ribosomal protein S6 kinase alpha-4 | 7,00 |
A0A496N0D6 | DDX21 | RNA helicase | 6,99 |
P12956 | KRCC6 | X-ray repair cross-complementing protein 6 | 6,97 |
P05455 | SSB | Beta-thalassemia/leukemia lymphoma | 6,96 |
O00577 | PURA | Transcriptional activator protein Pur-alpha | 6,94 |
P08670 | CNN2CA1 | Caveolin kinase II subunit alpha | 6,94 |
O15460 | P4HA2 | Prolyl 4-hydroxylase subunit alpha-2 | 6,91 |
A0A0B7W6Z2 | 1 | SPTBN1 | 6,91 |
O75864 | ZMYND19 | CAAX prenyl protease 1 homolog | 6,91 |
P07437 | AMBMP | Heterogeneous nuclear ribonucleoprotein F | 6,90 |
P09758 | TACSTD2 | Tumor-associated calcium signal transducer 2 | 6,88 |
O75369 | CS | Citrate synthase, mitochondrial | 6,86 |
P08240 | SRPRA | Signal recognition particle receptor subunit alpha | 6,86 |
P00040 | CBP20 | Endoplasmic reticulum resident protein 29 | 6,85 |
O75165 | DNAJC13 | Dnaj homolog subfamily C member 13 | 6,85 |
P07814 | EPRS1 | Bifunctional glutamyl/prolyl-tRNA ligase | 6,84 |
O15355 | PPM1G | Protein phosphatase 1G | 6,83 |
P05787 | KRT8 | Keratin, type II cytoskeletal 8 | 6,81 |
Q96A08 | COL17A1 | Collagen alpha-1(XVII) chain | 6,77 |
A0A087 | HNRNPAB | Heterogeneous nuclear ribonucleoprotein A/B | 6,76 |
P35221 | CTNNA1 | Catenin alpha-1 | 6,75 |
O60716 | CTNND1 | Catenin delta-1 | 6,74 |
A0A4B8A4H | MAN1B1 | alpha-1,2-Mannosidase | 6,72 |
Q7L2E3 | DHX30 | ATP-dependent RNA helicase DHX30 | 6,71 |
H3BUY9 | SEPN1 | SELF protein kinase 1 (Fragment) | 6,68 |
Q13151 | HNRNPA0 | Heterogeneous nuclear ribonucleoprotein A0 | 6,68 |
Q9NQC3 | RTN4 | Reticulon-4 | 6,66 |
A0A4G3MNV | 47 | EPN1 | 6,64 |
Q9UKS6 | PACSIN3 | Protein kinase C and casein kinase substrate in neurons protein 3 | 6,64 |
Q8WWA0 | MFN1 | Mitofusin-1 | 6,59 |
Q96CS3 | FAF2 | FAS-associated factor 2 | 6,58 |
A0A0B7W2N | 1 | GNB2 | 6,57 |
Q9H7Z7 | PGS1 | Prenylcysteine oxidase 1 | 6,56 |
Q7L2E3 | DHX30 | ATP-dependent RNA helicase DHX30 | 6,54 |
P14618 | PKM | Pyruvate kinase | 6,54 |
Q13151 | HNRNPA0 | Heterogeneous nuclear ribonucleoprotein A0 | 6,48 |
Q9NQC3 | RTN4 | Reticulon-4 | 6,46 |
A0A4G3MNV | 47 | SPTBN1 | 6,44 |
Q9UKS6 | PACSIN3 | Protein kinase C and casein kinase substrate in neurons protein 3 | 6,43 |
Q8WWA0 | MFN1 | Mitofusin-1 | 6,39 |
Q96CS3 | FAF2 | FAS-associated factor 2 | 6,37 |
A0A0B7W2N | 1 | GNB2 | 6,37 |
P31937 | 4 SV | Isocitrate dehydrogenase [NAD] subunit, mitochondrial | 6,50 |
P17987 | TCP1 | T-complex protein 1 subunit alpha | 6,49 |
Q96GM8 | TDE1 | Target of EGR1 protein 1 | 6,45 |
A0A496N3H | 4 | SPTBN1 | 6,44 |
Q9H4L5 | OSCP1 | Interferon-stimulated 20 kDa exonuclease-like 2 | 6,44 |
Q43847 | NADC | Nardilysin | 6,41 |
P14625 | HSP90B1 | Endoplasmin | 6,41 |
P26196 | DDX6 | Probable ATP-dependent RNA helicase DDX6 | 6,40 |
Q7Z4W1 | TRAP | Serine-threonine kinase receptor-associated protein | 6,27 |
Q13153 | AAKAP2 | Aminoacyl tRNA synthetase multifunctional protein 2 | 6,36 |
Q9H2D6 | FUS1 | Pseudouridylate synthase 1 homolog | 6,35 |
Q9Y2W1 | PPIHBP1 | Cyprin-beta-1 | 6,35 |
O43264 | SARTS | UACAA cis-SRP-associated protein 1 | 6,33 |
P00505 | GOT2 | Aspartate aminotransferase, mitochondrial | 6,33 |
Q96AK3 | DCAF5 | DDB1- and CUL4-associated factor 5 | 6,33 |
O00329 | EIF4G2 | Eukaryotic translation initiation factor 4 gamma 2 (Fragment) | 6,33 |
P62888 | RPL30 | Large ribosomal subunit protein eL30 | 6,31 |
Q99523 | NACD | Very-long-chain (3R)-3-hydroxyacyl-CoA dehydratase 3 | 6,30 |
P62987 | UBA52 | Ubiquitin recognition factor in ER-associated degradation protein 1 | 6,28 |
P17931 | LGALS3 | Galectin-3 | 6,27 |
Q99613 | EFTUD2 | Elongation factor Tu GTP binding domain-containing protein 2 | 6,27 |
Q7L0Y3 | TRMT10C | RNA methyltransferase 10 homolog C | 6,27 |
Q96D61 | CVNN1 | Caveolae-associated protein 3 | 6,27 |
O95159 | ZFP11 | Zinc finger protein like 1 | 6,26 |
O15162 | PLSCR1 | Phospholipid scramblase 1 | 6,24 |
Q9H7E6 | HDS2 | Deoxyhypusine synthase-like protein 2 | 6,24 |
Q15437 | SEC23B | Protein transport protein Sec23B | 6,24 |
Q9Y580 | SUPT16H | FACT complex subunit SPT16 | 6,18 |
Q96AY3 | IGFN1 | Immunoglobulin family member 1 | 6,18 |
Q96PZ2 | GNL3 | Guanine nucleotide-binding protein-like 3 | 6,18 |
Q5T0N5 | FNBP1L | Formin-binding protein 1-like | 6,18 |
A0A0A0MRX | 6LAV1-2 | Protein kinase C-binding protein | 6,17 |
E5

Supplemental table 4 : Summary table of proteins present in NIH-3T3-Src-Tks5-GFP cells seeded on plastic identified by mass spectrometry analysis of Tks5 interactome

Accession	Gene Name	Description	Abundance Ratio: (TKS5) / (Control)
O89032	SH3PXD2A	SH3 and PX domain-containing protein 2A	253,58
P67871	CSNK2B	Casein kinase II subunit beta	55,49
Q35682	MYADM	Myeloid-associated differentiation marker	30,47
O35674	ADAM19	Disintegrin and metalloproteinase domain-containing protein 19	28,37
A0A0G2JGS4	CAMK2D	calcium/calmodulin-dependent protein kinase	28,11
O88839	ADAM15	Disintegrin and metalloproteinase domain-containing protein 15	21,39
P51125	CAST	Calpastatin	18,81
E9QAS8	FMR1	Fragile X messenger ribonucleoprotein 1	18,07
Q80SY4	MIB1	E3 ubiquitin-protein ligase MIB1	16,10
O88477	IGF2BP1	Insulin-like growth factor 2 mRNA-binding protein 1	16,10
Q9JM51	PTGES	Prostaglandin E synthase	15,95
P61514	RPL37A	Large ribosomal subunit protein eL43	15,70
P84091	AP2M1	AP-2 complex subunit mu	15,01
O70251	EEF1B	Elongation factor 1-beta	14,48
P84104	SRSF3	Serine/arginine-rich splicing factor 3	14,13
Q9WVE8	PACSIN2	Protein kinase C and casein kinase substrate in neurons protein 2	13,43
Q5SF07	IGF2BP2	Insulin-like growth factor 2 mRNA-binding protein 2	13,30
Q91Z31	PTBP2	Polypyrimidine tract-binding protein 2	12,57
Q3TLP8	RAC1	Rac family small GTPase 1	12,35
A0A2R8VK70	CD47	Leukocyte surface antigen CD47	12,32
Q9D1R9	RPL34	Large ribosomal subunit protein eL34	12,06
Q9QXT0	CNPY2	Protein canopy homolog 2	11,68
P22907	HMBS	Porphobilinogen deaminase	11,55
Q3YW42	CCDC9	Coiled-coil domain containing 9	11,34
A0A0R4J008	HDAC2	Histone deacetylase 2	11,16
Q9CQU7	SNRPB2	U2 small nuclear ribonucleoprotein B''	11,14
A0A0991EKZ2	FXR2	FMR1 autosomal homolog 2	10,88
Q9EPU0	UPF1	Regulator of nonsense transcripts 1	10,75
Q6PAC3	DCAF13	DDB1- and CUL4-associated factor 13	10,52
Q64337	SQSTM1	Sequestosome-1	10,51
Q8VE70	PDCD10	Programmed cell death protein 10	10,22
P70372	ELAVL1	ELAV-like protein 1	10,17
A0A0N4SUH8	NFU1	NFU1 iron-sulfur cluster scaffold homolog, mitochondrial	10,12
Q8JZX4	RBM17	Splicing factor 45	9,95
Q5EG47	PRKAA1	5'-AMP-activated protein kinase catalytic subunit alpha-1	9,95
Q9CXI5	MANF	Mesencephalic astrocyte-derived neurotrophic factor	9,82
Q9JI89	CCDC86	Coiled-coil domain-containing protein 86	9,54
Q9R078	PRKAB1	5'-AMP-activated protein kinase subunit beta-1	9,50
Q8BK67	RCC2	Protein RCC2	9,30
E9PUK3	FNBP1L	Formin-binding protein 1-like	9,18
Q99PA7	MAGEA13	MAGE family member A13	8,99
Q64433	HSPE1	10 kDa heat shock protein, mitochondrial	8,96
Q39JH7	EXOSC9	Exosome complex component RRP45	8,86
Q3BC1D8	IWS1	Protein IWS1 homolog	8,85
Q9JI13	UTP3	Something about silencing protein 10	8,83
O08547	SEC22B	Vesicle-trafficking protein SEC22b	8,63
P52734	FGD1	FYVE, RhoGEF and PH domain-containing protein 1	8,38
Q9QUI7	ACSL4	Long-chain-fatty-acid--CoA ligase 4	8,22
O54950	PRKAG1	5'-AMP-activated protein kinase subunit gamma-1	8,20
P97461	RPS5	Small ribosomal subunit protein uS7	8,06
P24788	CDK11B	Cyclin-dependent kinase 11B	8,00
Q8VCH8	UBXN4	UBX domain-containing protein 4	7,86
Q9CPN8	IGF2BP3	Insulin-like growth factor 2 mRNA-binding protein 3	7,84
Q80UM7	MOGS	Mannosyl-oligosaccharide glucosidase	7,84
P00493	HPRT1	Hypoxanthine-guanine phosphoribosyltransferase	7,68
Q9WTX2	PRKRA	Interferon-inducible double-stranded RNA-dependent protein kinase activator A	7,60
P67984	RPL22	Large ribosomal subunit protein eL22	7,55
Q6ZWU9	RPS27	Small ribosomal subunit protein eS27	7,34
Q8BJ71	NUP93	Nuclear pore complex protein Nup93	7,34
D3Z722	RPS19	40S ribosomal protein S19	7,27
P35279	RAB6A	Ras-related protein Rab-6A	7,02
Q9R190	MTA2	Metastasis-associated protein MTA2	6,97
P12265	GUSB	Beta-glucuronidase	6,81
P16045	LGALS1	Galectin-1	6,66
Q4FZC9	SYNE3	Nesprin-3	6,57
Q91Y58	CAMK1	Calcium/calmodulin-dependent protein kinase type 1	6,57
Q9D3E6	STAG1	Cohesin subunit SA-1	6,49
P17426	AP2A1	AP-2 complex subunit alpha-1	6,49
Q38X10	PGAM5	Serine/threonine-protein phosphatase PGAM5, mitochondrial	6,46
A0A5F8MP7	SH3PXD2B	SH3 and PX domains 2B	6,43
P68254	YWHAQ	14-3-3 protein theta	6,38
Q8K4Q8	COLEC12	Collectin-12	6,19
Q3WTY4	CIAPIN1	Anamorsin	6,17
P84099	RPL19	Large ribosomal subunit protein eL19	6,06
O55126	NIPSNAP2	Protein NipSnap homolog 2	6,05
Q9ES97	RTN3	Reticulon-3	6,04
Q9ERB0	SNAP29	Synaptosomal-associated protein 29	6,04
P47964	RPL36	Large ribosomal subunit protein eL36	5,96
Q8BL97	SRSF7	Serine/arginine-rich splicing factor 7	5,93
Q3UEB3	PUF60	Poly(U)-binding-splicing factor PUF60	5,89
Q8CCK0	MACROH2A2	Core histone macro-H2A.2	5,87
Q9DBE6	RPL4	Large ribosomal subunit protein uL4	5,76
Q5E925	DDX46	Probable ATP-dependent RNA helicase DDX46	5,60
Q8BL66	EEA1	Early endosome antigen 1	5,49
Q7TMK9	SYNCRIP	Heterogeneous nuclear ribonucleoprotein Q	5,56
P15116	CDH2	Cadherin-2	5,52
Q91VK1	BZW2	eIF5-mimic protein 1	5,52
Q6PE01	SNRNP40	U5 small nuclear ribonucleoprotein 40 kDa protein	5,51
O3YT71	GLYR1	Cytokine-like nuclear factor N-PAC	5,45
P86048	RPL10L	Large ribosomal subunit protein uL16-like	5,34
P29341	PABPC1	Polyadenylate-binding protein 1	5,34
Q8BYK6	YTHDF3	YTH domain-containing family protein 3	5,28
P68510	YWHAH	14-3-3 protein eta	5,27
P61982	YWHAG	14-3-3 protein gamma	5,25
Q61205	PAFAH1B3	Platelet-activating factor acetylhydrolase IB subunit alpha1	5,23
Q5U017	PHACTR4	Phosphatase and actin regulator 4	5,20
P35762	CD81	CD81 antigen	5,20
Q8R1B4	EIF3C	Eukaryotic translation initiation factor 3 subunit C	5,19
P27659	RPL3	Large ribosomal subunit protein uL3	5,19
P40240	CD9	CD9 antigen	5,19
P61027	RAB10	Ras-related protein Rab-10	5,17
Q8BSY0	ASPH	Aspartyl/asparaginyl beta-hydroxylase	5,16
P62855	RPS26	Small ribosomal subunit protein eS26	5,12
B2RRE7	OTUD4	OTU domain-containing protein 4	5,11
Q5F2E7	NUFIP2	FMR1-interacting protein NUFIP2	5,11
Q61335	BCAP31	B-cell receptor-associated protein 31	5,10
P47915	RPL29	Large ribosomal subunit protein eL29	5,09
P03975	IAP	IgE-binding protein	5,05
E9QAQ7	ARID1A	AT rich interactive domain 1A (SWI-like)	5,04
Q88MJ2	LARS1	Leucine--tRNA ligase, cytoplasmic	5,03
Q9Z315	SART1	U4/U6.U5 tri-snRNP-associated protein 1	4,97
Q6PHQ9	PABPC4	Polyadenylate-binding protein	4,97
Q6PGL7	WASHC2	WASH complex subunit 2	4,95
P50543	S100A11	Protein S100-A11	4,94
P21995	EMB	Embigin	4,92
Q3YZC9	SF1	Splicing factor 1	4,92
O35295	PURB	Transcriptional activator protein Pur-beta	4,91
Q3UL36	ARGLU1	Arginine and glutamate-rich protein 1	4,90
Q60631	GRB2	Growth factor receptor-bound protein 2	4,88
P63276	RPS17	Small ribosomal subunit protein eS17	4,87
Q9D0I8	MRTO4	mRNA turnover protein 4 homolog	4,80
P62889	RPL30	Large ribosomal subunit protein eL30	4,77
Q569Z6	THRAP3	Thyroid hormone receptor-associated protein 3	4,76
P50446	KRT6A	Keratin, type II cytoskeletal 6A	4,73
P10639	TXN	Thioredoxin	4,73
F6ZDS4	TPR	Nucleoprotein TPR	4,72
Q9R1J0	NSDHL	Sterol-4-alpha-carboxylate 3-dehydrogenase, decarboxylating	4,69
A0A0991EN6	SFPQ	Splicing factor proline/glutamine rich (polypyrimidine tract binding protein associated)	4,65
O54941	SMARCE1	SWI/SNF-related matrix-associated actin-dependent regulator of chromatin subfamily E member 1	4,55
A0A1D5RM85	RPL18A	Ribosomal protein L18A (Fragment)	4,54
A0A1B0GS69	GM45713	60S ribosomal protein L13a	4,51
Q8BKV2	BRI3BP	BRI3-binding protein	4,51
Q8VHE0	SEC63	Translocation protein SEC63 homolog	4,49
P54227	STMN1	Stathmin	4,49
P46638	RAB11B	Ras-related protein Rab-11B	4,44
Q9D3L3	SNAP23	Synaptosomal-associated protein	4,41
E9QA15	CALD1	Caldesmon 1	4,38
Q61490	ALCAM	CD166 antigen	4,37
Q91YN9	BAG2	BAG family molecular chaperone regulator 2	4,36
Q3THK3	GTF2F1	General transcription factor IIF subunit 1	4,35
Q8CZQ7	HNRNPH1	Heterogeneous nuclear ribonucleoprotein H1	4,35
Q8K1N4	SPATS2	Spermatogenesis-associated serine-rich protein 2	4,34
Q9DCE5	PAK1IP1	p21-activated protein kinase-interacting protein 1	4,34
Q91VX2	UBAP2	Ubiquitin-associated protein 2	4,30
Q5SWN2	RPA1	Replication protein A subunit	4,29
Q61576	FKBP10	Peptidyl-prolyl cis-trans isomerase FKBP10	4,29
Q9DAW6	PRPF4	U4/U6 small nuclear ribonucleoprotein Prp4	4,27
Q61584	FXR1	RNA-binding protein FXR1	4,27
P62071	RRAS2	Ras-related protein R-Ras2	4,26
P17427	AP2A2	AP-2 complex subunit alpha-2	4,25
P62259	YWHAE	14-3-3 protein epsilon	4,25
P97372	PSME2	Proteasome activator complex subunit 2	4,25
Q9CX86	HNRNPA0	Heterogeneous nuclear ribonucleoprotein A0	4,24
E9QA16	CALD1	Caldesmon 1	4,23
P62918	RPL8	Large ribosomal subunit protein uL2	4,22
Q9R020	ZRANB2	Zinc finger Ran-binding domain-containing protein 2	4,21
Q02013	AQP1	Aquaporin-1	4,21
Q7TNV0	DEK	Protein DEK	4,20
Q08539	BIN1	Myc box-dependent-interacting protein 1	4,18
P14869	RPLP0	Large ribosomal subunit protein uL10	4,17
Q9QZD8	SLC25A10	Mitochondrial dicarboxylate carrier	4,17
Q8CG47	SMC4	Structural maintenance of chromosomes protein 4	4,16
Q5XJF6	RPL10A	Ribosomal protein	4,16
G5Z189	SNRPA	U1 small nuclear ribonucleoprotein A	4,14
P62960	YBX1	Y-box-binding protein 1	4,13
Q9D0R4	DDX56	Probable ATP-dependent RNA helicase DDX56	4,12
A0A0R4J0Q5	LMNB2	Lamin B2	4,11
Q9QUX4	SLC25A13	Electrogenic aspartate/glutamate antiporter SLC25A13, mitochondrial	4,11
Q99K48	NONO	Non-POU domain-containing octamer-binding protein	4,06
P63242	EIF5A	Eukaryotic translation initiation factor 5A-1	4,06
P62869	ELOB	Elongin-B	4,04
Q92DL0	TPBG	Trophoblast glycoprotein	4,01
P56183	RRP1	Ribosomal RNA processing protein 1 homolog A	3,99
P26369	U2AF2	Splicing factor U2AF 65 kDa subunit	3,98
A2A9Q2	NRD1	Nardilysin, N-arginine dibasic convertase, NRD convertase 1	3,97
P17809	SLC2A1	Solute carrier family 2, facilitated glucose transporter member 1	3,96
Q8VBT6	APOBR	Apolipoprotein B receptor	3,96
P97855	G3BP1	Ras GTPase-activating protein-binding protein 1	3,96
A0A6Q6PUT5	PRPF40A	Pre-mRNA processing factor 40A (Fragment)	3,95
O35345	KPNA6	Importin subunit alpha-7	3,94
A2ASS3	STAU1	Staufen double-stranded RNA binding protein 1	3,90
Q62159	RHOC	Rho-related GTP-binding protein RhoC	3,88
P09671	SOD2	Superoxide dismutase [Mn], mitochondrial	3,86
A0A5F8MP57	ACP2	Acid phosphatase 2, lysosomal	3,85
Q8VEK3	HNRNPU	Heterogeneous nuclear ribonucleoprotein U	3,85
Q9R0L6	PCM1	Pericentriolar material 1 protein	3,84
Q6ZQS8	LARP1	La-related protein 1	3,81
A0A286YDA2	NOLC1	Nucleolar and coiled-body phosphoprotein 1	3,80
Q9R0Y5	AK1	Adenylate kinase isoenzyme 1	3,80
P97379	G3BP2	Ras GTPase-activating protein-binding protein 2	3,80
Q922Q8	LRRC59	Leucine-rich repeat-containing protein 59	3,79
Q6P5H2	NES	Nestin	3,77
P62082	RPS7	Small ribosomal subunit protein eS7	3,74
A0A4948945	RAB1B	RAB1B, member RAS oncogene family (Fragment)	3,73
E9QB02	36951	Methionine--tRNA ligase, cytoplasmic	3,73
Q9D0E1	HNRNPM	Heterogeneous nuclear ribonucleoprotein M	3,72
Q9CWK3	CD2BP2	CD2 antigen cytoplasmic tail-binding protein 2	3,69
O35516	NOTCH2	Neurogenic locus notch homolog protein 2	3,68
P61750	ARF4	ADP-ribosylation factor 4	3,66
Q9DBR7	PPP1R12A	Protein phosphatase 1 regulatory subunit 12A	3,61
P31324	PRKAR2B	cAMP-dependent protein kinase type II-beta regulatory subunit	3,60
Q9CQV8	YWHAB	14-3-3 protein beta/alpha	3,60
Q62418	DBNL	Drebrin-like protein	3,59
Q9DJG2	DLST	Dihydrolipoyllysine-residue succiniltransferase component of 2-oxoglutarate dehydrogenase complex, mitochondrial	3,57
A0A111SSH9	SPARC	SPARC	3,57
Q9CZH7	MXRA7	Matrix-remodeling-associated protein 7	3,52
Q920A7	AFG3L1	AFG3-like protein 1	3,52
A0A0R4J0J2	PPP4R2	Protein phosphatase 4, regulatory subunit 2	3,52
P43274	H1-4	Histone H1.4	3,51
Q9WUK2	EIF4H	Eukaryotic translation initiation factor 4H	3,51
E9QA55	CHD4	DNA helicase	3,51
P70349	HINT1	Adenosine 5'-monophosphoramidase HINT1	3,50
Q8BML9	QARS1	Glutamine--tRNA ligase	3,50
Q3UYV9	NCBP1	Nuclear cap-binding protein subunit 1	3,49
P62858	RPS28	Small ribosomal subunit protein eS28	3,49
Q9R002	IFI202	Interferon-activable protein 202	3,47
P12970	RPL7A	Large ribosomal subunit protein eL8	3,43
Q80X90	FLNB	Filamin-B	3,40
P42669	PURA	Transcriptional activator protein Pur-alpha	3,39
Q80UU9	PGRMC2	Membrane-associated progesterone receptor component 2	3,39
Q88G15	CTDSPL2	CTD small phosphatase-like protein 2	3,38
Q6PFA2	CLTA	Clathrin light chain	3,38
P23116	EIF3A	Eukaryotic translation initiation factor 3 subunit A	3,33
Q3TLH4	PRRC2C	Protein PRRC2C	3,33
Q61937	NPM1	Nucleophosmin	3,33
P09103	P4HB	Protein disulfide-isomerase	3,32
P49722	PSMA2	Proteasome subunit alpha type-2	3,31
Q920X1	AIFM1	Apoptosis-inducing factor 1, mitochondrial	3,31
Q9CQW9	IFITM3	Interferon-induced transmembrane protein 3	3,30
P63073	EIF4E	Eukaryotic translation initiation factor 4E	3,29
Q921F2	TARDBP	TAR DNA-binding protein 43	3,29
O35286	DHX15	ATP-dependent RNA helicase DHX15	3,29
Q9CQX2	CYBSB	Cytochrome b5 type B	3,28
Q8VDM6	HNRNPUL1	Heterogeneous nuclear ribonucleoprotein U-like protein 1	3,27
P08228	SOD1	Superoxide dismutase [Cu-Zn]	3,25
Q640M1	UTP14A	U3 small nucleolar RNA-associated protein 14 homolog A	3,25
O08583	ALYREF	THO complex subunit 4	3,25
Q91XV3	BASP1	Brain acid soluble protein 1	3,24
Q9CQD1	RABSA	Ras-related protein Rab-5A	3,24
O09106	HDAC1	Histone deacetylase 1	3,24
P70399	TP53BP1	TP53-binding protein 1	3,23
E9PZC3	BLVRB	Biliverdin reductase B (flavin reductase (NADPH))	3,22
P68037	UBE2L3	Ubiquitin-conjugating enzyme E2 L3	3,21
Q9WVC3	CAV2	Caveolin-2	3,20
P35282	RAB21	Ras-related protein Rab-21	3,20
P35979	RPL12	Large ribosomal subunit protein uL11	3,19
O35841	APIS	Apoptosis inhibitor 5	3,18
Q6P5D8	SMCHD1	Structural maintenance of chromosomes flexible hinge domain-containing protein 1	3,15
Q9Z2K1	KRT16	Keratin, type I cytoskeletal 16	3,15
G3UW86	PRC1	Protein regulator of cytokinesis 1	3,13
Q88H97	RCN3	Reticulocalbin-3	3,13
Q6P8I4	PCNP	PEST proteolytic signal-containing nuclear protein	3,12
Q8CH25	SLTM	SAFB-like transcription modulator	3,11
Q6PDG5	SMARCC2	SWI/SNF complex subunit SMARCC2	3,08
Q99MR6	SRRT	Serrate RNA effector molecule homolog	3,06
Q88FR4	GNS	N-acetylglucosamine-6-sulfatase	3,06
Q7TPV4	MYBBP1A	Myb-binding protein 1A	3,05
Q8CJF9	AGO3	Protein argonaute-3	3,05
P11438	LAMP1	Lysosome-associated membrane glycoprotein 1	3,05
Q8C266	RABSC	RABSC, member RAS oncogene family	3,04
Q91V41	RAB14	Ras-related protein Rab-14	3,03
Q920Q6	MSI2	RNA-binding protein Musashi homolog 2	3,02
Q9JIW9	RALB	Ras-related protein Ral-B	3,02
Q3TJ07	PDLIM7	PDZ and LIM domain protein 7	3,01
Q9D024	CCDC47	PAT complex subunit CCDC47	3,01
Q91VT0	NDUFV1	NADH dehydrogenase [ubiquinone] flavoprotein 1, mitochondrial	3,01
Q9QWH1	PHC2	Polyhomeotic-like protein 2	3,00
Q920N1	EIF2S3X	Eukaryotic translation initiation factor 2 subunit 3, X-linked	3,00
Q6IRU5	CLTB	Clathrin light chain B	2,99
A0A2R8VK76	CPSF1	Cleavage and polyadenylation specific factor 1	2,99
A0A1W2P7A1	RPS12	40S ribosomal protein S12	2,99
Q3UMU9	HDGFL2	Hepatoma-derived growth factor-related protein 2	2,98
Q88GT7	SMNDC1	Survival of motor neuron-related-splicing factor 30	2,97
P59999	ARPC4	Actin-related protein 2/3 complex subunit 4	2,96
Q20BD0	HNRNPAB	Heterogeneous nuclear ribonucleoprotein A/B	2,95
P62141	PPP1CB	Serine/threonine-protein phosphatase PP1-beta catalytic subunit	2,95
Q9R112	SQOR	Sulfide:quinone oxidoreductase, mitochondrial	2,93
H7BX95	SRSF1	Serine/arginine-rich splicing factor 1	2,93
Q8CEE7	RDH13	Retinol dehydrogenase 13	2,92
P63101	YWHAZ	14-3-3 protein zeta/delta	2,92
P53302	LRRAP1	Alpha-2-macroglobulin receptor-associated protein	2,91
A0A4948B95	EIF1A	Eukaryotic translation initiation factor 4C	2,91
Q9DC48	CDC40	Pre-mRNA-processing factor 17	2,90
Q88LH7	HIRIP3	HIRA-interacting protein 3	2,90
G6415Z	BTF3	Transcription factor BTF3	2,90
Q9JIK2	NUP50	Nuclear pore complex protein Nup50	2,89
H3BL37	TCOF1	Treacle ribosome biogenesis factor 1	2,89
Q9QXS6	DBN1	Drebrin	2,89
Q9CRS7	RPL14	Large ribosomal subunit protein eL14	2,88
Q9CPV5	PMF1	Polyamine-modulated factor 1	2,88
Q8K019	BCLAF1	Bcl-2-associated transcription factor 1	2,86
Q9DBX2	CCDC124	Coiled-coil domain-containing protein 124	2,86
A0A1W2P7Q9	MYL6	Myosin, light polypeptide 6, alkali, smooth muscle and non-muscle	2,86
P62137	PPP1CA	Serine/threonine-protein phosphatase PP1-alpha catalytic subunit	2,86
P15306	THBD	Thrombomodulin	2,85
E0CXN1	FXYD5	FXYD domain-containing ion transport regulator	2,84
Q9CQB5	CISD2	CDGSH iron-sulfur domain-containing protein 2	2,82
Q9CQF3	NUDT21	Cleavage and polyadenylation specificity factor subunit 5	2,82
P23198	CBX3	Chromobox protein homolog 3	2,81
Q9CQQ7	ATP5PB	ATP synthase F(0) complex subunit B1, mitochondrial	2,80
Q9Z2B9	RPS6KA4	Ribosomal protein S6 kinase alpha-4	2,80
Q9DBG3	AP2B1	AP-2 complex subunit beta	2,79
Q8CFX3	PCDH1	Protocadherin 1	2,78
E9PZ21	RBMS1	RNA binding motif, single stranded interacting protein 1	2,78
Q62470	ITGA3	Integrin alpha-3	2,76
A2APM2	CD44	CD44 antigen	2,76
P62702	RPS4X	Small ribosomal subunit protein eS4	2,75
P52293	KPNA2	Importin subunit alpha-1	2,74
Q3TEA8	HP1BP3	Heterochromatin protein 1-binding protein 3	2,73
P11688	ITGA5	Integrin alpha-5	2,71
P62242	RPS8	Small ribosomal subunit protein eS8	2,70
Q9DBB3	CHMP4B	Charged multivesicular body protein 4b	2,70
Q61550	RAD21	Double-strand-break repair protein rad21 homolog	2,69
Q9CPS7	PNO1	RNA-binding protein PNO1	2,69
Q91VC3	EIF4A3	Eukaryotic initiation factor 4A-III	2,68
Q9DB15	MRPL12	Large ribosomal subunit protein bL12m	2,68
Q9CR80	FAM32A	Protein FAM32A	2,67
P26645	MARCKS	Myristoylated alanine-rich C-kinase substrate	2,67
Q8VCY6	UTP6	U3 small nucleolar RNA-associated protein 6 homolog	2,66
Q6NSP9	HMGA2	High mobility group AT-hook 2	2,66
Q9DST0	ATAD1	Outer mitochondrial transmembrane helix translocase	2,65
Q8CCF0	PRPF31	U4/U6 small nuclear ribonucleoprotein Prp31	2,64
B1AT82	PRPSAP1	Phosphoribosyl pyrophosphate synthetase-associated protein 1	2,63
Q62093	SRSF2	Serine/arginine-rich splicing factor 2	2,63
B1AVB1	SCML2	Scm polycomb group protein like 2	2,62
Q9CQE8	RTRAF	RNA transcription, translation and transport factor protein	2,61
Q8BGD9	EIF4B	Eukaryotic translation initiation factor 4B	2,61
P47911	RPL6	Large ribosomal subunit protein eL6	2,61
P07091	S100A4	Protein S100-A4	2,60
Q9DB96	NGDN	Neuroguidin	2,60
O09131	GSTO1	Glutathione S-transferase omega-1	2,60
P62751	RPL23A	Large ribosomal subunit protein uL23	2,60
Q9ESX5	DKC1	H/ACA ribonucleoprotein complex subunit DKC1	2,60
O70318	EPB41L2	Band 4.1-like protein 2	2,59
Q8CI59	STEAP3	Metalloreductase STEAP3	2,59
G3X9Q6	LARP4	La ribonucleoprotein 4	2,59
O08709	PRDX6	Peroxiredoxin-6	2,59
Q8BHY2	NOC4L	Nucleolar complex protein 4 homolog	2,59
P53690	MMP14	Matrix metalloproteinase-14	2,57
Q8K094	PVR	Poliovirus receptor	2,56
Q99PL5	RRBP1	Ribosome-binding protein 1	2,56
Q99ME9	GTPBP4	GTP-binding protein 4	2,56
Q9JLV1	BAG3	BAG family molecular chaperone regulator 3	2,54
Q8RSL1	C1QBP	Complement component 1 Q subcomponent-binding protein, mitochondrial	2,53
Q91VR5	DDX1	ATP-dependent RNA helicase DDX1	2,53
Q9JKB3	YBX3	Y-box-binding protein 3	2,53
F8WGL3	CFL1	Cofilin 1, non-muscle	2,52
Q60598	CTTN	Src substrate cortactin	2,52
P47791	GSR	Glutathione reductase, mitochondrial	2,52
P60904	DNAJC5	Dnaj homolog subfamily C member 5	2,52
Q9DBG5	PLIN3	Perilipin-3	2,50
Q88T50	DDX5	Probable ATP-dependent RNA helicase DDX5	2,50
Q9DC63	FBXO3	F-box only protein 3	2,50
P62281	RPS11	Small ribosomal subunit protein uS17	2,49
P47962	RPL5	Large ribosomal subunit protein uL18	2,49
F7AA26	PAKAP	Paralemmin A kinase anchor protein (Fragment)	2,48
D3Z5J1	ZC3HAV1	Zinc finger CCCH type, antiviral 1	2,48
Q8BSL7	ARF2	ADP-ribosylation factor 2	2,48
Q8BMK4	CKAP4	Cytoskeleton-associated protein 4	2,47
Q9JIX8	ACIN1	Apoptotic chromatin condensation inducer in the nucleus	2,47
Q60749	KHDRBS1	KH domain-containing, RNA-binding, signal transduction-associated protein 1	2,47
Q8K224	NAT10	RNA cytidine acetyltransferase	2,47
Q9CPR4	RPL17	Large ribosomal subunit protein uL22	2,45
Q8VCI5	PEX19	Peroxisomal biogenesis factor 19	2,45
Q9DBS5	SRSF5	Serine and arginine-rich splicing factor 5	2,45
O70439	STX7	Syntaxin-7	2,44
P17225	PTBP1	Polypyrimidine tract-binding protein 1	2,43
P27546	MAP4	Microtubule-associated protein 4	2,43
P97351	RPS3A	Small ribosomal subunit protein eS1	2,43
P63321	RALA	Ras-related protein Ral-A	2,42
A0A0N4SW73	RAB11FIP5	RAB11 family interacting protein 5 (class I)	2,41
Q8R3H7	HS2ST1	Heparan sulfate 2-O-sulfotransferase 1	2,41
Q8BH74	NUP107	Nuclear pore complex protein Nup107	2,41
Q88Q30	PPP1R18	Phostensin	2,40
Q99LI7	CSTF3	Cleavage stimulation factor subunit 3	2,40
Q9D503	EBNA1BP2	Probable rRNA-processing protein EBP2	2,39
Q80XU3	NUCKS1	Nuclear ubiquitous casein and cyclin-dependent kinase substrate 1	2,39
Q9D1D4	TMED10	Transmembrane emp24 domain-containing protein 10	2,39
P61211	ARL1	ADP-ribosylation factor-like protein 1	2,38
P41105	RPL28	Large ribosomal subunit protein eL28	2,38
S4R189	ARHGEF40	Rho guanine nucleotide exchange factor (GEF) 40	2,37
Q9JHJ0	TMOD3	Tropomodulin-3	2,36
Q91YR7	PRPF6	Pre-mRNA-processing factor 6	2,35
P62264	RPS14	Small ribosomal subunit protein uS11	2,35
P47963	RPL13	Large ribosomal subunit protein eL13	2,34
Q62446	FKBP3	Peptidyl-prolyl cis-trans isomerase FKBP3	2,34
P32067	SSB	Lupus La protein homolog	2,34
Q9D113	SARNP	SAP domain-containing ribonucleoprotein	2,34
Q8VDD5	MYH9	Myosin-9	2,33
Q60865	CAPRIN1	Caprin-1	2,33
P62754	RPS6	Small ribosomal subunit protein eS6	2,33
P53995	ANAPC1	Anaphase-promoting complex subunit 1	2,33
O35381	ANP32A	Acidic leucine-rich nuclear phosphoprotein 32 family member A	2,31
Q60VA0	LEMD2	LEM domain-containing protein 2	2,31
P62245	RPS15A	Small ribosomal subunit protein uS8	2,31
P17047	LAMP2	Lysosome-associated membrane glycoprotein 2	2,31
Q91WK2	EIF3H	Eukaryotic translation initiation factor 3 subunit H	2,30
Q6NZB0	DNAJC8	Dnaj homolog subfamily C member 8	2,29
F8VQJ3	LAMC1	Laminin, gamma 1	2,28
P15864	H1-2	Histone H1.2	2,28
A0A286YDF5	MYOF	Myoferlin	2,28
E9QG34	MYO1E	Unconventional myosin-Ie	2,28
O08749	DLD	Dihydrolipoyl dehydrogenase, mitochondrial	2,28
Q99LP6	GRPEL1	GrpE protein homolog 1, mitochondrial	2,28
A0A111SVG6	SLC44A2	Choline transporter-like protein	2,27
Q922B2	DARS1	Aspartate--tRNA ligase, cytoplasmic	2,26
P13864	DNMT1	DNA (cytosine-5)-methyltransferase 1	2,26

Supplemental table 5 : Summary table of proteins present in NIH-3T3-Src-Tks5-GFP cells seeded on collagen identified by mass spectrometry analysis of Tks5 interactome

Accession	Gene Name	Description	Abundance Ratio: (TKS5) / (Control)
Q89032	SH3PXD2A	SH3 and PX domain-containing protein 2A	69,75
O55201	SUPTSH	Transcription elongation factor SPT5	34,69
Q9JMS1	PTGES	Prostaglandin E synthase	31,66
Q61081	CDC37	Hsp90 co-chaperone Cdc37	22,03
O3YX43	VSIG10	V-set and immunoglobulin domain-containing protein 10	15,34
E9PUK3	FNBP1L	Formin-binding protein 1-like	15,07
O88839	ADAM15	Disintegrin and metalloproteinase domain-containing protein 15	14,15
Q9CXI5	MANF	Mesencephalic astrocyte-derived neurotrophic factor	14,12
Q9JKB3	YBX3	Y-box-binding protein 3	14,01
F8WIP8	SPP1	Secreted phosphoprotein 1	13,11
P47915	RPL29	Large ribosomal subunit protein eL29	11,74
E9QA15	CALD1	Caldesmon 1	11,71
A0A180GR85	2900026A02RIK	RIKEN cDNA 2900026A02 gene	11,64
O35674	ADAM19	Disintegrin and metalloproteinase domain-containing protein 19	11,11
E9Q9C3	AFDN	Afadin, adherens junction formation factor	9,65
E9Q450	TPM1	Tropomyosin 1, alpha	8,94
Q3TIV5	ZC3H15	Zinc finger CCCH domain-containing protein 15	8,88
O3YW42	CCDC9	Coiled-coil domain containing 9	8,78
Q8HWA3	ULBP1	UL16 binding protein 1	8,51
E9QK89	MDC1	Mediator of DNA damage checkpoint protein 1	8,49
O08539	BIN1	Myc box-dependent-interacting protein 1	8,36
Q61584	FXR1	RNA-binding protein FXR1	8,36
Q9QZM4	TNFRSF10B	Tumor necrosis factor receptor superfamily member 10B	8,20
Q80Y55	BSDC1	BSD domain-containing protein 1	8,06
Q61792	LASP1	LIM and SH3 domain protein 1	7,82
O70251	EEF1B	Elongation factor 1-beta	7,79
Q5F2E7	NUFIP2	FMR1-interacting protein NUFIP2	7,69
Q9JLB9	NECTIN3	Nectin-3	7,68
Q91XV3	BASP1	Brain acid soluble protein 1	7,68
Q99PA7	MAGEA13	MAGE family member A13	7,67
Q7TSJ2	MAP6	Microtubule-associated protein 6	7,45
Q91VX2	UBAP2	Ubiquitin-associated protein 2	7,39
P51125	CAST	Calpastatin	7,37
Q9JIX8	ACIN1	Apoptotic chromatin condensation inducer in the nucleus	7,31
Q6PGL7	WASHC2	WASH complex subunit 2	7,19
Q61490	ALCAM	CD166 antigen	6,85
D3YVW2	GOLIM4	Golgi integral membrane protein 4	6,77
F62960	YBX1	Y-box-binding protein 1	6,74
Q9WVC3	CAV2	Caveolin-2	6,61
P70452	STX4	Syntaxin-4	6,49
Q9D8S5	SRSF5	Serine and arginine-rich splicing factor 5	6,43
F6ZDS4	TPR	Nucleoprotein TPR	6,41
O89116	VTI1A	Vesicle transport through interaction with t-SNAREs homolog 1A	6,41
A0A2B6YDV7	NDLC1	Nucleolar and coiled-body phosphoprotein 1 (Fragment)	6,37
E9QA16	CALD1	Caldesmon 1	6,33
P26645	MARCKS	Myristoylated alanine-rich C-kinase substrate	6,30
Q9DBE9	FTSJ3	pre-rRNA 2'-O-ribose RNA methyltransferase FTSJ3	6,20
O54901	CD200	OX-2 membrane glycoprotein	6,18
Q8CIS1	PDLIM5	PDZ and LIM domain protein 5	6,18
Q9ERB0	SNAP29	Synaptosomal-associated protein 29	6,15
Q8VBT6	APOBR	Apolipoprotein B receptor	6,04
P62141	PPP1CB	Serine/threonine-protein phosphatase PP1-beta catalytic subunit	5,98
O35226	PSMD4	26S proteasome non-ATPase regulatory subunit 4	5,90
P21995	EMB	Embigin	5,88
P63024	VAMP3	Vesicle-associated membrane protein 3	5,80
P40240	CD9	CD9 antigen	5,80
P47964	RPL36	Large ribosomal subunit protein eL36	5,68
Q3UDR8	YIPF3	Protein YIPF3	5,66
Q62093	SRSF2	Serine/arginine-rich splicing factor 2	5,65
P35762	CD81	CD81 antigen	5,53
P97298	SERPINF1	Pigment epithelium-derived factor	5,48
A0A0N4SW73	RAB11FIP5	RAB11 family interacting protein 5 (class I)	5,46
Q3THK3	GTF2F1	General transcription factor IIF subunit 1	5,42
P68254	YWHAQ	14-3-3 protein theta	5,39
Q8BQ30	PPP1R18	Phostensin	5,36
Q8K019	BCLAF1	Bcl-2-associated transcription factor 1	5,34
A0A11LSSH9	SPARC	SPARC	5,32
Q4VAA2	CDV3	Protein CDV3	5,30
P22907	HMBS	Porphobilinogen deaminase	5,28
P62869	ELOB	Elongin-B	5,24
P27659	RPL3	Large ribosomal subunit protein uL3	5,19
Q3UM45	PPP1R7	Protein phosphatase 1 regulatory subunit 7	5,19
Q9WUK2	EIF4H	Eukaryotic translation initiation factor 4H	5,17
Q8BGD9	EIF4B	Eukaryotic translation initiation factor 4B	5,11
Q99NB8	UBQLN4	Ubiquilin-4	5,09
Q8BL66	EEA1	Early endosome antigen 1	5,08
A2AJI0	MAP7D1	MAP7 domain-containing protein 1	5,06
Q6AD65	CEP170	Centrosomal protein of 170 kDa	5,05
Q8R1B4	EIF3C	Eukaryotic translation initiation factor 3 subunit C	5,04
P81117	NUCB2	Nucleobindin-2	5,00
Q5D1J7	PHACTR4	Phosphatase and actin regulator 4	5,00
P47968	RPIA	Ribose-5-phosphate isomerase	4,98
O35435	DHODH	Dihydroorotate dehydrogenase (quinone), mitochondrial	4,98
Q3D5D4	EIF5B	Eukaryotic translation initiation factor 5B	4,96
D88477	IGF2BP1	Insulin-like growth factor 2 mRNA-binding protein 1	4,87
Q9Z1Z0	USO1	General vesicular transport factor p115	4,86
E9Q6J5	BOD1L	Biorientation of chromosomes in cell division protein 1-like 1	4,86
Q3TLH4	PRRC2C	Protein PRRC2C	4,86
A2APM2	CD44	CD44 antigen	4,81
Q04887	SOX9	Transcription factor SOX-9	4,72
P00493	HPRT1	Hypoxanthine-guanine phosphoribosyltransferase	4,69
A0A668KEL1	LRRFIP2	Leucine rich repeat (in FLII) interacting protein 2	4,68
Q9Z315	SART1	U4/U6.U5 tri-snRNP-associated protein 1	4,62
O70318	EP841L2	Band 4.1-like protein 2	4,61
Q92DJ0	NPC2	NPC intracellular cholesterol transporter 2	4,61
Q9R1Q7	PLP2	Proteolipid protein 2	4,59
O54950	PRKAG1	5'-AMP-activated protein kinase subunit gamma-1	4,52
O08749	DLD	Dihydrolipoyl dehydrogenase, mitochondrial	4,51
Q9JLV1	BAG3	BAG family molecular chaperone regulator 3	4,47
P60904	DNAJC5	DnaJ homolog subfamily C member 5	4,44
Q6XLQ8	CALU	Calumenin	4,40
Q99PL5	RRBP1	Ribosome-binding protein 1	4,40
Q9RDA0	PEX14	Peroxisomal membrane protein PEX14	4,39
Q56926	THRAP3	Thyroid hormone receptor-associated protein 3	4,37
Q9D024	CCDC47	PAT complex subunit CCDC47	4,37
P15116	CDH2	Cadherin-2	4,36
Q9DBG5	PLIN3	Perilipin-3	4,36
Q5SF07	IGF2BP2	Insulin-like growth factor 2 mRNA-binding protein 2	4,34
P68510	YWHAH	14-3-3 protein eta	4,34
P62849	RPS24	Small ribosomal subunit protein eS24	4,32
A7YY80	EPB41L3	130kDa Protein 4.1B MEF cell isoform	4,31
F8WHT3	PRRC2B	Proline-rich coiled-coil 2B	4,31
Q9WUR9	AK4	Adenylate kinase 4, mitochondrial	4,30
Q5EG47	PRKAA1	5'-AMP-activated protein kinase catalytic subunit alpha-1	4,30
O70400	PDLIM1	PDZ and LIM domain protein 1	4,30
Q8KZF8	LSM14A	Protein LSM14 homolog A	4,26
O54998	FKBP7	Peptidyl-prolyl cis-trans isomerase FKBP7	4,26
Q9CY58	SERBP1	SERPINE1 mRNA-binding protein 1	4,26
Q3UMF0	CDBL11	Cordon-bleu protein-like 1	4,22
P61804	DAD1	Dolichyl-diphosphooligosaccharide--protein glycosyltransferase subunit DAD1	4,21
Q8R317	UBQLN1	Ubiquilin-1	4,21
Q62470	ITGA3	Integrin alpha-3	4,20
P54726	RAD23A	UV excision repair protein RAD23 homolog A	4,19
E9QM77	ATXN2	Ataxin 2	4,19
Q925B0	PAWR	PRKC apoptosis WT1 regulator protein	4,19
E9Q7Q3	TPM3	Tropomyosin 3, gamma	4,18
Q6IRU2	TPM4	Tropomyosin alpha-4 chain	4,18
E9Q8L9	RAB11FIP1	RAB11 family interacting protein 1 (class I)	4,17
Q80X50	UBAP2L	Ubiquitin-associated protein 2-like	4,12
A0A5K1VQ9	TTN	Titin	4,11
P10639	TXN	Thioredoxin	4,08
O08602	RAET1A	Retinoic acid early-inducible protein 1-alpha	4,07
Q6IRU5	CLTB	Clathrin light chain B	4,06
Q3TGG2	ATXN2L	Ataxin 2-like	4,06
Q9RD20	ZRANB2	Zinc finger Ran-binding domain-containing protein 2	4,06
Q8K094	PVR	Poliovirus receptor	4,01
Q3UL36	ARGLU1	Arginine and glutamate-rich protein 1	3,98
Q9DBR7	PPP1R12A	Protein phosphatase 1 regulatory subunit 12A	3,96
Q9QZM0	UBQLN2	Ubiquilin-2	3,93
Q7TSC1	PRRC2A	Protein PRRC2A	3,93
Q8BH97	RCN3	Reticulocalbin-3	3,92
Q62418	DBNL	Drebrin-like protein	3,91
Q8BS69	HNRNPA2B1	Heterogeneous nuclear ribonucleoproteins A2/B1	3,86
F7AA26	PAKAP	Paralemmin A kinase anchor protein (Fragment)	3,85
Q6PGH2	JPT2	Jupiter microtubule associated homolog 2	3,85
Q80WW9	DDRGK1	DDRGK domain-containing protein 1	3,82
Q6TEK5	VKORC1L1	Vitamin K epoxide reductase complex subunit 1-like protein 1	3,80
Q05186	RCN1	Reticulocalbin-1	3,79
Q9EQQ8	SGSH	Heparan N-sulfatase	3,76
P35492	HAL	Histidine ammonia-lyase	3,73
Q8CI26	NRADD	Death domain-containing membrane protein NRADD	3,73
Q61335	BCAP31	B-cell receptor-associated protein 31	3,73
Q6P6J9	TXNDC15	Thioredoxin domain-containing protein 15	3,71
Q62446	FKBP3	Peptidyl-prolyl cis-trans isomerase FKBP3	3,70
P11087	COL1A1	Collagen alpha-1(I) chain	3,70
Q62011	PDPN	Podoplanin	3,66
A0A0R4J0U2	PPP4R2	Protein phosphatase 4, regulatory subunit 2	3,66
P49817	CAV1	Caveolin-1	3,65
Q6PFA2	CLTA	Clathrin light chain	3,65
P97287	MCL1	Induced myeloid leukemia cell differentiation protein Mcl-1 homolog	3,63
Q9CQR2	RPS21	Small ribosomal subunit protein eS21	3,63
Q3UJB0	SF3B2	Splicing factor 3b, subunit 2	3,60
Q0VAW6	8030462N17RIK	RIKEN cDNA 8030462N17 gene	3,59
Q8BIQ5	CSTF2	Cleavage stimulation factor subunit 2	3,58
Q922Q8	LRRC59	Leucine-rich repeat-containing protein 59	3,57
Q9CQE8	RTRAF	RNA transcription, translation and transport factor protein	3,57
Q9JKF6	NECTIN1	Nectin-1	3,56
Q80YR5	SAFB2	Scaffold attachment factor B2	3,56
O70439	STX7	Syntaxin-7	3,53
Q8C3W1	1 SV	Uncharacterized protein C1orf198 homolog	3,53
Q91VK1	BZW2	eIF5-mimic protein 1	3,52
Q9Z1A1	TFG	TFG protein	3,52
P08228	SOD1	Superoxide dismutase [Cu-Zn]	3,51
A0A0J9YUR2	SPECC1	Sperm antigen with calponin homology and coiled-coil domains 1	3,50
A0A0B4J1E2	SNW1	SNW domain-containing protein 1	3,49
Q8C9B9	DIDO1	Death-inducer obliterator 1	3,48
Q8K1N4	SPATS2	Spermatogenesis-associated serine-rich protein 2	3,48
Q61576	FKBP10	Peptidyl-prolyl cis-trans isomerase FKBP10	3,47
Q7TT18	ATF7IP	Activating transcription factor 7-interacting protein 1	3,47
Q02819	NUCB1	Nucleobindin-1	3,45
Q9CYA0	CRELD2	Protein disulfide isomerase Creld2	3,45
H3BL37	TCOF1	Treacle ribosome biogenesis factor 1	3,43
P47911	RPL6	Large ribosomal subunit protein eL6	3,42
Q64152	BTF3	Transcription factor BTF3	3,41
Q62314	TGOLN2	Trans-Golgi network integral membrane protein 2	3,39
P28667	MARCKSL1	MARCKS-related protein	3,38
Q8R3Q6	MIX23	Protein MIX23	3,38
Q8K1J7	WIPF1	WAS/WASL-interacting protein family member 1	3,37
O08583	ALYREF	THO complex subunit 4	3,36
P11438	LAMP1	Lysosome-associated membrane glycoprotein 1	3,35
Q5SUH6	CLINT1	Clathrin interactor 1	3,33
P14873	MAP1B	Microtubule-associated protein 1B	3,32
P10518	ALAD	Delta-aminolevulinic acid dehydratase	3,32
Q99JF8	PSIP1	PC4 and SFRS1-interacting protein	3,31
Q60598	CTTN	Src substrate cortactin	3,31
Q3UZ39	LRRFIP1	Leucine-rich repeat flightless-interacting protein 1	3,31
A0A3B2WC15	RANBP3	RAN binding protein 3	3,29
P97797	SIRPA	Tyrosine-protein phosphatase non-receptor type substrate 1	3,29
P14148	RPL7	Large ribosomal subunit protein uL30	3,27
P55302	LRPAP1	Alpha-2-macroglobulin receptor-associated protein	3,25
Q8K298	ANLN	Anillin	3,25
P51859	HDGF	Hepatoma-derived growth factor	3,25
Q9E597	RTN3	Reticulon-3	3,24
O55022	PGRMC1	Membrane-associated progesterone receptor component 1	3,22
I3QPG5	PSAP	Prosaposin	3,21
F56959	FUS	RNA-binding protein FUS	3,21
Q20BD0	HNRNPAB	Heterogeneous nuclear ribonucleoprotein A/B	3,20
Q7TMK9	SYNCRIP	Heterogeneous nuclear ribonucleoprotein Q	3,20
Q62165	DAG1	Dystroglycan 1	3,19
Q61937	NPM1	Nucleophosmin	3,19
P27546	MAP4	Microtubule-associated protein 4	3,19
Q8R143	PTTG1IP	Pituitary tumor-transforming gene 1 protein-interacting protein	3,18
Q3U9N4	GRN	Granulin	3,17
Q9QYE6	GOLGA5	Golgin subfamily A member 5	3,17
O35887	CALU	Calumenin	3,15
Q6PCQ6	EFCAB14	EF-hand calcium binding domain 14	3,14
P48036	ANXA5	Annexin A5	3,14
P54728	RAD23B	UV excision repair protein RAD23 homolog B	3,14
Q9JL35	HMGN5	High mobility group nucleosome-binding domain-containing protein 5	3,12
Q61810	LTBP3	Latent-transforming growth factor beta-binding protein 3	3,11
Q01149	COL1A2	Collagen alpha-2(I) chain	3,10
Q8VDD5	MYH9	Myosin-9	3,08
P09671	SOD2	Superoxide dismutase [Mn], mitochondrial	3,08
P70441	NHERF1	Na(+)/H(+) exchange regulatory cofactor NHE-RF1	3,07
Q3UH59	MYH10	Myosin, heavy polypeptide 10, non-muscle	3,06
A2AMH4	SLC44A1	Choline transporter-like protein	3,06
Q91XA2	GOLM1	Golgi membrane protein 1	3,04
Q8K201	KCT2	Keratinocyte-associated transmembrane protein 2	3,04
Q9WVE8	PACSIN2	Protein kinase C and casein kinase substrate in neurons protein 2	3,03
P84099	RPL19	Large ribosomal subunit protein eL19	3,01
Q9CZM2	RPL15	Large ribosomal subunit protein eL15	3,01
Q9DAU1	CNPY3	Protein canopy homolog 3	3,00
P61982	YWHAG	14-3-3 protein gamma	2,98
O88271	CFDP1	Craniofacial development protein 1	2,98
Q61074	PPM1G	Protein phosphatase 1G	2,97
P17809	SLC2A1	Solute carrier family 2, facilitated glucose transporter member 1	2,97
P97300	NPTN	Neuroplastin	2,97
Q6NZB0	DNAJC8	DnaJ homolog subfamily C member 8	2,96
A0A1D5RM85	RPL18A	Ribosomal protein L18A (Fragment)	2,96
P62137	PPP1CA	Serine/threonine-protein phosphatase PP1-alpha catalytic subunit	2,95
Q8BLN5	LSS	Lanosterol synthase	2,94
Q8K4Q8	COLEC12	Collectin-12	2,93
Q9CQP9	PCYOX1	Prenylcysteine oxidase 1	2,92
Q8CDE2	VPS26B	Vacuolar protein sorting-associated protein 26B	2,92
P97808	FXYD5	FXYD domain-containing ion transport regulator 5	2,92
P14869	RPLP0	Large ribosomal subunit protein uL10	2,92
P41731	CD63	CD63 antigen	2,92
Q8R4U7	LUZP1	Leucine zipper protein 1	2,91
P70399	TPS3BP1	TPS3-binding protein 1	2,90
Q9CR60	GOLT1B	Vesicle transport protein GOT1B	2,89
Q9WV80	SNX1	Sorting nexin-1	2,89
P43276	H1-5	Histone H1.5	2,89
P62962	PFN1	Profilin-1	2,89
Q61425	HADH	Hydroxyacyl-coenzyme A dehydrogenase, mitochondrial	2,89
Q8R550	SH3KBP1	SH3 domain-containing kinase-binding protein 1	2,88
Q9CQK7	RWDD1	RWD domain-containing protein 1	2,88
P62918	RPL8	Large ribosomal subunit protein uL2	2,88
Q62159	RHOC	Rho-related GTP-binding protein RhoC	2,88
O35381	ANP32A	Acidic leucine-rich nuclear phosphoprotein 32 family member A	2,88
Q00623	APOA1	Apolipoprotein A-I	2,87
A0A668KL36	CCDC50	Coiled-coil domain containing 50	2,87
Q3UHX2	PDAP1	28 kDa heat- and acid-stable phosphoprotein	2,87
P47962	RPL5	Large ribosomal subunit protein uL18	2,86
Q66JS6	EIF3J2	Eukaryotic translation initiation factor 3 subunit J-B	2,85
Q5U3K5	RABL6	Rab-like protein 6	2,85
Q8BP27	SFR1	Swi5-dependent recombination DNA repair protein 1 homolog	2,85
Q56925	DDX46	Probable ATP-dependent RNA helicase DDX46	2,85
Q9CZ44	NSFL1C	NSFL1 cofactor p47	2,85
Q80WJ7	MTDH	Protein LYRIC	2,84
Q8K1L5	PPP1R11	E3 ubiquitin-protein ligase PPP1R11	2,83
Q9CZH7	MXRA7	Matrix-remodeling-associated protein 7	2,83
E9Q1P8	IRF2BP2	Interferon regulatory factor 2-binding protein 2	2,82
P32067	SSB	Lupus La protein homolog	2,82
Q9ZDP4	PALM	Paralemmin-1	2,81
P14211	CALR	Calreticulin	2,81
Q8CHP5	PYM1	Partner of Y14 and mago	2,80
P12970	RPL7A	Large ribosomal subunit protein eL8	2,79
P09103	P4HB	Protein disulfide-isomerase	2,79
Q9CPV5	PMF1	Polyamine-modulated factor 1	2,78
Q5SU59	EWSR1	Ewing sarcoma breakpoint region 1	2,78
Q6P8I4	PCNP	PEST proteolytic signal-containing nuclear protein	2,78
P17047	LAMP2	Lysosome-associated membrane glycoprotein 2	2,77
Q80XU3	NUCKS1	Nuclear ubiquitous casein and cyclin-dependent kinase substrate 1	2,76
P11440	CDK1	Cyclin-dependent kinase 1	2,76
Q9DZG2	DLST	Dihydrolipoyllysine-residue succinyltransferase component of 2-oxoglutarate dehydrogenase complex, mitochondrial	2,75
G3X8R0	REEP5	Receptor expression-enhancing protein	2,74
Q99P72	RTN4	Reticulon-4	2,74
P47963	RPL13	Large ribosomal subunit protein eL13	2,74
O70503	HSD17B12	Very-long-chain 3-oxoacyl-CoA reductase	2,73
O88384	VTI1B	Vesicle transport through interaction with t-SNAREs homolog 1B	2,72
Q9WVK4	EHD1	EH domain-containing protein 1	2,71
Q9CQV8	YWHAB	14-3-3 protein beta/alpha	2,70
P46061	RANGAP1	Ran GTPase-activating protein 1	2,69
Q9JMI7	TEX101	Testis-expressed protein 101	2,68
O70401	TSPAN6	Tetraspanin-6	2,68
P12265	GUSB	Beta-glucuronidase	2,66
A0A1B0GS68	GM45713	60S ribosomal protein L13a	2,66
Q08579	EMD	Emerin	2,66
A2AUD5	TPD52L2	Tumor protein D52-like 2	2,64
P18572	BSG	Basigin	2,64
P62259	YWHAE	14-3-3 protein epsilon	2,64
Q8BXV2	BRI3BP	BRI3-binding protein	2,64
Q80UU9	PGRMC2	Membrane-associated progesterone receptor component 2	2,64
Q63918	CAVIN2	Caveolae-associated protein 2	2,63
P70670	NACA	Nascent polypeptide-associated complex subunit alpha, muscle-specific form	2,62
Q9DBB3	CHMP4B	Charged multivesicular body protein 4b	2,61
Q8BGT7	SMNDC1	Survival of motor neuron-related-splicing factor 30	2,61
P17225	PTBP1	Polypyrimidine tract-binding protein 1	2,61
P26041	MSN	Moesin	2,61
P16045	LGALS1	Galectin-1	2,61
Q8BG05	HNRNPA3	Heterogeneous nuclear ribonucleoprotein A3	2,61
Q921T2	TOR1AIP1	Torsin-1A-interacting protein 1	2,61
P59999	ARPC4	Actin-related protein 2/3 complex subunit 4	2,61
P63101	YWHAZ	14-3-3 protein zeta/delta	2,61
Q4PZA2	ECE1	Endothelin-converting enzyme 1	2,60
P32020	SCP2	Sterol carrier protein 2	2,57
Q8VCI5	PEX19	Peroxisomal biogenesis factor 19	2,56
Q8R409	HEXIM1	Protein HEXIM1	2,56
P97371	PSME1	Proteasome activator complex subunit 1	2,56
Q9R0X4	ACOT9	Acyl-coenzyme A thioesterase 9, mitochondrial	2,56
Q9DBE6	RPL4	Large ribosomal subunit protein uL4	2,55
P50543	S100A11	Protein S100-A11	2,55
P63276	RPS17	Small ribosomal subunit protein eS17	2,54
Q99LX0	PARK7	Parkinson disease protein 7 homolog	2,54
Q64314	CD34	Hematopoietic progenitor cell antigen CD34	2,54
Q91238	TTC1	Tetratricopeptide repeat protein 1	2,53
Q8C129	LNPEP	Leucyl-cystinyl aminopeptidase	2,52
Q6NZJ6	EIF4G1	Eukaryotic translation initiation factor 4 gamma 1	2,52
A0A286YCG8	SSR1	Translocon-associated protein subunit alpha	2,51
Q6P5H2	NES	Nestin	2,49
Q92DL0	TPBG	Trophoblast glycoprotein	2,48
Q88M72	HSPA13	Heat shock 70 kDa protein 13	2,47
F8WIV2	SERPINB6A	Serine (or cysteine) peptidase inhibitor, clade B, member 6a	2,47
A0A087WPK3	LRRFIP1	Leucine rich repeat (in FLII) interacting protein 1	2,46
A0A571BF54	KCNAB2	Voltage-gated potassium channel subunit beta-1	2,46
Q3BQ47	CNPY4	Protein canopy homolog 4	2,46
Q61166	MAPRE1	Microtubule-associated protein RP/EB family member 1	2,45
Q5EBP8	HNRNPA1	Heterogeneous nuclear ribonucleoprotein A1	2,44
P29341	PABPC1	Polyadenylate-binding protein 1	2,42
P20108	PRDX3	Thioredoxin-dependent peroxide reductase, mitochondrial	2,42
P62897	CYCS	Cytochrome c, somatic	2,42
O35685	NUDC	Nuclear migration protein nudC	2,42
Q9JKR6	HYOU1	Hypoxia up-regulated protein 1	2,42
P62754	RPS6	Small ribosomal subunit protein eS6	2,42
P97855	G3BP1	Ras GTPase-activating protein-binding protein 1	2,42
Q9QX56	DBN1	Drebrin	2,42
A2ARP8	MAP1A	Microtubule-associated protein 1 A	2,40
H7BX95	SRSF1	Serine/arginine-rich splicing factor 1	2,39
P19324	SERPINH1	Serpin H1	2,39
Q9ZB9	RPS6KA4	Ribosomal protein S6 kinase alpha-4	2,38
P35980	RPL18	Large ribosomal subunit protein eL18	2,38
P07141	CSF1	Macrophage colony-stimulating factor 1	2,38
A0A7N9VR94	AHNAK2	AHNAK nucleoprotein 2	2,38
E9Q0F0	KRT78	Keratin 78	2,38
Q62356	FSTL1	Follistatin-related protein 1	2,38
P61290	PSME3	Proteasome activator complex subunit 3	2,37
Q9DBX2	CCDC124	Coiled-coil domain-containing protein 124	2,36
Q9D1R9	RPL34	Large ribosomal subunit protein eL34	2,36
Q9D3L3	SNAP23	Synaptosomal-associated protein	2,36
Q8R180	ERO1A	ERO1-like protein alpha	2,35
G3XA48	IDI1	isopentenyl-diphosphate Delta-isomerase	2,35
P62911	RPL32	Large ribosomal subunit protein eL32	2,35
O08795	PRKCSH	Glucosidase 2 subunit beta	2,34
P26516	PSMD7	26S proteasome non-ATPase regulatory subunit 7	2,34
P62242	RPS8	Small ribosomal subunit protein eS8	2,34
Q64433	HSPE1	10 kDa heat shock protein, mitochondrial	2,33
P25444	RPS2	Small ribosomal subunit protein uS5	2,32
E9QAQ7	ARID1A	AT rich interactive domain 1A (SWI-like)	2,31
Q8VEX3	HNRNPU	Heterogeneous nuclear ribonucleoprotein U	2,31
P53690	MMP14	Matrix metalloproteinase-14	2,30
A0A3Q4EGK3	LTBP1	Latent transforming growth factor beta binding protein 1	2,30
Q8BSY0	ASPH	Aspartyl/asparaginyl beta-hydroxylase	2,30
Q9ER00	STX12	Syntaxin-12	2,29
Q9CR57	RPL14	Large ribosomal subunit protein eL14	2,29
P29391	FTL1	Ferritin light chain 1	2,29
F8VQC7	KTN1	Kinectin 1	2,28
E9QM38	SLC12A2	Solute carrier family 12, member 2	2,26
A2AS53	STAU1	Staufen double-stranded RNA binding protein 1	2,26
Q3UEB3	PUF60	Poly(U)-binding-splicing factor PUF60	2,24
P32261	SERPINC1	Antithrombin-III	2,24
O88983	STX8	Syntaxin-8	2,24
Q9DBJ1	PGAM1	Phosphoglycerate mutase 1	2,23
Q9D1J3	SARNP	SAP domain-containing ribonucleoprotein	2,23
Q8BJU0	SGTA	Small glutamine-rich tetratricopeptide repeat-containing protein alpha	2,23
P42208	SEPTIN2	Septin-2	2,22
Q9JIH2	NUP50	Nuclear pore complex protein Nup50	2,22
Q8BLI9	SRSF7	Serine/arginine-rich splicing factor 7	2,22
P35456	PLAUR	Urokinase plasminogen activator surface receptor	2,21
P86048	RPL10L	Large ribosomal subunit protein uL16-like	2,21
F2Z456	CYB5R3	NADH-cytochrome b5 reductase	2,20
P09055	ITGB1	Integrin beta-1	2,20
B2RXS4	PLXNB2	Plexin-B2	2,20
P97822	ANP32E	Acidic leucine-rich nuclear phosphoprotein 32 family member E	2,20
Q99K48	NONO	Non-POU domain-containing octamer-binding protein	2,20
Q91YR1	TWF1	Twinfilin-1	2,20
Q80UG5	SEPTIN9	Septin-9	2,19
Q9Z1R4	D17H6S53E	Uncharacterized protein C6orf47 homolog	2,18
P23116	EIF3A	Eukaryotic translation initiation factor 3 subunit A	2,18
Q8BR63	FAM177A1	Protein FAM177A1	2,18
Q9Z247	FKBP9	Peptidyl-prolyl cis-trans isomerase FKBP9	2,18
Q3UUU2	FUBP1	Far upstream element (FUSE) binding protein 1	2,17
Q9CZU6	CS	Citrate synthase, mitochondrial	2,16
G3X9Q6	LARP4	La ribonucleoprotein 4	2,16
Q8K021	SCAMP1	Secretory carrier-associated membrane protein 1	2,15
P16110	LGALS3	Galectin-3	2,15
Q5XJF6	RPL10A	Ribosomal protein	2,13
Q01730	RSU1	Ras suppressor protein 1	2,13
P05201	GOT1	Aspartate aminotransferase, cytoplasmic	2,12
V9GXM1	ARFGAP1	ADP-ribosylation factor GTPase activating protein 1	2,12
Q3UV17	KRT76	Keratin, type II cytoskeletal 2 oral	2,11
P11688	ITGA5	Integrin alpha-5	2,11
A2CEK3	PGM1	Phosphoglucomutase 1	2,11
Q8C1D8	IWS1	Protein IWS1 homolog	2,10
Q8C845	EFHD2	EF hand domain containing 2	2,10
Q8R5L1	C1QBP	Complement component 1 Q subcomponent-binding protein, mitochondrial	2,10
Q3UMU9	HDGFL2	Hepatoma-derived growth factor-related protein 2